ARL-CR-0774 ● JUNE 2015

US Army Research Laboratory

# Report of Research at Technische Universität Darmstadt on Ultrahard Materials in the B-C-N-Si System

**edited by Ralf Riedel**
*Technische Universität Darmstadt*
*Fachbereich Material- und Geowissenschaften*
*Fachgebiet Disperse Feststoffe*
*Petersenstr. 32*
*D-64287 Darmstadt*
*Germany*

**and**

**James W McCauley (Emeritus)**
*US Army Research Laboratory*
*Weapons and Materials Research Directorate, ARL*
*Aberdeen Proving Ground, MD 21005-5066*

**under contract W911NF-09-1-0576**

## NOTICES

### Disclaimers

The findings in this report are not to be construed as an official Department of the Army position unless so designated by other authorized documents.

Citation of manufacturer's or trade names does not constitute an official endorsement or approval of the use thereof.

Destroy this report when it is no longer needed. Do not return it to the originator.

ARL-CR-0774 ● JUNE 2015

US Army Research Laboratory

# Report of Research at Technische Universität Darmstadt on Ultrahard Materials in the B-C-N-Si System

**edited by Ralf Riedel**
*Technische Universität Darmstadt*
*Fachbereich Material- und Geowissenschaften*
*Fachgebiet Disperse Feststoffe*
*Petersenstr. 32*
*D-64287 Darmstadt*
*Germany*

**and**

**James W McCauley (Emeritus)**
*US Army Research Laboratory*
*Weapons and Materials Research Directorate, ARL*
*Aberdeen Proving Ground, MD 21005-5066*

**under contract W911NF-09-1-0576**

# REPORT DOCUMENTATION PAGE

*Form Approved*
*OMB No. 0704-0188*



| 1. REPORT DATE *(DD-MM-YYYY)* | 2. REPORT TYPE | 3. DATES COVERED (From - To) |
|---|---|---|
| June 2015 | Final | 1 August 2009–31 December 2012 |

**4. TITLE AND SUBTITLE**
Report of Research at Technische Universität Darmstadt on Ultrahard Materials in the B-C-N-Si System

**5a. CONTRACT NUMBER**
W911NF-09-1-0576

**5b. GRANT NUMBER**

**5c. PROGRAM ELEMENT NUMBER**

**6. EDITOR(S)**
Ralf Riedel and James W McCauley

**5d. PROJECT NUMBER**
1375-MS-01

**5e. TASK NUMBER**

**5f. WORK UNIT NUMBER**

**7. PERFORMING ORGANIZATION NAME(S) AND ADDRESS(ES)**
US Army International Technology Center–Atlantic

**8. PERFORMING ORGANIZATION REPORT NUMBER**

**9. SPONSORING/MONITORING AGENCY NAME(S) AND ADDRESS(ES)**
US Army Research Laboratory
ATTN: RDRL-WM
Aberdeen Proving Ground, MD 21005-5069

**10. SPONSOR/MONITOR'S ACRONYM(S)**

**11. SPONSOR/MONITOR'S REPORT NUMBER(S)**
ARL-CR-0774

**12. DISTRIBUTION/AVAILABILITY STATEMENT**
Approved for public release; distribution is unlimited.

**13. SUPPLEMENTARY NOTES**

**14. ABSTRACT**

There are 3 phases of this research program:

1) The synthesis of a boron carbide ($B_4C$) ceramic powder by means of a polymer pyrolysis route. The synthesis involves the polycondensation of single molecules and subsequent thermal decomposition of the resulting boron-containing polymer at 1,100 °C. The product is annealed in a second step at 2,000 °C to form polycrystalline $B_4C$. The work is divided into 3 parts: i) synthesis of the educts—namely, bis(trimethylsilyl)carbodiimide and 2,4,6-trichloroborazine; ii) synthesis of the preceramic polymer by reaction of the aforementioned educts; and iii) thermolysis of the polymer up to 2,000 °C in a helium atmosphere.
2) A comprehensive literature review on superhard materials and their method of fabrication, projected properties, and possible scale-up, with a focus on the B-C-N system.
3) Attempting to fabricate, using the multianvil press, larger samples of c-$Si_3N_4$ (transparent if possible)—a spinel structure material.

**15. SUBJECT TERMS**
boron, carbon, nitrogen, silicon, cubic-$Si_3N_4$, boron carbide, ultrahard materials, high pressure

| 16. SECURITY CLASSIFICATION OF: | | | 17. LIMITATION OF ABSTRACT | 18. NUMBER OF PAGES | 19a. NAME OF RESPONSIBLE PERSON |
|---|---|---|---|---|---|
| a. REPORT | b. ABSTRACT | c. THIS PAGE | | | James W McCauley |
| Unclassified | Unclassified | Unclassified | UU | 98 | 19b. TELEPHONE NUMBER (Include area code) 410-306-0711 |

## Contents

## List of Figures

## List of Tables

# 1. Nonaqueous Sol-Gel Synthesis of Boron Carbide–Based Materials

Gabriela Mera and Ralf Riedel

## 1.1 Interim Report (Project Start Date: December 1, 2009)

### 1.1.1 Summary

The aim of the present project is the synthesis of a boron carbide ($B_4C$) ceramic powder by means of a polymer pyrolysis route. The synthesis involves polycondensation of single molecules and subsequent thermal decomposition of the resulting boron-containing polymer at 1,100 °C. The product is annealed in a second step at 2,000 °C to form polycrystalline $B_4C$. The work is divided into 3 parts: i) synthesis of the educts—namely, bis(trimethylsilyl)carbodiimide and 2,4,6-trichloroborazine; ii) synthesis of the preceramic polymer by reaction of the aforementioned educts; and iii) thermolysis of the polymer up to 2,000 °C in a helium atmosphere.

### 1.1.2 Experimental Work

The synthesis of bis(trimethylsilyl)carbodiimide was performed as reported in the literature, starting from hexamethyldisilazane **1** (purum, ≥98.0% [gas chromatograph], Fluka, Germany), dicyandiamide **2** (99%, Aldrich, Germany; 19.70 Euros for 1 kg), and ammonium sulfate as the catalyst (SigmaUltra, ≥99.0%, Sigma-Aldrich, Germany; 32.90 Euros for 100 g) as shown in Scheme 1.

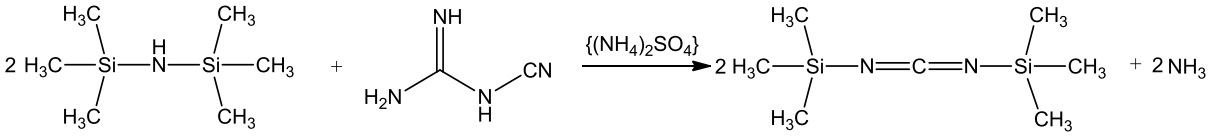


**1** **2** **3**

**Scheme 1**

The reaction mixture was heated at 164 °C for 8 h, followed by a fractional distillation over a Vigreux column. The yield of the product, bis(trimethylsilyl) carbodiimide **3**, was 65 wt%.

The maximum amount of product per batch that can be produced in our lab is 250 mL. Until now, we have produced 0.5 L of pure bis(trimethylsilyl) carbodiimide.

The synthesis of 2,4,6-trichloroborazine was achieved by an improved synthetic route, which has not been reported in the literature yet. The novel synthesis approach allows us to use $BCl_3 \cdot SMe_2$ **4** instead of $BCl_3$ gas, which is highly reactive and toxic. Accordingly, hexamethyldisilazane **1** (purum, ≥98.0% (GC), Fluka, Germany) was reacted with $BCl_3 \cdot SMe_2$ **4** in dichloromethane as the solvent (2.0 M in methylene chloride, Aldrich, Germany) (Scheme 2).

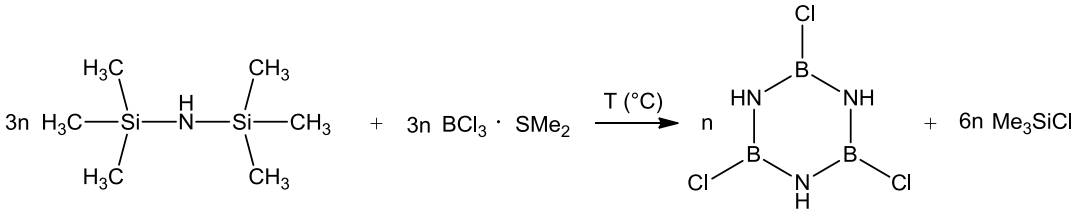


**1** **4** **5**

**Scheme 2**

Several reaction conditions were tested to produce a pure product **5** with an improved yield. The progress of the reactions were followed by means of liquid-state $^{1}H$, $^{13}C\{^{1}H\}$, $^{13}C$ DEPT (distortionless enhancement by polarization transfer), $^{29}Si$ DEPT, and $^{11}B$ NMR (nuclear magnetic resonance) in $C_6D_6$.

Independently of the starting temperature or the ratio of the educts, 2,4,6-trichloroborazine **5** was obtained as the major product, together with some traces of residual $BCl_3 \cdot SMe_2$. The reactions were performed at starting temperatures –25, 0, and 25 °C, followed by refluxing at 66 °C and drying of the solid product **5** in vacuum.

In the next step, the product 2,4,6-trichloroborazine **5** has to be purified by sublimation in vacuum at 60 °C. Subsequently, 2,4,6-trichloroborazine **5** will be reacted with bis(trimethylsilyl)carbodiimide **3** to form the preceramic polymer **6** (Scheme 3).

The synthesis of the educts and of the polymer will be done in several batches to produce the required amount of $B_4C$.

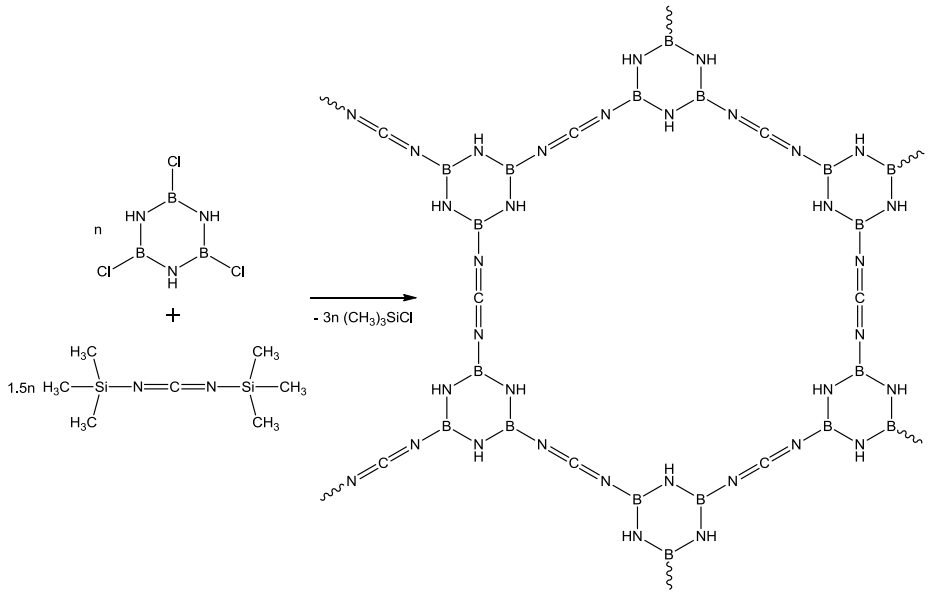


**6**

**Scheme 3**

## 1.2 Final Report (Project Start Date: December 15, 2009)

### 1.2.1 Summary

The aim of the present project is the synthesis of a boron carbide ($B_4C$) ceramic powder by means of a polymer pyrolysis route. The synthesis involves polycondensation of single molecules and subsequent thermal decomposition of the resulting boron-containing polymer at 1,100 °C. The product is annealed in a second step at 2,000 °C to form polycrystalline $B_4C$. The work is divided into 3 parts: i) synthesis of the educts—namely, bis(trimethylsilyl)carbodiimide and 2,4,6-trichloroborazine; ii) synthesis of the preceramic polymer by reaction of the aforementioned educts; and iii) thermolysis of the polymer up to 2,000 °C in a helium atmosphere.

### 1.2.2 Experimental Work

The synthesis and purification of bis(trimethylsilyl)carbodiimide **2** was done as described in the interim report above.

For the synthesis of 2,4,6-trichloroborazine **5**, several routes were proved. As described in the interim report, the product was firstly produced by the reaction of hexamethyldisilazane with $BCl_3 \cdot SMe_2$ **4** in dichloromethane as solvent (2.0 M in methylene chloride, Aldrich, Germany) as shown in Scheme 1.

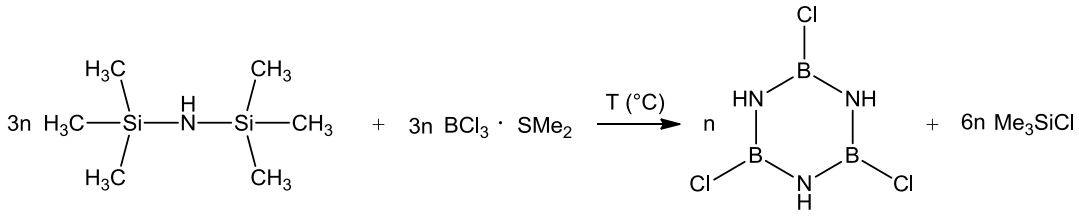


**1** **4** **5**

**Scheme 1**

Several reaction conditions were tested to produce a pure product **5** with improved yield. The progress of the reactions were followed by means of liquid-state $^{1}H$, $^{13}C\{^{1}H\}$, $^{13}C$ DEPT, $^{29}Si$ DEPT, and $^{11}B$ NMR in $C_6D_6$. Independently of the starting temperature or the ratio of the educts, 2,4,6-trichloroborazine **5** was obtained as the major product, together with some traces of residual $BCl_3{\cdot}SMe_2$ **4**. The reactions were performed at starting temperatures –25, 0, and 25 °C, followed by refluxing at 66 °C and drying of the solid product **5** in vacuum. In the next step, the product 2,4,6-trichloroborazine **5** has to be purified by sublimation in vacuo at 60 °C. Subsequently, 2,4,6-trichloroborazine **5** is reacted with bis(trimethylsilyl) carbodiimide **3** to form the preceramic polymer **6** (Scheme 2).

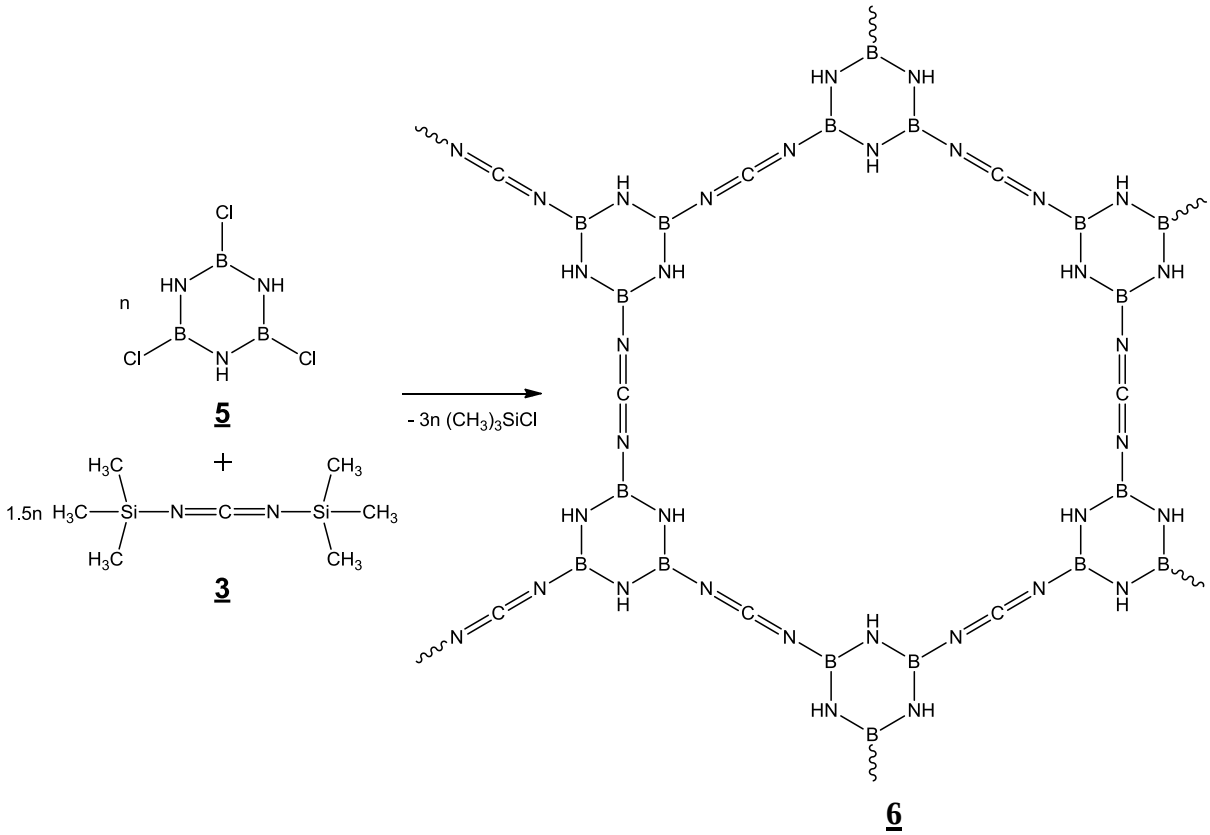


**Scheme 2**

The synthesis of the educts and of the polymer will be done in several batches to produce the required amount of boron carbide ($B_4C$).

The polymer **6** was pyrolyzed at 1100 °C to produce an amorphous $B_xC_yN_z$ ceramic **7**. The pyrolysis program was as follows: 100 °C/h heating rate to 200 °C, holding time 2 h, heating to 1,100 °C with 100 °C/h, and dwelling time 2 h. After holding at the final temperature, the sample was allowed to cool to room temperature. The ceramic yield was ≈25 wt%. This process is summarized in Scheme 3.

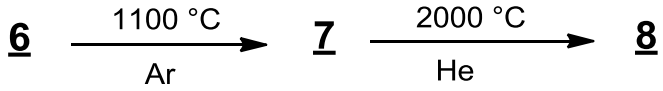


**Scheme 3**

The amorphous $B_xC_yN_z$ ceramic **7** (Fig. 1.1) was further pyrolyzed to 2000 °C in an Astro furnace. The yield after thermolysis of $B_xC_yN_z$ was ≈50 wt%. The product **8** obtained at 2,000 °C is not pure $B_4C$—it still contains ß-SiC and graphite as crystalline phases (Fig. 1.2) together with an amorphous phase. Moreover, contamination of sulfur was analysed (specific smell of the samples and coloration of the crucible).

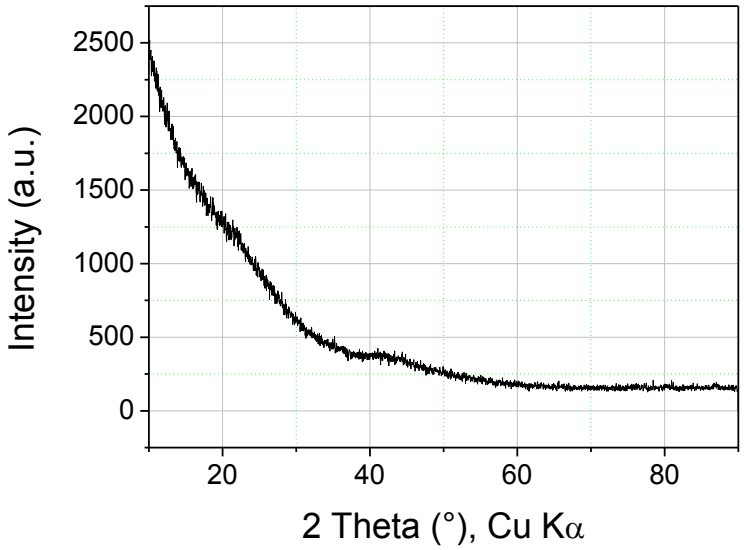


**Fig. 1.1 X-ray diffraction (XRD) of the synthesized $B_xC_yN_z$ ceramic 7 at 1,100 °C**

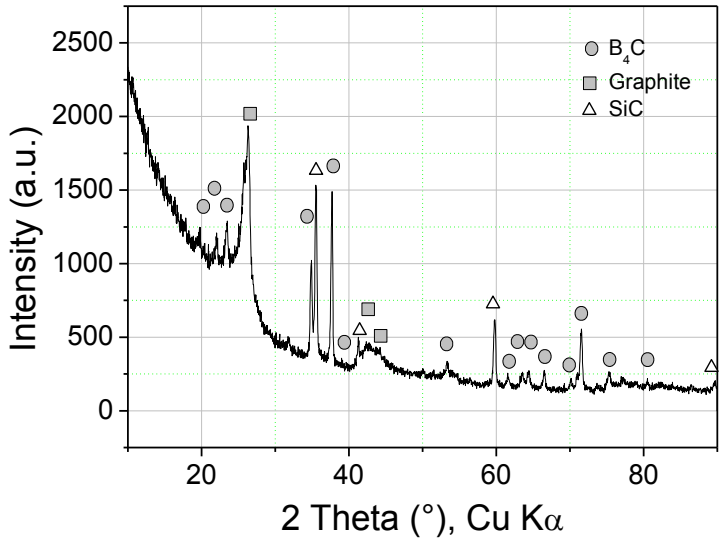


**Fig. 1.2 X-ray diffraction (XRD) analysis of the sample 7 at 2,000 °C**

The results are also in agreement with micro-Raman spectroscopy studies (514.5-nm laser). Figure 1.3 shows the results obtained for the regions containing $B_4C$ and amorphous carbon (Fig. 1.3a) and for the regions containing ß-SiC and amorphous carbon (Fig. 1.3b). The presence of graphite phase was not identified by Raman spectroscopy.

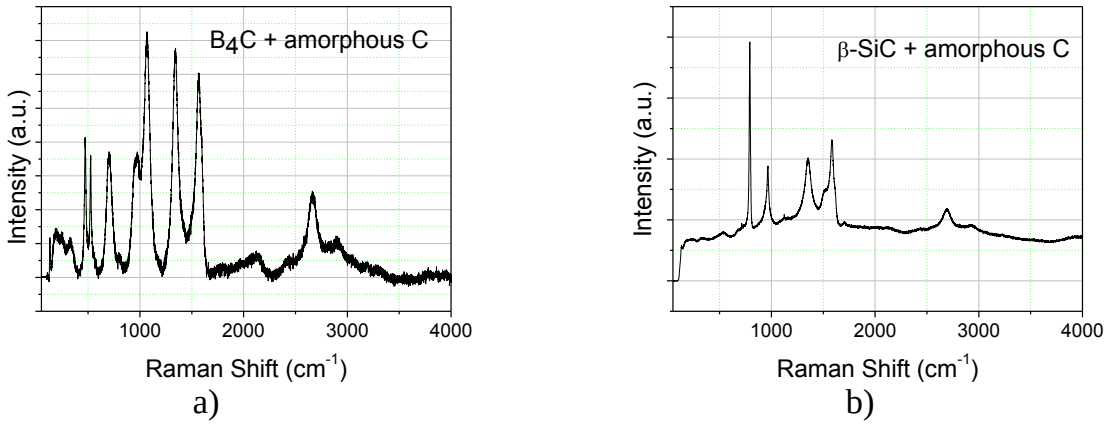


**Fig. 1.3 Raman spectroscopy of 8 (at 2,000 °C): a) regions containing $B_4C$ and amorphous carbon and b) regions containing ß-SiC and amorphous carbon**

To improve the purity of the products, 2,4,6-trichloroborazine was also synthesized from hexamethyldisilazane and trichloroborane 1M in hexane (Scheme 4).

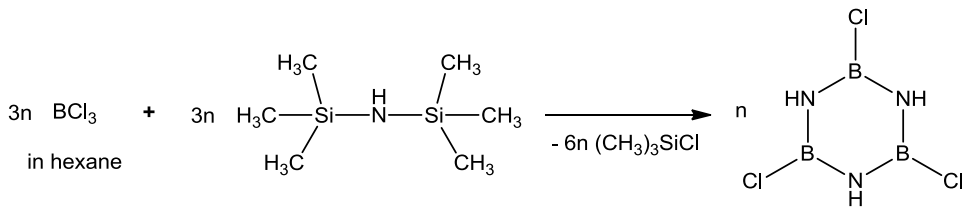


**9** **1** **5`**

**Scheme 4**

The trichloroborane solution violently reacts with moisture; therefore, the synthesis can be made only in small amounts, high dilution, and at low temperature (–65 °C). The highest amount of product **5'** that can be produced in one batch in our laboratory is 5 g. The yield of the reaction is ≈45 wt%, and the product was further used without purification. The quantitative polymerization of **5'** with bis(trimethylsilyl)carbodiimide yields polymer **6'** having the same structure as **6** but containing no sulfur impurities.

Similar to the pyrolysis of **6**, the amorphous product **7'** obtained at 1100 °C and crystalline **8'** synthesized at 2000 °C can be produced according to Scheme 5.

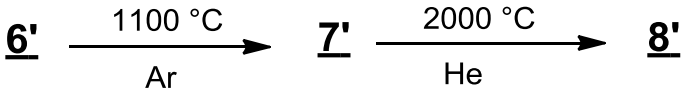


**Scheme 5**

Product **8'** is a $B_4C$-containing ceramic as proved by Raman spectroscopy (514.5 nm) (Fig. 1.4) and by X-ray diffraction (XRD) analysis (Fig. 1.5).

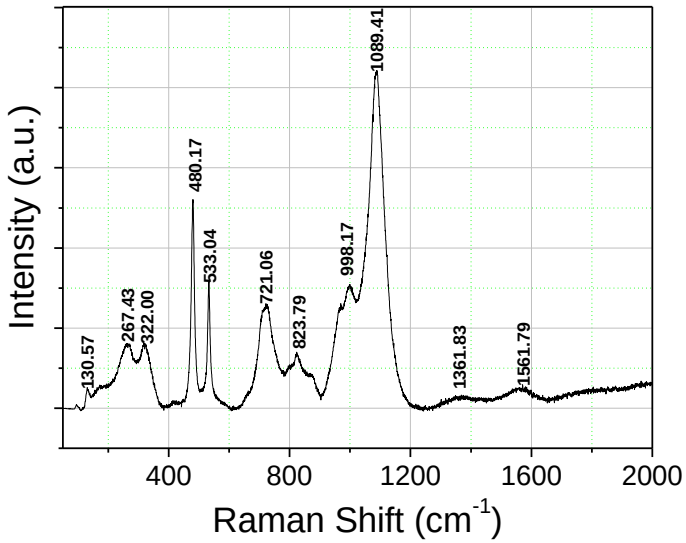


**Fig. 1.4 Raman spectrum of 8' (at 2,000 °C)**

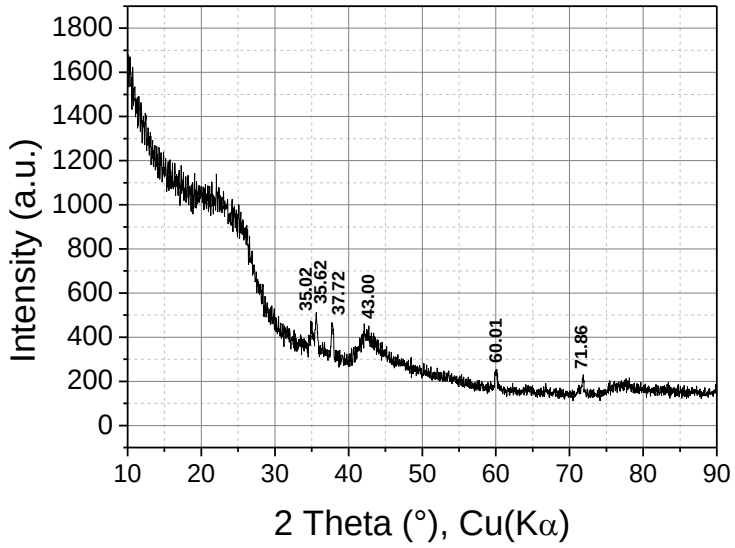


**Fig. 1.5 X-ray diffraction (XRD) analysis of 8' (at 2,000 °C)**

The evidence for the formation of $B_4C$ is also clearly shown by Raman spectroscopy. Figure 1.4 shows the micro-Raman spectra of sample **8'**. Three wide bands at 721.06, 823.79, and 1,089.41 $cm^{-1}$ and a double narrow band at 480.17/533.04 $cm^{-1}$ can be clearly distinguished, which are characteristic for the presence of rhombohedral $B_4C$. Two other broad lines at 1,361.83 and 1,561.79 $cm^{-1}$ can also be found, corresponding to the D and G absorption bands of residual amorphous carbon, nevertheless of low intensity. From the Raman studies it is obvious that sample **8'** exhibits the band pattern of that of $B_4C$ with low excess carbon impurities.

The XRD diffractogram shows weak reflections in part related to rhombohedral $B_4C$ according to the PDF database (Powder Diffraction Files [PDF], International Center for Diffraction Data: Swarthmore, PA). The sample is not completely crystallized, and it looks similar to $B_4CN_4$ synthesized at 1,800 °C as reported in Kroke et al.[1] and Völger et al.[2]

The broad and weak (100) reflex of turbostratically disordered graphite-like $B_xC_yN_z$ around $2\theta = 43°$ is also found. To completely crystallize the sample, higher temperatures and/or longer annealing times are required. The experiments are currently under investigation.

The microstructure of **8'** was analyzed also by means of scanning electron microscope (SEM) analysis. Figure 1.6 presents the micrograph of the ceramic sample composed of 2 phases, one with a high porosity and a second one with dense regions.

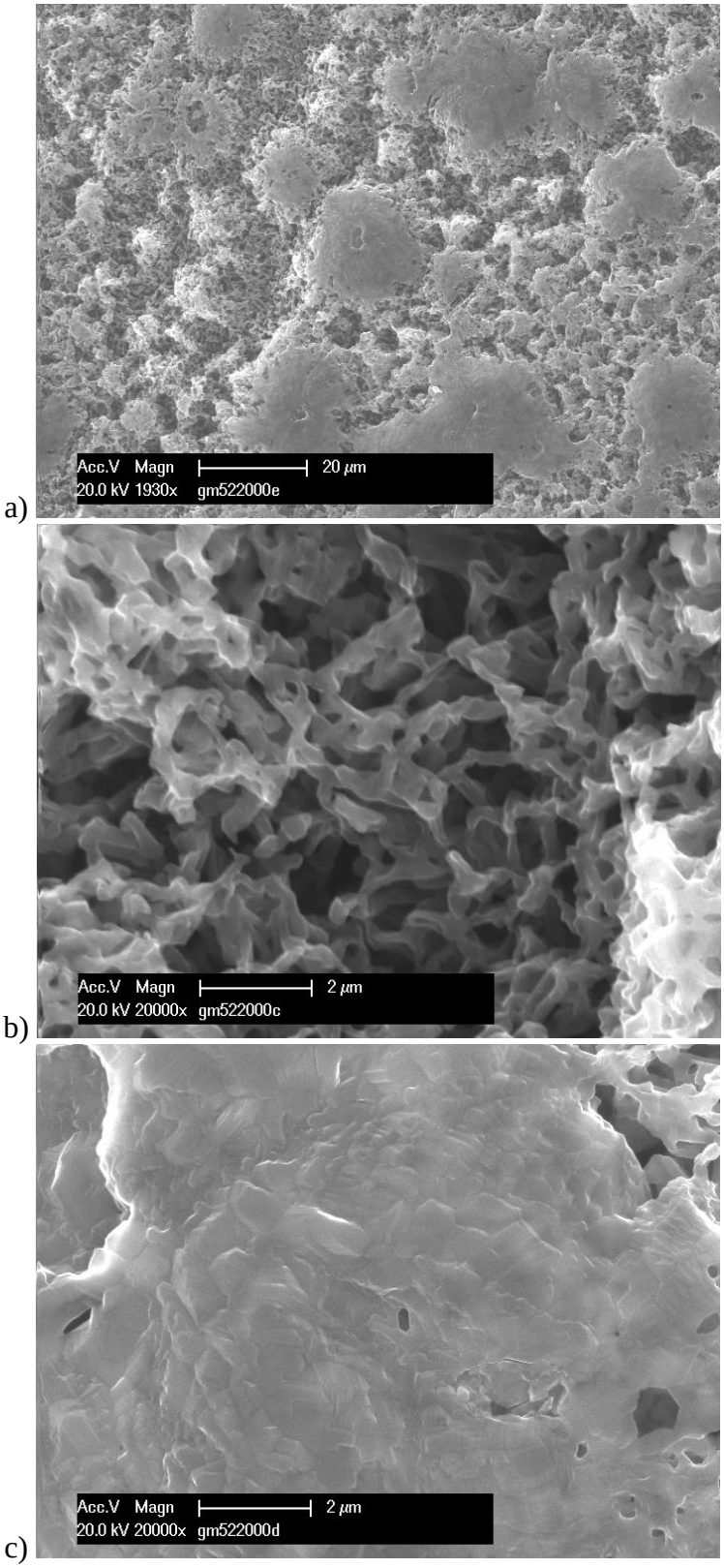


**Fig. 1.6 Scanning electron micrograph of product 8': a) overall microstructure of the sample; b) porous part of the microstructure; and c) dense part of the microstructure**

The elemental analysis of the product **8'** has shown that the sample still contains nitrogen and some oxygen impurities. The calculated molecular formula is $B_{4.9}C_1N_{2.3}O_{0.1}$ corresponding to 11.67 wt% C, 2.60 wt% O, 33.84 wt% N, and 51.89 wt% B. The decomposition of $BC_xN_y$ to $B_4C$ with elimination of nitrogen gas (reported to take place at 1,850 °C) is obviously occurring at higher temperatures than the one used in the present study.

Therefore, product **7'** ($BC_xN_y$, 1,100 °C) is presently synthesized in several batches and pyrolyzed up to 2,100 and 2,200 °C with annealing times of 4 to 10 h to achieve the requested amount of pure $B_4C$ ceramic.

At this point in the project it became clear that the original goal of making large quantities of pure $B_4C$ powder in a time- and cost-effective manner was probably not possible with the available funding. The main problem was that the cost of the starting material, trichloroborazine, was just too high (500 g for 55,000.00 Euros) from the standpoint of this project or for future commercialization. It was therefore decided to refocus the project on the following tasks:

- Compose a short review paper on superhard materials and their method of fabrication, projected properties, and possible scale up, with a focus on the B-C-N system.
- Try to fabricate, using the multianvil press (MAP), larger samples of c-$Si_3N_4$ (transparent if possible).

The reports of these 2 tasks follow in Parts 2 and 3.

### 1.2.3 References


1. Kroke E, Völger KW, Klonczynski A, Riedel R. Angew Chem Int Ed. 2001;40(9):1698–1700.
2. Völger KW, Kroke E, Gervais C, Saito T, Babonneau F, Riedel R, Iwamoto Y, Hirayama T. Chem Mater. 2003;15:755–764.

## 2. Review: Synthesis Routes to Ultrahard B-C-N Phases

Dmytro Dzivenko and Ralf Riedel

Finding substances harder than diamond appears to be a real challenge. Rather than harder, it might be more productive to consider the possibility of novel superhard substances and/or materials that are more useful than diamond for certain applications. While diamond exhibits extreme hardness, its actual performance as a superabrasive or electronic material is somewhat limited. It easily oxidizes in air at even moderate temperatures and cannot be used as an abrasive for machining of ferrous alloys. Cubic BN (c-BN) exhibits greater thermal stability and is the superabrasive of choice for machining of steels but has only half of the hardness of diamond. A possible solution to improve useful properties is to synthesize dense binary or ternary phases containing second-row main group elements (B, C, N) with the goal that these materials might be more thermally and chemically stable than diamond, and harder than c-BN, and thus should be excellent materials for high-speed cutting and polishing of different materials including ferrous alloys. There is also potential that new dense binary and ternary compounds in the B-C-N system will demonstrate important optoelectronic and/or superconducting properties in combination with exceptional hardness.

Thus, the search for a superhard substance that might surpass (or at least combine) advanced properties of diamond and c-BN goes on, supported by continuous improvement of experimental techniques and growth of computational capacities; this search is important both for understanding the fundamental correlations between microscopic characteristics of interatomic interactions and macroscopic properties, and for pure technological applications. Taking into account the existence of correlations between hardness and unambiguously determined physical characteristics of substances (such as elastic properties, density, etc.), the scientific community was able to sort out “islands” of existent and hypothetical (super)hard substances. They can be tentatively divided into 3 classes: i) covalent and ionic-covalent compounds formed by light elements from the middles of the second and third rows of the periodic table (low-Z compounds); ii) covalently bonded crystalline and disordered carbon modifications; and iii) partially covalent compounds of transition metals with light elements, such as borides, carbides, nitrides, and oxides.[1,2] To synthesize such compounds and substances, characterized by short bonds with high cohesive energy and rigid structures, the extreme conditions, such as high pressures (HPs) and high temperatures (HTs), or chemical vapor deposition (CVD) techniques are generally required. CVD techniques, however, do not provide bulk products and are, therefore, beyond the scope of the present report.

An alternative way to the superstrength and superhardness lies in the development of new materials, based on the existent (super)hard substances, via manipulation of their structure at the micro- and nanoscale. In other words, development of nanocomposites, multilayers, and superlattices via appropriate design and control of the material's morphology would allow bringing its hardness and other mechanical characteristics closer to or even surpass the "ideal" values. This approach has been successfully applied, for example, to fabricate c-BN, $Si_3N_4$, TiN-based nanocomposites, multilayers, and heterostructures with hardness approaching and even surpassing that of diamond.[3]

The present review is focused on the most promising class of potential superhard compounds—namely, covalent binary and ternary phases in the B-C-N system: diamond-like $B_xC_yN_z$ and $BC_x$ and dense $C_3N_4$ phases. It includes an overview of the theoretical works on the prediction of possible structures in the B-C-N system, investigation of their stability, and potentially interesting (in particular, elasto-mechanical) properties. It also describes the most prominent experimental approaches to obtain bulk superhard B-C-N compounds, including preparation of starting materials (precursors), experimental high-pressure high-temperature synthesis conditions, and results of characterization of the high-pressure products.

## 2.1 Ternary B-C-N Compounds

Ternary B-C-N compounds have drawn considerable attention during the last 2 decades because of the similarity in atom sizes and structures of carbon and boron nitride (i.e., diamond and cubic boron nitride, or graphite and hexagonal graphite-like boron nitride), which suggested that it should be possible to synthesize phases containing all 3 elements. Indeed, the existence of many low-density $B_xC_yN_z$ phases with hexagonal or turbostratic structure has been reported. They can be synthesized via i) nitriding of solid-phase precursors at high temperatures, ii) using CVD technique, or iii) pyrolysis of inorganic polymers containing boron, carbon, and nitrogen. These compounds are of broad interest because graphitic $B_xC_yN_z$ can be considered for applications as high-temperature semiconductors, especially if they can be altered by doping or structural changes.[4] Moreover, it is expected that the dense forms of ternary B-C-N compounds or diamond-like solid solution with the general formula $(BN)_xC_y$ can exhibit extreme hardness approaching that of diamond,[4–9] in combination with excellent thermal and chemical stability (superior to those of diamond)[10], and would therefore be indispensable abrasive materials for high-speed machining of ferrous alloys. Even though interesting properties like photoluminescence[11], hydrogen absorption and storage[12], and exhaust gas absorption[13] have been claimed for various B-C-N compounds (e.g., graphitic- or turbostratic-BCN, hexagonal-BCN, cubic-BCN, BCN-nanotubes)[14], the

present review will be generally focused on preparing dense ultrahard phases of B-C-N. This implies consideration of synthesis routes employing extreme pressures and temperatures or, to a lesser extent, CVD technique, which does not provide bulk superhard materials. The synthetic approaches resulting in low-density B-C-N ceramics or films (polymer routes, CVD, sputtering, etc.) will be also briefly considered in a sense of preparation of starting materials for subsequent high-pressure high-temperature (HP-HT) treatment, leading to the formation of hard phases.

### 2.1.1 Theoretical Predictions

Theoreticians have taken the first step in the late 1980s to investigate the electronic structure, bonding, and properties of this interesting class of materials prior to thorough experimental characterization. All the theoretical predictions can be roughly classified in investigation of structural stability, mechanical properties, and electronic properties.

#### 2.1.1.1 Structural Stability

Liu et al.[15] was one of the first to calculate the electronic structure of graphitic $BC_2N$ compounds using the local density functional formalism. The structural stability of $BC_2N$ has also been studied by Nozaki et al.[16] using an empirical molecular mechanics simulation. Both studies had 8 constituent atoms in a unit cell even though different structural models with different atomic arrangements were considered. These initial studies were focused on structural stability using monolayer-model and nearest neighbor environments. It has been predicted that $BC_2N$ is formed by maximizing C-C and B-N bonds. It has also been found that a structure with alternate -C-C- and -B-N- chains or rings is the most stable one. These predicted structures can be assigned to graphitic-$BC_2N$ type; some of the earlier experiments reported similar structures[17,18]. Quite recently the structural and electronic properties of boron ternary graphite-like monolayers (BCN) were investigated using a pseudopotential method within density functional theory with an emphasis on the effect of composition and atomic arrangement on the structural stability and electronic properties in a 32-atom unit cell.[19] The calculations confirm that the stable structure of boron ternary monolayers (BCN) is formed by increasing the number of both C-C and B-N bonds and, independent of the unit cell size, in agreement with earlier results,[15,16] obtained applying another approach. The structure, stability, and nature of the bonding of $BC_2N$ have been compared with the tetra-atomic carbon and BN molecules by Tapas Kar et al.[20] They predicted that the most stable structure of $BC_2N$ is linear, whereas $C_4$ and $(BN)_2$ are cyclic. However, as per our knowledge, experiments have not come up with linear-type $BC_2N$.

Regarding the cubic B-C-N materials, some early studies of diamond/c-BN superlattices and alloys indicated very limited miscibility with respect to c-BN

and diamond in the solid state around atmospheric pressure.[21,22] In order to explore possible synthetic routes to the single-phase "heterodiamond" $BC_2N$ phase, Tateyama et al.[23] investigated the effect of compression on graphitic $BC_2N$ (g-$BC_2N$) using the monolayer structure proposed by Liu et al.[15] and Nozaki et al.[16] Structure optimization was done using monoclinic unit cells with 8 atoms. The results showed that a more stable structure corresponds to that with no B-B or N-N bonds and more C-C and B-N bonds, so-called β-$BC_2N$ (Fig. 2.1). It seems that earlier predictions of the structural stability based on the number of B-N and C-C bonds (bond counting rule) in a monolayer structure hold here also. Among the 4 possible transformation structures, g-$BC_2N$ to β-$BC_2N$ was the most energetically favorable. Calculations predicted that β-$BC_2N$ can be synthesized from g-$BC_2N$ at nearly ambient pressure while the superlattice $BN/C_2$ by compression of g-$BC_2N$ to about 16 GPa[23]. The bulk modulus of dense β-$BC_2N$ is calculated to be between 374 and 409 GPa.[23–26] Mattesini et al.[24] predicted the metastable orthorhombic Λ-$BC_2N$ and trigonal Φ-$BC_2N$, "the most stable forms of the three-dimensional $BC_2N$ system", by replacing the carbon atoms with boron and nitrogen in the crystalline phase of fcc diamond. In new ternary B-C-N phases, the substitution was performed by taking the consideration of bond counting rule used by Tateyama et al.[23] and density functional theory (DFT) and local density approximation (LDA) were used for the calculation. Later, Sun et al.[27] confirmed that the above described β-$BC_2N$ has the lowest total energy among other possible atomic arrangements, although all the structures seem to be metastable and tend to separate into diamond and c-BN.

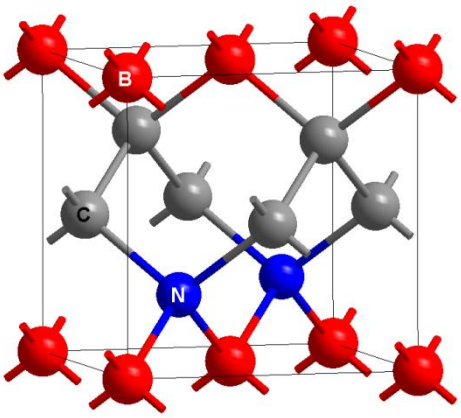


**Fig. 2.1 A representative atomic arrangement in the unit cell of cubic β-$BC_2N$ structure**

Yuge et al.[28] examined the phase stability of c-BCN (diamond-like) with a composition range of $(BN)_{(1-x)}(C_2)_x$ $(0 \leq x \leq 1)$ around atmospheric pressure by the combination of the cluster expansion technique and Monte Carlo simulation–based on first-principles calculations. In their work the authors doubted the results of a few earlier calculations that addressed the phase stability of c-BNC with respect to the c-BN and diamond, showing a significant discrepancy in the predicted phase diagrams due to the differences in the used

model: One achieves complete miscibility around T = 3,546 K, which is slightly below the melting line between c-BN and diamond.[29] Another reaches complete miscibility at T = 8,500 K, which is much higher than the melting line.[22] In their work, Yuge et al.[28] carefully considered the dependence of enthalpy on atomic arrangements, the effect of atomic orderings on configuration entropy, and the effect of lattice vibration, which were neglected in earlier theoretical predictions. The final result predicts strong preference of B-N and C-C bonding and disfavors B-C, C-N, B-B, and N-N bonds, which suggests phase separation to c-BN and diamond. Complete miscibility is achieved over T = 4,500 K, which is higher than the melting points of both diamond and c-BN.[28] Similar trends are found for the miscibility in the wurtzitic w-BCN between hexagonal diamond (londsdaleite) and w-BN, although a significant anisotropy in solubility for the wurtzite-like structure is observed, which leads to a 2-dimensional (2-D)-like solid solution in dilute composition despite its 3-dimensional (3-D) $sp^3$ bonding.[30] Furthermore, examination of pressure effects on the phase stability of c-BNC[31] has shown that at a pressure of 10 GPa, the solution energies of neighboring B–N and C–C atoms into diamond and cubic BN are both higher than those at 0 GPa, indicating a decrease of solubility in c-BNC under applied pressure. This decrease can mainly be attributed to the increase of volume with the formation of a c-BNC solid solution. The authors note that the success in synthesis of c-BNC compounds under high pressure should relate to the kinetic reason but not to a reason of the energetic in thermodynamic equilibrium.[31]

The structural stability and mechanical and electronic properties of cubic $BC_xN$ ($0.21 < x < 19.28$) crystals within a random solid solution model were investigated by Zhuang et al.[32] from the first principles. The authors have shown that, compared to c-$BC_2N$, the $BC_xN$ solids with higher carbon content ($x > 2$) exhibit better structural stability and higher elastic moduli. Moreover, significant deviations of the elastic moduli and lattice parameters from the predictions of Vegard's law have indicated that the $BC_xN$ solid solutions are not a simple mixing of diamond and cubic-BN. The computed band gaps are substantially lower than those of diamond and c-BN approaching the lowest value of 2 eV for $x = 4.4$.

Sun et al.[33] studied $BC_2N$ in cubic structure forms using ab initio pseudo-potential LDA calculations. The authors compared the recent experimental claim of cubic-$BC_2N$ of that time[5,7] with 8 atom zinc-blende structured cubic unit cells (the experimental results will be discussed in the next section). Fortunately, out of 420 different configurations, only 7 are topologically different because of the high symmetry of the zinc-blende-structured lattice, which makes their study possible. Even though predicted structures (1) and (2) (Fig. 2.2) are more stable and have the lowest energies, all 7 possible structures are metastable and tend to separate into diamond and cubic BN. Structures (1)

and (2) do not have B-B and N-N bonds, which is also consistent with earlier predictions. However, the full bond counting rule is not satisfied because they do have the same number of C-B and C-N bonds as C-C and B-N bonds. Later, the same research group, based on first-principles total-energy, and dynamic phonon calculations, investigated the structural transformation to and stability of cubic $BC_2N$ phases under pressure.[34,35] The authors showed that different starting material forms (graphitic $BC_2N$ with different atomic arrangement) lead to distinct synthesis routes, yielding end products with drastically different physical properties. Among all the considered structures, a high-density phase with no B-B or N-N bonding (phases 1 or 2 in Fig. 2.2) showed the highest structural stability and lowest compressibility at high pressure.

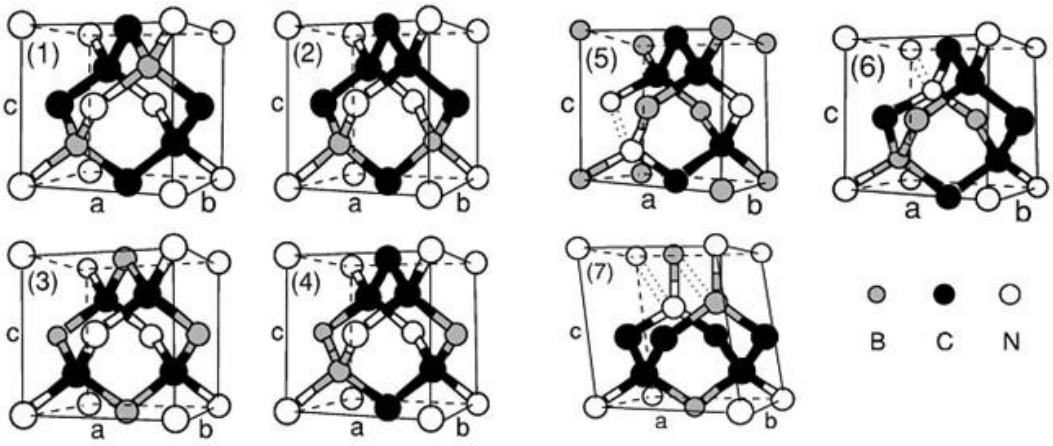


**Fig. 2.2 All the possible topologically different c-$BC_2N$ structures (after structural relaxation) starting from an 8-atom zinc-blende structured unit cell.[33] The dotted bonds indicate the broken covalent bonds between N atoms.**

There were many other structures proposed for $BC_2N$ ternary phases, like pseudocubic superlattice $BC_2N_{1x1}$,[36] "low-density" cubic LD-$BC_2N$,[37] tetragonal z-$BC_2N$,[38] z*-$BC_2N$ and t-$BC_2N$ (Fig. 2.3),[39] wurtzite-type w-$BC_2N$,[40] chalcopyrite-type cp-$BC_2N$,[25] body-centered bc6-$BC_2N$,[41] etc. (see Table 2.1). By comparing the simulated and experimental X-ray diffraction (XRD) patterns of $BC_2N$, Zhou et al.[39] have shown that for nanocrystalline powder z-$BC_2N$, z*-$BC_2N$ and t-$BC_2N$ reveal no significant difference and are in excellent agreement with the experimental results of Solozhenko et al.[7] However, only tetragonal t-$BC_2N$[39] seems to address most of the difficulties in explaining Raman splitting of LO and TO modes and higher experimental Vickers hardness values.[7] Another research group employed an ab initio evolutionary algorithm[42] to resolve the crystal structure of the observed superhard $BC_2N$ from 2 independent experiments. Among 12 considered structures, the authors uncovered 2 polymorphs with rhombohedral and orthorhombic symmetries, with which the experimental XRD pattern is well reproduced. Analysis of the total energy results and the simulated energy-loss near-edge spectroscopy suggested that the rhombohedral structure (*R*3*m* with 2

$BC_2N$ units in primitive cell) is the best candidate for the superhard $BC_2N$. The calculated electronic structures show that rh-$BC_2N$ is a wide-gap semiconductor with an indirect DFT band gap of 3.8 eV.

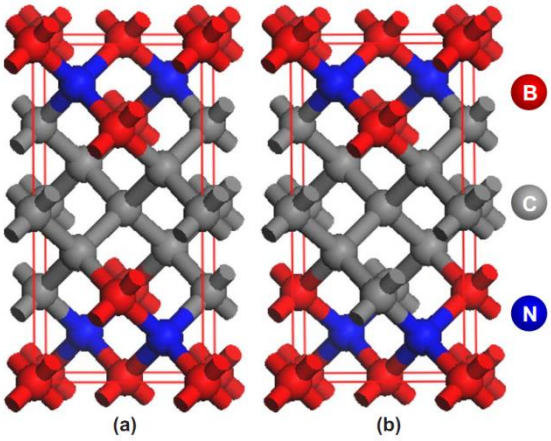


**Fig. 2.3 Proposed tetragonal crystal structures of diamond-like $BC_2N$: a) z*-$BC_2N$ with *P*-42*m* symmetry and b) t-$BC_2N$ with *P*-$42_1$*m* symmetry[38,39]**

Luo et al.[43] studied the $BC_4N$ crystal structure using DFT with LDA. They tried to correlate the experimentally derived $BC_4N$ structure and properties reported by Zhao et al.[9] (see Section 2.1.3). The authors proposed 3C-$BC_4N$ configurations constructed with Ramsdell notation and ruled out the modeling $BC_4N$ (unit cell consists of 6 or 12 atoms) with a zinc blende structure, which has 8 atoms in its unit cell. A simulated XRD pattern of the 3C-$BC_4N$ model matches the experimental XRD pattern of c-$BC_4N$.

The same research group has also considered the B-C-N phases with other stoichiometries—structural, electronic, and mechanical properties as well as phase transitions under hydrostatic pressures have been investigated for 6 possible $B_2C_2N_2$ structures deduced from the 3C-SiC unit cell.[44] The calculations have shown that $B_2C_2N_2$ with the maximum numbers of C–C and B–N bonds has the lowest total energy and is a large-gap semiconductor with an indirect band gap of 4.10 eV. The calculated bulk-, shear moduli, and Vickers hardness of 398.4, 440.7, and 84.3 GPa of the $B_2C_2N_2$ indicate that it is one potential superhard material with a hardness larger than that of cubic boron nitride. The pressure-induced structural transition from its low-pressure graphitic counterpart is estimated to occur above 11.4 GPa.[44] Tang et al.[45] investigated 5 nonequivalent atomic configurations of the suggested 3C-$BC_4N$ structure using first-principle calculations. All the configurations were found to be metastable. The band gap was calculated to be highly dependent on the atomic arrangement, thus a different 3C-$BC_4N$ configuration revealed insulating, semiconductor, semimetallic, or even metallic behavior.[45] Two possible metastable high-density $BC_6N$ phases originating from the diamond structure were suggested by Luo et al.[46] The calculations have shown that both $BC_6N$ phases are semiconductors with a direct generalized gradient

approximation (GGA) energy gap of about 2.1 eV and have Vickers hardness about 79–80 GPa, higher than the values for c-$BC_2N$ and c-BN.

Weihrich et al.[47] investigated a selective substitution of nitrogen with boron in the $C_3N_4$ for the 2- and 3-D structures using pseudo-potential and full-potential computations in the framework of the local DFT. This substitution led to the structures with the experimentally observed $BC_3N_3$ stoichiometry. The authors proposed a 2-D structure for the B-C-N precursor and a new ultrahard rhombohedral (*R*3*m*) compound, rh-$BC_3N_3$, with a bulk modulus of approximately 405 GPa reaching the range of the other studied $BC_2N$ structures.

Very recently, the formation ability of B-C-N ternary phases was studied by Jiang et al.[48] using DFT based on the model of the previously synthesized tetrahedral amorphous carbon (ta-C).[49] The "ta-C" modification was reported to possess not only high mass density (3.2 g/cm$^3$) and large amounts of sp$^3$ hybridized carbon (84%−88%) but also superior hardness (45 GPa) and Young's modulus (340 GPa). Possible B-C-N ternary phases were studied and plotted in a full-spectrum triangular phase diagram (Fig. 2.4). Formation energies are plotted accordingly and compared with experiential compositions reported to date. It is interesting that the formation energy distributes symmetrically along the C−BN isoelectronic line, in which the compositions in the range of B: 15–35 at%; C: 30–55 at%; N: 15–35 at% are relatively easier to form owing to their negative formation energy. Notably, most of the $B_xC_yN_z$ compositions synthesized in experiments are located in this area.

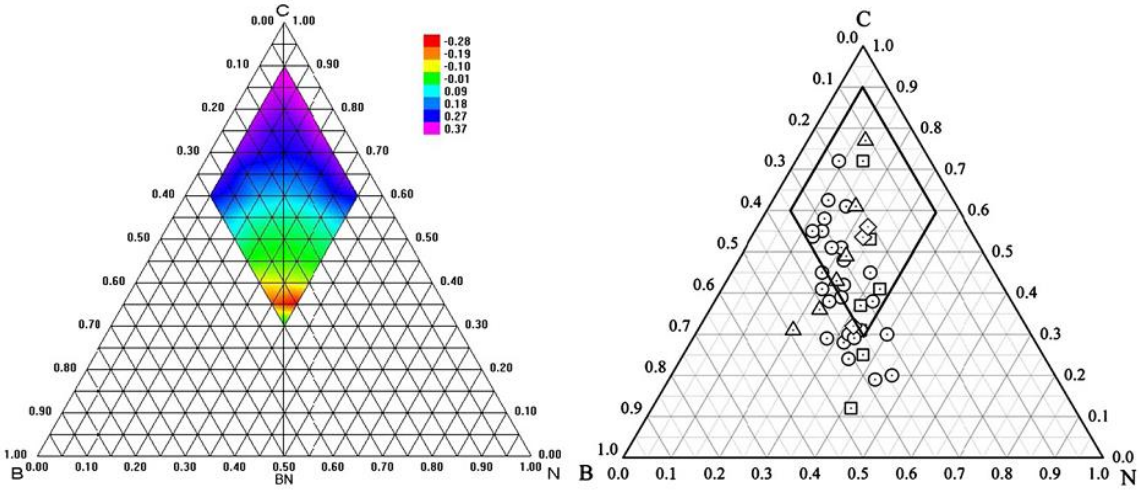


(a) (b)

**Fig. 2.4 a) Distribution of formation energy (eV/atom) on the upper rhombus of ternary B−C−N phase diagram using full spectrum. Less formation energy means that the corresponding composition is easier to form. b) $B_xC_yN_z$ compositions synthesized in previous experiments. Most compositions are located in the area with negative formation energy, in agreement with the theoretical prediction.[48]**

#### 2.1.1.2 Mechanical and Electronic Properties

In this report, the considered mechanical properties of the B-C-N ternary phase are mainly restricted to bulk modulus (B), shear modulus (G), and hardness (Vickers microhardness, Hv). The great interest in a superdard phase has been aroused because solid solutions (prepared by Knittle et al.[5]) of carbon and boron nitride showed a bulk modulus value of 355 GPa. Tateyama et al.[23] was the first to calculate a bulk modulus of 438±14 GPa for his predicted β-$BC_2N$ structure, which is slightly less than that of diamond. Thereafter, many theoretical predictions came with different bulk moduli and hardness depending on the considered structure predicted and the model used for calculations. The available theoretical values of lattice parameters, bulk and shear moduli, and estimated hardness of the predicted superhard $BC_2N$ structures, as well as of dense BCN phases with compositions different from $BC_2N$, are summarized in Table 2.1. The predicted bulk moduli for all the different structures generally exceed the experimental ones of c-BN (369–401 GPa) with most of them approaching those of diamond (433–442 GPa).[1,50]

**Table 2.1 Calculated lattice parameters, bulk moduli, shear moduli, and estimated hardness (if available) of the predicted superhard B-C-N phases. The experimental values for dense carbon and BN modifications are given for comparison.**

| Structure | a (nm) | b (nm) | c (nm) | α (°) | β (°) | γ (°) | B (GPa) | G (GPa) | Hv (GPa) | Ref. |
|---|---|---|---|---|---|---|---|---|---|---|
| Diamond[1] | 0.3567 | 0.3567 | 0.3567 | 90 | 90 | 90 | 442–433 | 534-544 | 60–150 | [1, 50] |
| C-ondsdaleite[1] | 0.252 | 0.252 | 0.412 | 90 | 90 | 120 | … | 382 | 60–70 | [1, 50] |
| c-BN[1] | 0.3616 | 0.3616 | 0.3616 | 90 | 90 | 90 | 369–401 | 409 | 46–80 | [1, 50] |
| w-BN[1] | 0.254 | 0.254 | 0.420 | 90 | 90 | 120 | 390 | 330 | 34–60 | [1, 50] |
| c-$BC_2N$[1] | 0.3642 | 0.3642 | 0.3642 | 90 | 90 | 90 | 282 | 447 | 76 | [7, 51] |
| | 0.3595 | 0.3595 | 0.3595 | 90 | 90 | 90 | … | … | 62 | [9] |
| c-$BC_4N$[1] | 0.3586 | 0.3586 | 0.3586 | 90 | 90 | 90 | … | … | 68 | [9] |
| β-$BC_2N$ | 0.3577 | 0.3577 | 0.3577 | 89.38 | 90.62 | 90.62 | 438±14 | … | … | [23] |
| | 0.3579 | 0.3579 | 0.3612 | 90 | 90 | 89.32 | 383.3 | … | … | [52] |
| | 0.361 | 0.361 | 0.361 | 90 | 90 | 90 | 342.4 | 453.6 | … | [37] |
| o-$BC_2N$ | 0.2528 | 0.2502 | 0.3587 | 90 | 90 | 90 | 408.9 | … | … | [24] |
| | 0.2529 | 0.2502 | 0.3591 | 90 | 90 | 90 | 403.1 | 446 | … | [26] |
| Φ-$BC_2N$ | 0.2496 | 0.2496 | 0.4192 | 90 | 90 | 120 | 420.1 | … | … | [53] |
| Λ-$BC_2N$ | 0.3554 | 0.3599 | 0.3553 | 90 | 90 | 90 | 459.4 | 481.96 | … | [24, 53] |
| c-$BC_2N$-1 | 0.3570 | 0.3609 | 0.3570 | 89.5 | 90 | 90 | 399.7 | … | … | [33] |
| c-$BC_2N$-2 | 0.3568 | 0.3564 | 0.3613 | 90 | 90 | 90 | 400.1 | … | … | [33] |
| $BC_2N_{1x1}$ | 0.4355 | 0.2514 | 1.2483 | 90 | 90 | 90 | 419.5 | … | 75.8(21) | [36] |
| | 0.3579 | 0.3579 | 1.074 | 90 | 90 | 90 | 420 | … | … | [54] |
| z-$BC_2N$ | 0.3565 | 0.3565 | 0.7168 | 90 | 90 | 90 | 402.7 | 447.4 | 75.9 | [38] |
| | 0.3604 | 0.3604 | 0.7247 | 90 | 90 | 90 | 385 | … | 65.0 | [42] |
| z*-$BC_2N$ | 0.3577 | 0.3577 | 0.7122 | 90 | 90 | 90 | 423.3 | 471.7 | 75.6 | [39] |
| t-$BC_2N$ | 0.3579 | 0.3579 | 0.7116 | 90 | 90 | 90 | 422.1 | 466.9 | 75.3 | [39] |
| r-$BC_2N$ | 0.3602 | 0.3602 | 0.3602 | n.d. | … | … | 382 | … | … | [54] |
| rh-$BC_2N$ | 0.2545 | 0.2545 | 2.5068 | 90 | 90 | 120 | 395 | … | 62.1 | [42] |
| w-$BC_2N$ | 0.2501 | 0.2501 | 0.4205 | 90 | 90 | 90 | 407.5 | 466.5 | 76.8 | [40] |
| cp-$BC_2N$ | 0.3613 | 0.3613 | 0.7146 | 90 | 90 | 90 | 367.4 | 432.0 | 72 | [25] |
| | 0.3653 | 0.3653 | 0.7228 | 90 | 90 | 90 | 349 | … | 67.5 | [42] |
| bc6-$BC_2N$ | 0.4361 | 0.4382 | 0.4405 | 90 | 90 | 90 | 305 | … | 60 | [41] |
| 3C-$BC_4N$ | 0.2507 | 0.2507 | 0.6196 | 90 | 90 | 120 | 418.8 | 521.3 | 84.3 | [43] |
| $BC_4N_{2x1}$ | 0.3567 | 0.3567 | n.d. | 90 | 90 | 90 | 428 | … | | [54] |
| t-$BC_6N$ | 0.3574 | 0.3574 | 0.3564 | 90 | 90 | 90 | 410.4 | … | 79.9 | [46] |
| r-$BC_6N$ | 0.3565 | 0.3565 | 0.3565 | 90.15 | 90.15 | 90.15 | 399.9 | … | 79.1 | [46] |
| $B_xC_yN_z$ | … | … | … | … | … | … | | (650–730)[2] | 45–50 | [48] |
| rh-$BC_3N_3$ | 0.3449 | 0.3449 | 0.3449 | 87.5 | … | … | 405.3 | … | … | [47] |
| $B_2C_2N_2$ | 0.2521 | 0.2521 | 0.6235 | 90 | 90 | 120 | 398.4 | … | 84.3 | [44] |

[1] Experimental values
[2] Values for the Young's modulus are given.

The claimed successful synthesis of cubic boron–carbonitride compounds $BC_2N$ with an experimentally determined extreme hardness second only to diamond and comparably low bulk modulus[7,9] initiated a systematic theoretical exploration of the nature of such a phenomenon. In particular, Zhang et al.[55] have examined the ideal strength of cubic $BC_2N$ using first-principles calculations. In contrast to the experiment, the authors revealed that, despite the large elastic parameters, compositional anisotropy and strain-dependent bonding character impose limitations on their strength. Consequently, the hardness of the optimal $BC_2N$ structure should be even lower than that of c-BN. The measured extreme hardness of $BC_2N$ nanocomposites is referred to the nanocrystalline size effect and the bonding to the surrounding amorphous carbon matrix. Zhuang et al.[56] have shown that the atomic arrangements (B, C, N) within the c-$BC_2N$ crystal lattice—namely, the different degrees of mixture of diamond and c-BN, may lead to distinctly different values of Vickers hardness and tensile strength. Similarly, Zhang et al.[57] have investigated elastic constants for several diamond-like $BC_2N$ structures from the first principles. The authors have shown that, although the deviations of the lattice constants from those of cubic lattices are small (about 1%), the differences among the elastic constant components, which should be the same for cubic lattices, can reach 75% because of the chemical anisotropy of the $BC_2N$ structures. For $BC_2N$ in which exact cubic symmetry is constrained, large residual stresses of 4–5 GPa in the structures were observed. Thus, the authors have concluded that any results derived by assuming exact cubic symmetry for $BC_2N$ structures may not be reliable.

Interest in electronic properties of B-C-N ternary phases started as early as their stability and structure prediction arose. Most of the theoretical calculations on structure and mechanical properties also predicted band gap values. However, predicted properties vary from semiconductor to insulator depending on the structure. For a layered structure, Liu et al.[15] predicted a band gap ($E_g$) of 1.6 eV, and for tubular and chiral structure, Miyamoto et al.[58] predicted 1.25–1.75 eV. Experimental results from Watanabe et al.[59] also confirmed semiconductor behavior of layered $BC_2N$. For $BC_2N$ heterodiamond, Tateyama et al.[23] predicted an indirect band gap of 3.97 eV. For orthorhombic $BC_2N$[24], a band gap of around 1.7–2.01 eV is predicted, whereas for c-$BC_2N$[33] derived from a zinc-blende structure, a bang gap of approximately 2.0 eV is calculated. Zhou et al.[38] have shown that despite the only difference between z*-$BC_2N$ and z-$BC_2N$ is that B and N atoms are interchanged with each other, the calculated band structures exhibit a significant difference: z*-$BC_2N$ is an indirect semiconductor with a band gap of 3.6 eV, while z-$BC_2N$ is a direct one with a band gap of 2.7 eV. The calculated electronic structures for chalcopyrite-type cp-$BC_2N$ showed that this compound is a wide gap semiconductor with a direct band gap about 3.3 eV, displaying some potential application ultraviolet luminescence.[25] Rhombohedral rh-$BC_2N$[42] and wurtzite-type w-$BC_2N$[40] are

predicted to have an indirect wide band gap of 3.6 and 3.99 eV, respectively. An even wider band gap is calculated for $BC_4N$, to be 4.06 eV.[43] In contrast, bc6-$BC_2N$ is an indirect semiconductor with band gap of 0.60 eV.[41] Several reports[23,24,33] also pointed out that the employment of LDA in calculation leads to significant underestimation of the band gap (65%–75%), thus the values calculated using this model cannot be considered as completely reliable.

### 2.1.2 Synthesis of B-C-N Precursors

A few recent first-principles studies of structural transformation and stability of B-C-N phases have indicated that different starting materials may lead to distinct synthesis routes, yielding various dense B-C-N end products with drastically different physical properties.[23,34] Therefore, different precursor materials used for HP-HT experiments on the synthesis of ultrahard dense B-C-N compounds will be considered below.

The oldest, simplest, and still widely used method is to synthesize boron carbonitrides from the elements at high temperatures. A typical reaction was used by Kosolapova et al.[60] in which boron and carbon powders were heated at 1,800–2,000 °C in $N_2/NH_3$ for prolonged periods promoting the reactions below:

$$\mathrm{B(s)+2C\ (s)+\tfrac{1}{2}N_2(g)} \xrightarrow{1800\text{-}2000\ ^\circ\mathrm{C}} \mathrm{BC_2N\ (s)}.$$

$$\mathrm{B(s)+2C\ (s)+\ NH_3(g)} \xrightarrow{\Delta} \mathrm{BC_2N\ (s)+\ \tfrac{3}{2}H_2(g)}.$$

The formation of $BC_2N$ in such reactions is diffusion controlled, occurring at the solid interfaces (B/C or B/$C_3N_4$) by a process of nucleation and growth. At elevated temperatures, the reactant atoms have enough energy to diffuse toward the interface forming the product. However, the process slows down as the interface thickens, and effectively, the reactants are no longer in contact.[60] Because of a complex process of diffusion of ions toward the thick interface, there is always some degree of inhomogeneity on the atomic level, which renders this method ineffective for the formation of complete solid solutions. Recently a stoichiometric ternary compound $B_4CN_4$ was obtained by direct nitridation of commercial $B_4C$ powder via heating in a stream of nitrogen at temperatures in the range of 1,600–1,900 °C.[61] The reaction was diffusion-controlled. The resulting powder with elemental composition $B_{3.96\text{-}4.03}C_{1.00}N_{3.96\text{-}4.07}O_{0.01\text{-}0.08}$ (~$B_4CN_4$) determined by electron probe microanalysis (EPMA) had the turbostratic layered structure, where carbon atoms form linear C $sp^2$–C $sp^2$ chains bonded to B and N within h-BN layers with a molar ratio C/BN = 1/4.

One of the first attempts of c-BN and diamond-mixed crystals by Badzian et al.[4] used graphitic g-BCN prepared by a CVD route. They used gaseous mixtures of $BCl_3/CCl_4/N_2/H_2$ at 1,900 °C to deposit polycrystalline BCN deposited on a graphite rod:

$$BCl_3 + CCl_4 + N_2 + H_2 \xrightarrow{1900\ °C} (BN)_xC_{1-x} + \ldots$$

As the CVD method employed 4 different gases, controlling the reaction and end product stoichiometry was very crucial. In further works, Bartlett and coworkers [62,63] conducted the reaction of boron trichloride with acetylene and ammonia at relatively low temperatures, which resulted in better ordering and more accurate compositions (e.g., $B_2CN_2$, $B_{0.485}C_{0.03}N_{0.485}$, $B_{0.35}C_{0.3}N_{0.35}$):

$$BCl_3 + y\ C_2H_2 + z\ NH_3 \xrightarrow{700\text{ -}800\ °C} B_xN_yC_z\ .$$

Instead of acetylene, other hydrocarbons, such as $CH_4$ and $C_3H_8$, have been used for the CVD preparation of other ternary B-C-N phases.[64] For example, Besmann[65] obtained single-phase $BC_{0.43}N_{0.29}$ with a graphite-like structure from $BCl_3$-$NH_3$-$CH_4$-$H_2$ mixtures at 1,650 K and 3.3 kPa. If boron trichloride and acetonitrile ($CH_3CN$) are used as the reactants, almost stoichiometric material with composition $BC_2N$ is obtained[62,63]:

$$BCl_3 + CH_3CN \xrightarrow{800\ °C} BC_2N + 3\ HCl\ .$$

The films produced by those methods consist of a turbostratic layered structure that contains $sp^2$-hybridized B, C, and N atoms according to XRD and transmission electron microscopy (TEM) studies. X-ray photoelectron spectroscopy (XPS) investigations reveal the presence of C-C, B-N, C-N, and B-C bonds. The same approach was successfully applied by Watanabe et al.[66] in order to produce amorphous $BC_2N$ films on polycrystalline Ni and quartz substrates. While using the same reactants in a hydrogen and nitrogen atmosphere, Kawaguchi et al.[67] deposited new graphite-like films of composition $BC_{0.9\text{-}1.3}N_{0.8\text{-}0.9}H_{0.4\text{-}0.7}$ and $BC_{3.0\text{-}3.2}N_{0.8\text{-}1.0}H_{0.2\text{-}2}$, which can be described as BCN(H) and $BC_3N$(H). X-ray and electron diffraction analyses indicate that these materials have hexagonal structures similar to that of graphite.

Hegermann et al.[68] investigated the influence of the carrier gases $N_2$, argon (Ar), and helium (He) and the applied power on the chemical composition of boron carbonitride films deposited by a PA-CVD process. Si(100) wafers were used as substrates and pyridine-borane and triazaborabicyclodecane as B-C-N-forming single-source precursors. Films that were either deposited in He using a low power density or in $N_2$ using a high power density revealed similar chemical composition of approximately $BC_4N$ as well as comparable properties (in particular, outstanding hardness ~60 GPa). XRD and TEM analysis of these films showed their amorphous nature. It should be noted that amorphous B–C–N films have been intensively studied during the last 2 decades since practically any composition within the B-C-N triangle can be synthesized by various conventional chemical and physical deposition methods, such as the previously

mentioned (PA)-CVD[66,67–69] as well as ion beam–assisted deposition,[70] pulsed laser deposition,[71] and magnetron sputtering.[72] Tuning different deposition parameters and choosing an appropriate atmosphere allows us to control not only the composition but also the bond contents in the resulting B-C-N films. This can play a key role when choosing precursors for the high-pressure synthesis of ultrahard diamond-like B-C-N phases, since the nature of the starting material is found to have a significant influence on the structural features and properties of the end product.

In contrast to the deposition routes to B-C-N materials resulting in ternary $B_xC_yN_z$ films, large amounts of similar phases can be synthesized via pyrolysis of polymeric B-C-N-based precursors at relatively low temperatures around 1,000 °C. In this way, thermal treatment of *B*-triphenylborazine and *N*-triphenylborazine in an autoclave at 1,000 °C results in boron carbonitrides with compositions of $BC_{3.9}N$ and $BC_{3.6}N$, respectively[73]. Ceramic $B_xC_yN_z$ powders with various nonstoichiometric compositions can be also obtained via pyrolysis of decaborane(12)-adducts of diamines $[–B_{10}H_{12}·\text{diamine}–]_n$,[74] pyroazabole polymer,[75] or polyethylene-iminoborane $[–CH_2–CH_2–N=BH_2–]_n$.[76]

Riedel and coworkers[17,77,78] reported the synthesis of turbostratic graphite-like $BC_2N$ and $BC_4N$ from piperazine borane and pyridine borane, respectively (the reactions A and B given below). This method can be ascribed to the so-called polymer-derived ceramic route, where a highly cross-linked insoluble, infusible polymeric intermediate is formed followed with pyrolysis under argon atmosphere at 1,050 °C. It is important to mention that in the latter reaction, utilization of nitrogen-containing atmosphere can lead to completely different results—namely, formation of almost pure boron nitride. In a subsequent work of the same research group, a crystalline ternary h-$BC_2N$ with a graphite-like structure was synthesized from these precursors at elevated pressures and temperatures.[79]

**(A)**

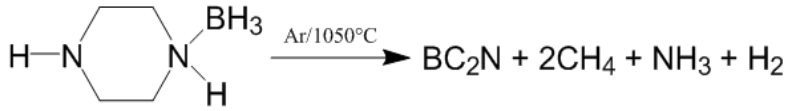


**(B)**

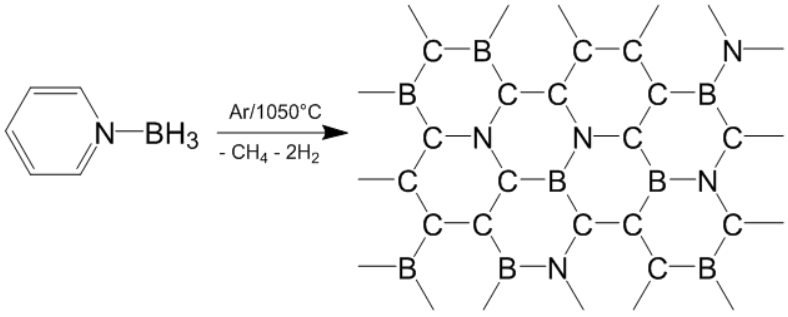


($BC_4N$)

Amorphous B-C-N ceramics were produced by thermolysis of poly(borosesquicarbodiimide) of idealized formula $[B_2(NCN)_3]_n$ at 1,100 °C in an argon atmosphere.[80] Wide-angle diffraction showed that the ceramics consist of an amorphous structure with hexagonal planar near-range ordered atomic arrangements similar to graphite. Nuclear magnetic resonance (NMR) investigation of the products showed the presence of BN structures with mainly trigonally coordinated boron and nitrogen nuclei and the presence of amorphous (graphite-like) carbon within the B-C-N ceramics at the same time. The authors concluded that the BCN phase tends to short-range phase separation into BN and C regions.

Another amorphous B-C-N ceramic with composition $B_4CN_4$ was prepared via a nonoxide sol-gel process.[81] In this approach *B*-trichloroborazene, $B_3N_3H_3Cl_3$, reacts with bis-(trimethylsilyl)-carbodiimide $Me_3Si\text{-}NCN\text{-}SiMe_3$ in tetrahydrofuran (THF) or toluene, or without any solvent, to form nonoxide gels. The $BCN_2H_2$-xerogels, obtained after aging and drying, are practically free of any chlorine or oxygen and contain only small amounts of silicon. At 1,200 °C a novel amorphous $B_4CN_4$ phase is formed, which is stable up to 1,600 °C where it starts to crystallize. This novel nitrogen-rich $B_4CN_4$ phase may be a promising amorphous precursor for high-pressure synthesis of crystalline BCN phases.

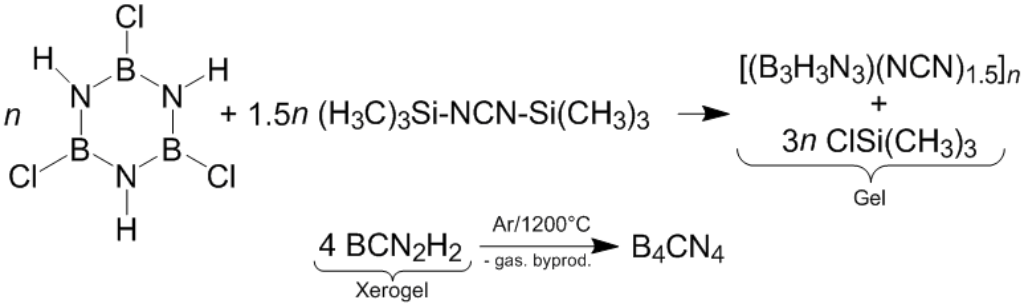


A series of graphitic B-C-N compounds (g-$BC_xN$) were prepared in good yield by pyrolysis of the polymers between $BCl_3$ and commercially available nitriles at 1,773 K.[82] Acrylonitrile, malononitrile, acetonitrile, tetracyanoethylene (TCNE), and polyacrylonitrile were used as the C-N sources while $BCl_3$ was used as the B-source. The g-$BC_xN$ samples were prepared in 3 steps: 1) adduct formation at ambient temperature, followed by dehydrochlorination /polymerization at temperatures up to 773 K; 2) carbonization of the polymeric materials at 1273 K; and 3) graphitization at 1,773 K. The products were characterized by combustion elemental analysis, XPS, Fourier-transform infrared (FTIR) spectroscopy, and XRD. The obtained powders of g-$BC_xN$ ($2 \leq x \leq 5$) were subsequently used for the shock synthesis of B-C-N heterodiamonds, c-$BC_xN$.[82]

Tian et al.[83] synthesized the B-C-N precursor by mixing boric acid $H_3BO_3$ with melamine $C_3N_6H_6$ (1:2 ratios) in an agate mortar. The mixture was heated to

200 °C for 1 h and then at 300 °C for an additional 2 h. After cooling, the pulverized powder was exposed to 1,600 °C in nitrogen atmosphere for 15 min. Li et al.,[84] in a similar approach, tried the mixture of boron oxide and melamine, subjecting it to 770 °C in vacuum for 2 h leading to B-C-N precursor. However, by knowing boric acid coverts into boron oxide at 300 °C, both reactions look the same, even though the starting material is different. Amorphous BCN was prepared by a solid-state reaction between boric acid and melamine via heat treatment at 1,273 K under $10^{-3}$ Pa.[85] For the $H_3BO_3$ to $C_3N_6H_6$ mass ratio of 1:3, the obtained B-C-N material revealed the chemical composition of $B_{0.48}C_{0.29}N_{0.23}$. Annealed for 40 min at 1,473 K under 4.0 GPa, the amorphous BCN crystallized into a single-phase hexagonal (h-BCN) compound with lattice constants of $a_0 = 0.2506$ nm and $c_0 = 0.6652$ nm.

Hubacek and Sato et al.[18] prepared a B-C-N precursor by simultaneous nitridation of boric acid and carbonization of saccharose in molten urea followed by annealing in nitrogen at 1,500 °C. The results showed graphite-like $BC_2N$ and $BC_4N$, depending on the saccharose content, having broad XRD lines like turbostratic layered structures. This precursor preparation method was later used by Solozhenko et al.[7] in the synthesis of the superhard c-$BC_2N$ phase. The reaction of low-surface-area amorphous carbon spheres with a mixture of urea and boric acid at 930 °C yields a composition close to $BC_4N$ with a graphitic structure.[86] The obtained product was characterized by electron energy loss spectroscopy (EELS), XPS, TEM, Raman spectroscopy, and XRD, revealing a porous ceramic material composed of BCN spheres (Fig. 2.5) with a layered structure involving random distribution of boron, carbon, and nitrogen atoms. In turn, the reaction of amorphous carbon nanotubes with boric acid and urea was shown to yield nanotubes with the approximate composition of $BC_4N$.[87]

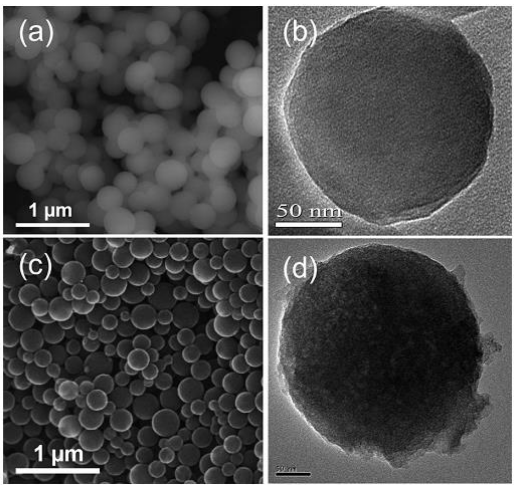


**Fig. 2.5 High-temperature reaction of amorphous carbon spheres. a) SEM and b) TEM image, with boric acid and urea yields spheres with graphitic structure and composition of $BC_4N$, c) SEM and d) TEM image.[86]**

A solvothermal reaction of $CH_3CN{\cdot}BCl_3$ and lithium nitride ($Li_3N$) using benzene as the solvent has been successfully applied to prepare boron carbonitride at 300 °C and less than about 7 MPa.[88] XRD and TEM investigation of the obtained powder revealed hexagonal ordering. The product predominately consisted of B, C, and N elements (B: 14.4%, C: 36.6%, N: 20.8%) with some amount of O and H (O: 8.0%, H: 4.2%) determined by combustion elemental analysis. XPS and FTIR spectroscopy confirmed the chemical composition and atomic-level hybrid. A hexagonal graphite-like BCN compound was also prepared by a reaction between carbon tetrachloride ($CCl_4$), boron tribromide ($BBr_3$), $Li_3N$, and sodium at 400 °C.[89] Measurements of FTIR, XRD, TEM, and EELS show that 2 kinds of compounds have been formed: hexagonal polycrystalline $BC_2N$ phase was found to coexist with hollow sphere-like amorphous C–N phase with composition close to $C_3N$.

Another approach to the low-density ternary B-C-N compounds implies mechanical mixing and alloying. In this method boron-, carbon-, and nitrogen-containing materials are mixed together to form a B-C-N complex in the easiest possible way—for example, boron nitride powder with carbon/graphite powder or boron powder with carbon nitride powder. Homogenous samples with well-distributed B, C, and N are obtained via prolonged (high-energy) ball milling. Knittle et al.[5] were the first to try mechanical mixtures of graphitic-boron nitride (h-BN) and graphite (g-C) in different compositions. The mixtures were ground together under acetone to get uniformity. The authors compared the results with that of chemically prepared BCN microcrystalline powders, and the performed high-pressure high-temperature experiments provided solid solutions of c-BN and diamond. Zhao et al.[9] tried a very similar approach to get $BC_2N$ and $BC_4N$ mixtures. Precursor materials were prepared by stoichiometric 2:1 and 4:1 molar ratio mixture of graphite and hexagonal boron nitride (h-BN) to get $BC_2N$ and $BC_4N$, respectively. The mixture was ball-milled for 34 h in a tungsten carbide vial to get good homogeneity. The idea was to break $sp^2$ bonding among hexagonal rings of graphite and h-BN crystal structure and to get amorphous BCN fine powder.[9] Huang et al.[90] applied a similar approach to synthesize the amorphous B-C-N (a-$BC_2N$) phase. EELS and TEM studies indicated the $sp^2$-hybridized bonding of the a-$BC_2N$; the mixing between the BN and the C species was achieved at a nanometer scale, thus a mechanical mixture rather than a chemical mixture is obtained. Filonenko et al.[91] used a starting material as mixtures of boron (B) (35%–50%) and carbon nitride powders. Commercially available boron ranging from 1 to 10 μm mainly consisting of β-phase was mechanically mixed with graphitic carbon nitride ($C_3N_4$) nanospheres. The authors reported that boron content in the mixture was varied from 20% to 80%, low B (<35%) leading to the decomposition of $C_3N_4$ and higher B (>50%) content leading to the synthesis of boron carbides at HP-HT conditions; however, the reaction mechanism is still unclear.

The techniques employed to synthesize low-density B-C-N phases—such as high-temperature nitriding, solid phase pyrolysis, chemical and physical vapor deposition, and ball milling—generally result in the poorly crystallized, turbostratic, or amorphous products. Well-crystallized B-C-N compounds having hexagonal structure (h-BCN) were successfully obtained by applying high pressures and high temperatures. Thus, amorphous B-C-N precursors were transformed into h-BCN using a belt-type apparatus[79] and Bridgman anvils[85] at pressures of 3–5 GPa and temperatures of 1,000–1,500 °C. Yamada[92] produced a graphite-like phase by shock synthesis of a mechanical mixture of graphite and h-BN. The hexagonal lattice parameters of $a_0$ = 0.2475 nm and $c_0$ = 0.676 nm were determined by TEM from a cluster of sheet-like particles, which composition corresponded to $BC_2N$. EELS confirmed the presence of boron, carbon, and nitrogen—all $sp^2$-hybridized—in a single graphite-like crystal. A highly crystalline hexagonal $BC_2N$ compound was prepared by the compression of a turbostratic B-C-N precursor (synthesized via high-temperature reaction of melamine and boric acid) with iron catalyst at the high temperature of 1,500 °C and the high pressure of 5.5 GPa.[93] Yang et al.[94] obtained h-BCN from a mixture of boron powder and a CNH compound prepared by pyrolysis of melamine ($C_3H_6N_6$) under high temperature (1,400–1,500 °C) and high pressure (5.0–5.5 GPa). XPS, FTIR, and Raman spectroscopy showed the presence of B-N, C-B-N, C-N, and B-C bonds in the product with the overall composition of $B_{0.18}C_{0.64}N_{0.16}$ (near $BC_4N$). X-ray diffraction analysis confirmed a hexagonal structure. Scanning and transmission electron microscopy revealed the flaky h-$BC_4N$ particles of about 1 μm with a thickness of 200 nm.

### 2.1.3 HP-HT Experiments and Results

The conditions normally employed to synthesize superhard materials require extreme pressures and temperatures or a chemical vapor deposition technique (the latter, however, does not provide bulk superhard materials). Badzian[4] prepared cubic BN-C mixed crystals by the HP-HT technique (14 GPa, 3,600 °C, Bridgman apparatus), using as the starting material hexagonal BN-C prepared from CVD. He believed that the material had a diamond-like structure and found that the material exhibited weak (200) and (420) reflections in the XRD pattern, suggesting the possibility of B-N pairs in the sublattices. Sasaki et al.[95] attempted the transformation of graphitic $BC_2N$[62] into a cubic phase under relatively mild HP-HT conditions (5.5 GPa, 1,400–1,600 °C, Belt Press) using a Co catalyst, but they obtained the phase-separated mixture of cubic phases (i.e., the well-crystallized diamond and c-BN crystals up to 3 μm in size). Expecting the catalytic promotion of the phase separation in the B-C-N system, Nakano et al.[96] attempted the direct transformation of g-$BC_2N$ into the cubic phase, without additives under higher HP-HT conditions (7.7 GPa, 2,000–2,400 °C, Belt Press). Several cubic phases with a diamond-like structure—namely, c-BN, diamond containing minor amount of B and N, and a cubic B-C-N

substance—were confirmed in the products above 2,150 °C by the powder XRD patterns. At 2,400 °C, however, the cubic B-C-N product tended to segregate into c-BN and diamond. Authors concluded that not a c-$BC_2N$ but a mixture of c-BN and diamond is thermodynamically stable in the B-C-N system under the conditions employed.[96] A similar result was reported recently by Huang et al.[90], where the HP-HT treatment at 7.7 GPa and 2,300 °C of the amorphous a-$BC_2N$ phase resulted in the complete segregation of the carbon and BN species—namely, c-BN, amorphous carbon, and turbostratic graphite. No mutual solubilities between c-BN and carbon were found at these P-T conditions.

Knittle et al.[5] prepared a cubic $C_x(BN)_{(1-x)}$ (x = 0.3–0.6) solid solution under high pressures (30–50 GPa) and high temperatures (2,000–2,500 K) from mechanical mixtures of graphitic-boron nitride and graphite using a laser-heated diamond anvil cell (LH-DAC). Measurements of the lattice parameters of samples quenched to ambient pressure showed that the solid solution series was nonideal, with molar volumes up to 1% larger than expected (Vegard's law) based on ideal mixing between C (diamond) and cubic-BN. The bulk modulus of $C_{0.3}(BN)_{0.7}$ was found to be 355±19 GPa, which was lower than the ideal solid solution of diamond and cubic BN but consistent with the expanded unit-cell volumes. The ionic bonding nature in these solid solutions was confirmed by Raman spectra of $C_{0.3}(BN)_{0.7}$, which exhibited LO-TO splitting of the phonon modes.

Komatsu et al.[6,10,82,97] converted the graphitic $BC_{2.5}N$ (g-$BC_{2.5}N$) obtained by CVD technique to heterodiamond c-$BC_{2.5}N$ using a cylindrical shock compression technique. The shock pressure and temperature on the sample were estimated to be 35–50 GPa and 3,000–10,000 °C, respectively. They also studied bulk synthesis from different starting materials, g-$BC_xN$ ($2 \leq x \leq 5$) obtained by both CVD or solid phase pyrolysis, using the shock compression method and explored properties like thermal oxidation resistance, thermal expansion coefficient, and bulk modulus of the high-pressure products[10,82]. Heterodiamond c-$BC_{2.5}N$ crystals (5–20 nm in size) showed polycrystalline behavior. The lattice constant was measured to be 3.605 Å—a value that was between those of diamond (3.5667 Å) and cubic BN (3.6158 Å). The material revealed a thermal oxidation resistance (stable up to 700 °C) higher than that of diamond, a low thermal expansion coefficient (~$10^{-6}$ $K^{-1}$), and a bulk modulus (401 GPa) higher than that of cubic BN.

Solozhenko et al.[7] prepared cubic $BC_2N$ from graphitic $BC_2N$ synthesized according to the method of Hubacek and Sato[18] using the HP-HT conditions (18–25 GPa /2,000–2,200 °C in a LH-DAC and multianvil press [MAP]). The lattice parameter of the c-$BC_2N$ determined at ambient conditions was 3.642±0.002 Å, much larger than those of diamond and c-BN (Fig. 2.6). For the large volume sample, the hardness ($H_v$) was measured to be 76 GPa, which is higher than that of c-BN. Surprisingly, the determined bulk modulus of the c-

$BC_2N$ was 282 GPa, which is significantly lower than the values for c-BN or c-$BC_2N$ reported by other authors.[5,10] Zhao et al.[9] pointed out a possible reaction of the sample with MgO capsule material in that work as well as a large deviation of the lattice constant of c-$BC_2N$ from Vegard's law. Solozhenko and coworkers came up with a detailed characterization of the synthesized c-$BC_2N$ sample.[51,98,99] Raman spectroscopy studies showed the Raman band 1326 $cm^{-1}$ attributed to the LO mode of c-$BC_2N$, whereas the TO mode was missing.[98] Atomic force microscopy images revealed the c-$BC_2N$ grains of 200 nm in size in contrast to initially reported 10–30 nm from TEM images.[99] The authors also reported a Knoop hardness ($H_K$) of 55 GPa, Young's modulus (E) of 980 GPa, sheer modulus (G) of 447 GPa, and fracture toughness ($K_{Ic}$) of 4.5 $MPa \cdot m^{1/2}$ for their c-$BC_2N$ and proclaim it the hardest-known solid after diamond.[51] Subsequent Brillouin scattering measurements on the same cubic $BC_2N$ phase provided even lower bulk modulus and shear modulus values of 259 and 238 GPa, respectively.[100] The authors relate these results to the dependence of elastic properties of diamond-like B-C-N phases on the structure of the phase and on the synthesis condition for that specific sample. Nevertheless, the B, E, and G values of c-$BC_2N$ reported by Solozhenko and coworkers significantly deviate from the elastic moduli relationship for homogeneous isotropic materials. Theoretical attempts to explain lower bulk modulus, large lattice constant, and missing TO modes in Raman spectra of the synthesized c-$BC_2N$ and to correlate these issues with possible B-C-N structure[33,38,39] could not give an unambiguous answer so far.

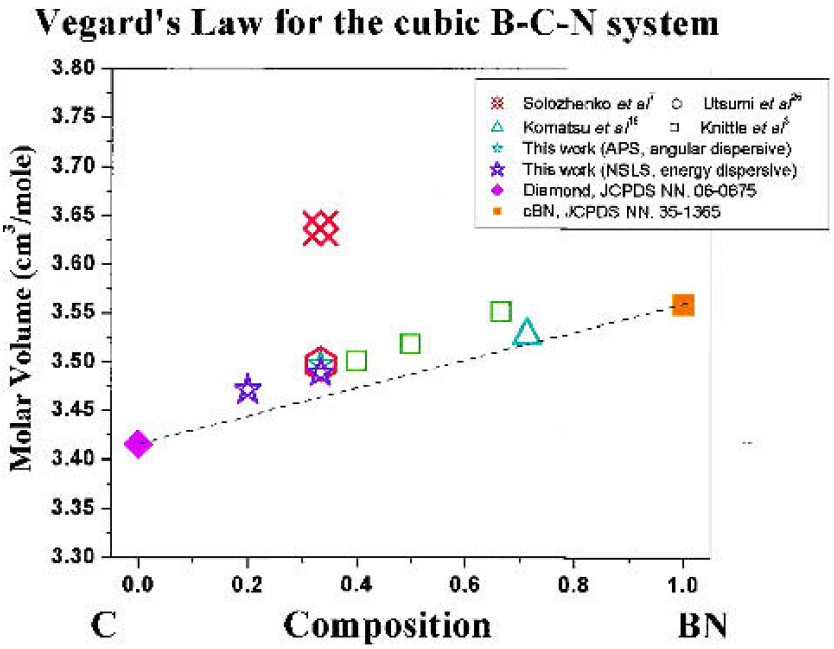


**Fig. 2.6 Plot of all observed unit-cell volumes in the B–C–N system of cubic zinc-blende structure.[9] The relationship of unit-cell volume vs. chemical composition shows a clear trend closely obeying Vegard's law for ideal solid solutions, except for data of Solozhenko et al.[7]**

Zhao et al.[9] synthesized a superhard phase of $BC_2N$ and $BC_4N$ in nanostructured bulks under HP-HT conditions (20 GPa, 2000 °C, MAP) from a mixture of the graphite and h-BN powders in 2:1 and 4:1 molar ratio, respectively. The mixture was ball-milled in a tungsten carbide vial for 34 h, which allowed them to obtain homogeneous starting materials with randomly bonded B, C, and N atoms. The authors expected to break the $sp^2$ bonding among the hexagonal rings of the graphite and h-BN crystal structures and to introduce some initial amount of hybrid $sp^3$ bonding. XRD, SEM, and Raman spectroscopy studies of the ball-milled mixture showed that the $BC_2N$ and $BC_4N$ starting material was completely amorphized with a median particle size of about 2–3 nm. Comparative studies of synchrotron XRD, HR-TEM, EELS, and Vegard's law of the unit-cell volume versus chemical compositions all indicated that the high-pressure $BC_2N$ and $BC_4N$ products were single B-C-N ternary phases with crystallites of about 5 nm in size. Assuming a face-centered cubic zinc-blende structure, the authors derived a unit-cell parameter of $a_0 = 3.595(7)$ Å and $a_0 = 3.586(9)$ Å for the synthesized $BC_2N$ and $BC_4N$ material, respectively. The hardness measurements showed the nominal hardness of 62 GPa for c-$BC_2N$ and 68 GPa for c-$BC_4N$, which is between the hardness values of diamond and cubic boron nitride. A plot of unit-cell parameters as a function of chemical composition showed good agreement with Vegard's law (Fig. 2.6), with the exception of Solozhenko et al.'s data,[7] which deviate significantly from the line. The authors suggested that the composition of Solozhenko et al.'s sample was not the solid solution of $BC_2N$ and clearly had a different chemistry.[9] Taking into account the XRD and Raman spectroscopy measurements of Solozhenko et al.[7] and Zhao et al.,[9] theoreticians suggested 2 tetragonal (z*-$BC_2N$ and t-$BC_2N$)[39] and one rhombohedral (rh-$BC_2N$)[42] as the most likely structures describing experimentally obtained c-$BC_2N$. In turn, the 3C-$BC_4N$ structure with trigonal symmetry[43] was found to give the best agreement with the experimental XRD pattern of c-$BC_4N$.[9]

Quite unusual boron-rich B-C-N stoichiometry, "$B(C_xN_{1-x})$", was chosen by Guo et al.[101] for their HP-HT experiments. A $B_2CN$ precursor was prepared by mechanical vibration-milling process from amorphous boron, graphite, and h-BN powders with a mole ratio of 1:1:1 and mixed with $Ca_3B_2N_4$ catalyst. The authors claimed that a boron-rich cubic phase is formed at 5.5 GPa and 1500 °C. The carbon content (detected by energy-dispersive X-ray [EDX] spectroscopy) was found to vary from 0 to 16 at% depending on the investigated crystal. The average composition is reported to be $B_{0.58}C_{0.16}N_{0.26}$. Despite the evident oxygen peak in the EDX spectra, the authors gave no comment on the oxygen presence in the product.[101] Moreover, the cubic lattice parameter of $a_0 = 3.618$ Å of the claimed BCN phase is similar to that of c-BN.

Nicolich et al.[102] attempted to form cubic ternary crystals from turbostratic BCN starting materials[77] at HP-HT conditions (3–5 GPa, 1,200–1,500 °C, belt-type

apparatus) obtained ternary graphitic crystals. In earlier attempts, Solozhenko et al.[103] tried to compress g-$BC_4N$ up to 7 GPa at 1900 °C in a multianvil press (MAP); they succeeded only to densify the starting material. Tian et al.[83], Li et al.[84], and Da-Peng et al.[94] studied the HP-HT behavior (5–6 GPa, 1,400–1,700 °C, MAP) of BCN precursor prepared by reaction of melamine and boric acid derivatives (method is explained in Section 2.1.2). This reaction lead to the formation of hexagonal-BCN (h-BCN). The lattice constants $a_0$ = 2.506 Å and $c_0$ = 6.657 Å, [83] and $a_0$ = 2.510 Å and $c_0$ = 6.690 Å,[84] were reported. A completely new $BC_{3.3}N$ crystalline compound with a low-density orthorhombic structure has been synthesized using an amorphous B-C-N precursor at 6 GPa and 1,773 K.[104] Results of energy-dispersive spectroscopy and EELS showed that the compound has a 1.04:3.27:1 B:C:N chemical stoichiometry. The lattice parameters of $BC_{3.3}N$ crystal were obtained to be $a_0$ = 6.610 Å, $b_0$= 4.977 Å, and $c_0$ = 8.509 Å by XRD and select area electron diffraction (SAED). On the basis of XRD refinement and EELS results, one possible $BC_{3.3}N$ ($B_3C_{10}N_3$) model with a space group *Pmma* (No. 51) is proposed.

Li et al.[105] studied high-pressure phase transition of h-BCN[83] having the composition of $B_{0.47}C_{0.23}N_{0.30}$ up to 30 GPa in a DAC. Transformation from h-BCN to the wurtzite BCN (w-BCN) structure was observed for pressures above 15 GPa, and a bulk modulus of 275 GPa was derived from the equation of state of the w-BCN. The bulk modulus value is very close to that earlier reported by Solozhenko et al. for c-$BC_2N$ and is significantly smaller than those of c-BN and w-BN. The authors, however, neither verify the composition of the new high-pressure phase nor provide the data about its stability at ambient pressure.

Filonenko et al.[91] reported high-pressure synthesis of the heterodiamond phase using the powder mixtures of graphite-like carbon nitride g-$C_3N_4$ and crystalline boron (35–50 wt%) as the starting material. A "toroid"-type apparatus was employed to apply high pressure (6–15 GPa) and high temperature (1,000–1,600 °C). Treatment at pressures above 8 GPa and temperatures in the range of 1,450–1,600 °C resulted in the formation of a cubic phase with the unit cell parameter $a_0$ = 3.6551 Å. It is noteworthy that the employed HP-HT conditions are very mild when compared to the other reports of the diamond-like B-C-N syntheses. The highest yield of the cubic BCN phase has been obtained from mixtures with approximately 50 wt% of boron. EDX analysis of the synthesized c-BCN crystals revealed an average atomic composition of 45.3% B, 36.5% N, 11.6% C (roughly ~$B_4CN_4$), and a considerable amount of oxygen (6.6 at%). On the basis of the Rietveld structure refinement of the c-BCN, the authors propose that carbon atoms partially replace boron and nitrogen in their positions in the structure of c-BN, while oxygen takes only nitrogen positions.[91] This statement, however, requires further experimental verification. Moreover, the reported unit cell parameter of 3.6551 Å exceeds that of c-BN, thus ruling out the possibility of matching with Vegard's law for diamond/c-BN alloys. A

detailed characterization of the synthesized c-BCN phase with respect to the chemical bonding and properties, as well as an unambiguous conclusion on the oxygen presence, are awaited.

Recently, a single-phase cubic $BC_4N$ was claimed to be formed at high pressure and temperature (18–20 GPa, 2,000–2,200 K, MAP) starting with either a mixture of diamond and c-BN or graphite and h-BN.[106] The authors reported extreme Vickers hardness (85 ± 4 GPa) of the HP products, reaching the hardness of single crystal diamond. Based on the measured and calculated XRD patterns, the authors concluded that the synthesized products are solid solutions of diamond and c-BN with a zinc-blende structure (*F*-43*m*) when starting from a mixture of C and BN but could be solid solutions based on the diamond-like structure (*Fd*-3*m*) if the starting materials are graphitic B-C-N compounds.[106] It should be, however, emphasized that presented XRD data alone do not provide unambiguous evidence of the presence of a single B-C-N phase. In particular, the formation of c-BN/diamond nanocomposites cannot be excluded.

Very intriguing results were reported lately by Liu et al.,[107] who succeeded in preparing diamond crystals doped with B and N atoms, starting from graphitic mixtures of C and BN with compositions of $C_{1-x}(BN)_x$, where x = 0.02, 0.1, or 0.5. The BN-doped diamond crystals were grown in a large volume cubic MAP using iron-nickel alloy as catalysts at pressures of 5.0–7.2 GPa and temperatures of 1,500–2,300 K. Variation in morphology and color of the obtained crystals (Fig. 2.7) were attributed to the different amounts of B and N atoms incorporated into the crystal structure. XRD, XPS, Raman-, and FT-IR spectroscopy were used to verify the structure, chemical composition, and bonding of the crystals—in particular, the presence of all 3 elements as well as of the C-C, B-N, B-C, and C-N bonds. The authors have noted that the $C_{0.9}(BN)_{0.1}$ tends to separate into several cubic phases having different B/N ratios, while in the $C_{0.5}(BN)_{0.5}$ system, no phase separation was found and the obtained single-phase "BCN"-diamond exhibited cuboctahedral shape, light yellow in color, and nearly transparent.[107] The derived cubic lattice parameter of the "BCN"-diamond of 3.575 Å is in a good agreement with Vegard's law for a diamond/c-BN alloy. The exact chemical composition of the BN-doped diamond crystal phases was not, however, determined.

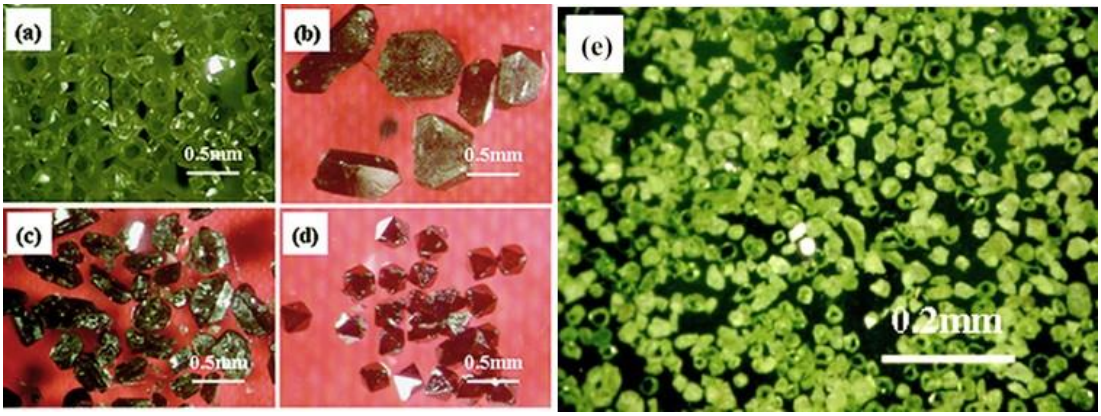


**Fig. 2.7 Optical images of diamond crystals obtained at HP-HT using Fe-Ni alloy as a catalyst starting from graphite a) or mixtures of graphite and h-BN with stoichiometries of b) C0.98(BN)0.02; c) C0.9(BN)0.1; d) C0.9(BN)0.1 with 1 wt% Al additive; and e) C0.5(BN)0.5.[107]**

## 2.2 C-N Compounds

For nearly 20 years, intense interest in the synthesis of new C-N materials has been generated by the prediction of unusual properties of saturated, i.e., carbon $sp^3$-hybridized, crystalline $C_3N_4$-phases.[108] The basis of this prediction was provided by a semi-empirical model developed by Cohen.[109] The effective correlation between bulk modulus ($B_V$) and bond length ($d$) was found to be $B_V = 1{,}972/d^{3.5}$. A typical bond length of 1.47 Å for a C–N single bond was derived from organic nitrogen-containing molecules, while the C–C distance in diamond is 1.54 Å. This means that the bulk moduli of dense $C_3N_4$ phases could probably be higher than those of diamond. Moreover, based on the controversial opinion that hardness of material is primarily determined by its bulk modulus,[109,110] the authors suggested that this hypothetical carbon nitride can surpass diamond in hardness. Such a daring statement excited the scientific community and, as a result, many theoretical investigations and experimental efforts to synthesize postulated carbon nitrides were made during the last 2 decades and continues up till now.

### 2.2.1 Postulated Carbon Nitrides

Several hypothetical carbon nitrides have been proposed and analyzed in literature: α-$C_3N_4$,[111] β-$C_3N_4$,[108] "defect zincblende" *dzb*-$C_3N_4$,[112] "pseudocubic" pc-$C_3N_4$ and "willemite-II" *wmII*-$C_3N_4$,[113] spinel γ-$C_3N_4$,[114] and λ-$C_3N_4$.[115] Their structural data together with calculated bulk moduli and hardness from different theoretical works are summarized in Table 2.2.

**Table 2.2 Predicted $C_3N_4$ phases and their calculated structural parameters, bulk moduli, and hardness**

| Modification | Space Group | a (Å) | c (Å) | α (°) | Density (g/cm$^3$) | $B_0$ (GPa) | Hardness (GPa) | Ref. |
|---|---|---|---|---|---|---|---|---|
| α-$C_3N_4$ | $P3_1c$ (159) | 6.35 | 4.46 | … | 3.78 | 189 | | [111] |
| | | 6.47 | 4.71 | … | 3.58 | 425 | | [113] |
| | | 6.45 | 4.70 | … | 3.61 | n.d. | | [116] |
| | | 6.47 | 4.71 | … | 3.58 | 379 | 82.7 | [117] |
| | | 6.45 | 4.70 | … | 3.61 | 367–449 | 84.2 | [118] |
| β-$C_3N_4$ | *P3* (143) | 6.35 | 2.46 | … | 3.56 | 250 | | [111] |
| | | 6.40 | 2.40 | … | 3.58 | 451 | | [113] |
| | | 6.40 | 2.41 | … | 3.58 | 419 | 85.7 | [117] |
| | $P6_3/m$ (176) | 6.39 | 2.40 | … | 3.60 | n.d. | | 116] |
| | | 6.44 | 2.47 | … | 3.58 | 427 | | [108] |
| | | 6.41 | 2.40 | … | 3.60 | 437 | | [112] |
| | | 6.38 | 2.39 | … | 3.63 | 409–448 | 84.5 | [118] |
| *dzb*-$C_3N_4$ | P-43m (215) | 3.43 | … | … | 3.79 | 425 | | [112] |
| | | 3.43 | … | … | 3.79 | 386–448 | 88.7 | [118] |
| *pc*-$C_3N_4$ | P-42m (111) | 3.42 | 3.42 | … | 3.81 | 448 | | [113] |
| | | 3.43 | 3.43 | … | 3.78 | 393 | 79.6 | [117] |
| *wmII*-$C_3N_4$ | I-43d (220) | 5.40 | … | … | 3.89 | 496 | | [113] |
| | | 5.44 | … | … | 3.79 | n.d. | | [119] |
| | | 5.41 | … | … | 3.86 | 449 | 92.0 | [117] |
| | | 5.39 | … | … | 3.91 | 441–485 | 90.7 | [118] |
| γ-$C_3N_4$ | Fd-3m (227) | 6.87 | … | … | 3.77 | 369 | | [114] |
| | | 6.78 | … | … | 3.92 | n.d. | | [119] |
| | | 6.71 | … | … | 4.04 | 379 | 62.3 | [117] |
| | | 6.81 | … | … | 3.87 | 376–432 | 59.4 | [118] |
| λ-$C_3N_4$ | $P4_322$ (95) | n.d. | … | … | 3.0 | n.d. | | [115] |
| g-$C_3N_4$ | P-6m2 (187) | 4.74 | 6.72 | … | 2.33 | n.d. | | [113] |
| | | 4.37 | 6.69 | … | 2.35 | n.d. | | [116] |
| rh-$C_3N_4$ | *R3m* (160) | 4.11 | … | 70.5 | 2.56 | 51 | | [112] |

The β-$C_3N_4$ polymorph is based on the β-$Si_3N_4$ structure, with C substituted for Si. This structure consists of 4-fold coordinated (sp$^3$-hybridized) carbons linked by 3-fold coordinated N-atoms into a network of corner-linked $CN_4$ tetrahedra (Fig. 2.8a). The hexagonal unit cell contains 14 atoms (2 $C_3N_4$ formula units) and has $P6_3/m$ or closely related $P3$ symmetry. In the former symmetry, all $NC_3$ polyhedra are considered to be planar in geometry, thus implying formal sp$^2$-hybridization of N-atoms similar to that observed for β-$Si_3N_4$.[108,112] Other authors considered only the half $NC_3$ units to be planar while the other half to have pyramidal geometry (sp$^3$ hybridized nitrogen), which resulted in the change of the symmetry to $P3$.[111,113]

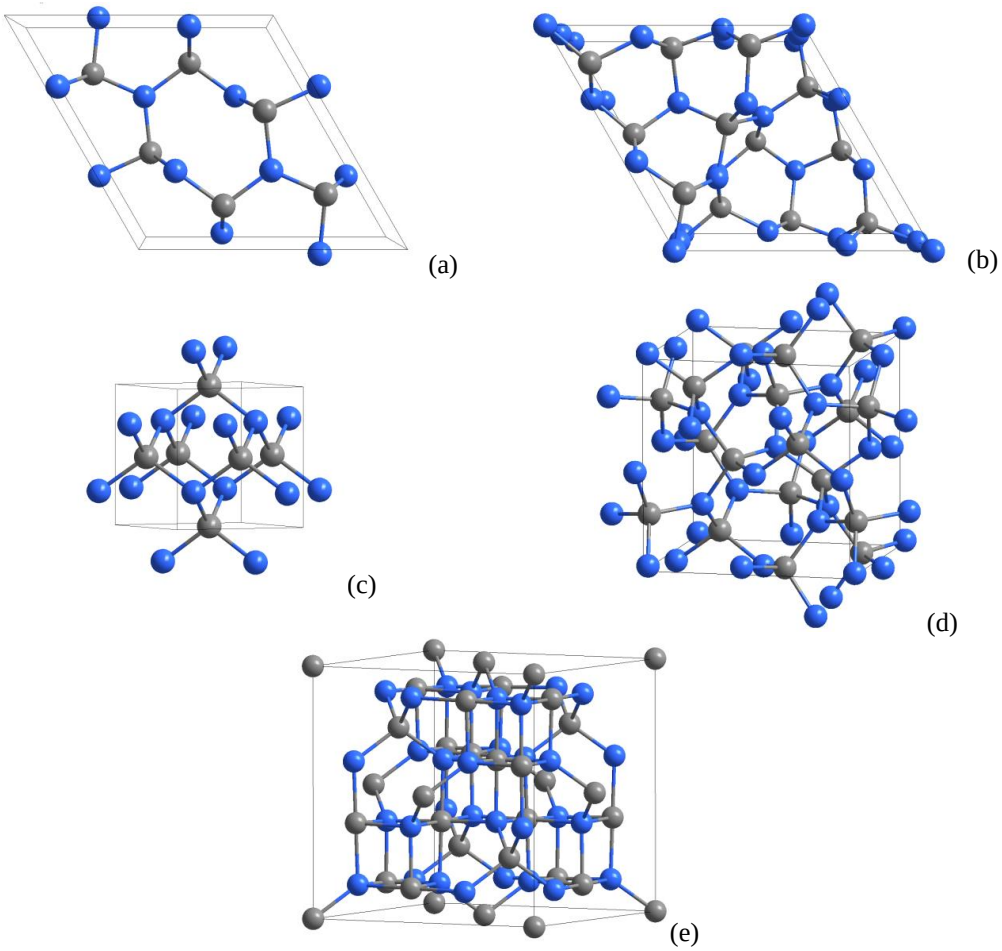


**Fig. 2.8 Theoretically predicted dense carbon(IV) nitride polymorphs that have been proposed in literature and which were examined theoretically: a) β-$C_3N_4$ (*P*6$_3$/*m*), b) α-$C_3N_4$ (*P*3$_1$*c*); c) "pseudo-cubic" or "defect zinc blende" $C_3N_4$ (*P*-43*m*); d) "cubic" or "willemite-II" $C_3N_4$ (*I*-43*d*); e) spinel-type γ-$C_3N_4$ (*Fd*-3*m*). The carbon and nitrogen atoms are represented as gray and blue spheres, respectively.**

Following the prediction of the β-phase, the α-$C_3N_4$ structure was similarly deduced from α-$Si_3N_4$. It can be described as an ABAB stacking sequence of layers of β-$C_3N_4$ (a) and its mirror image (b) (Fig. 2.8b). The hexagonal unit cell has *P*3$_1$*c* symmetry and contains 4 $C_3N_4$ formula units. According to theoretical calculation, $NC_3$ polyhedra are exclusively pyramidal in geometry, thus indicating $sp^3$-hybridization of nitrogen.[111,113] The issues of nitrogen hybridization and structural uncertainties in the predicted α- and β-$C_3N_4$ are critically reviewed by Malkow.[120]

Pseudocubic $C_3N_4$ polymorph represents a defect zinc blende structure (isostructural to α-$CdIn_2Se_4$). It can be constructed from a c-BN structure by substituting 4 B-atoms of the unit cell by 3 C-atoms and one vacancy. The structure exhibits either *P*-43*m* or *P*-42*m* symmetry with 7 atoms (one formula unit) in the unit cell. The network consists of corners-linked $CN_4$ tetrahedra (Fig. 2.8c) in such a way that the C-N-C angle is close to 109°, which suggests $sp^3$ hybridization for nitrogen.

The cubic "*wmII*"- type structure is derived from a high-pressure phase of a zinc silicate ($Zn_2SiO_4$) willemite-II, via replacing the cations (Zn and Si) by C and the anions (O) by N (Fig. 2.8d). The initially tetragonal structure was found to relax toward the more symmetrical cubic one having *I*-43*d* symmetry. For this structure the extremely high bulk moduli (~450–500 GPa), exceeding the experimental one of diamond (442 GPa), and high density 3.8–3.9 g/cm$^3$ were reported. However, both pseudocubic and cubic $C_3N_4$ phases were found to be less thermodynamically stable than the previously described α and β polymorphs.

Finally, the discovery of the high-pressure cubic spinel silicon nitride (γ-$Si_3N_4$)[121] suggested the existence of isostructural γ-$C_3N_4$.[114,119] The structure (space group *Fd*-3*m*) comprises C-atoms in 2 different environments: 8 tetrahedrally and 16 octahedrally coordinated carbons per unit cell (Fig. 2.8e). Despite the evident existence of 6 coordinated carbons in transition metal complex cations, octahedral carbon sites in γ-$C_3N_4$ are considered to be very unlikely in terms of hybridization. Nevertheless, this structural form is expected to be attainable under ultra-high-pressure conditions.[119]

By simulating the compression of polymeric carbon nitride precursors—in particular, carbon dicarbodiimide $C(NCN)_2$—Kroll and Hoffmann have found transformation to a completely novel and unusual solid structure having $C_3N_4$ stoichiometry.[115] The hypothetical λ-$C_3N_4$ consists of tetrahedrally coordinated carbon with nitrogen polyhedra both in planar ($sp^2$) and pyramidal ($sp^3$) geometry. However, the λ-phase also contains C-C and N-N bonds, which, in the sense of oxidation state formalism, does not allow to refer λ-$C_3N_4$ to carbon(IV) nitrides.

Despite most predicted carbon nitrides that exhibit the $C_3N_4$-stoichiometry, first synthesis attempts, mainly devoted to deposition of thin films, have indicated the difficulty to obtain a C:N ratio of 3:4. With this in view, Cote and Cohen have examined 8 new structural models for carbon nitrides with 1:1 stoichiometry by means of ab initio calculations.[122] They have considered cubic rock salt and zinc-blende types, rhombohedral (buckled carbon nitride sheets with interplanar covalent bonds), orthorhombic β-InS type, tetragonal GeP-type, and 3 hexagonal structures being 3-D networks of pure $sp^2$-bonded solids "bct-4", "H-6", and GaSe-type. The authors reported that for this stoichiometry, $sp^2$ bonding of nitrogen is energetically preferable to $sp^3$. The cubic phases were found to be mechanically unstable and relaxed to a rhombohedral phase with a bulk modulus of 253 GPa. The bulk moduli of 345 and 375 GPa were calculated for hexagonal H-6 and bct-4 phases, respectively. Finally, the GaSe structure, made of layers where the C-C bond is perpendicular to the plane of the layers, was found to be the most energetically favorable of all phases considered, and it has a bulk modulus of 199 GPa. Kim et al.[123] investigated cubic CN phases (rocksalt, BCC, and zinc-blende) using DFT and found that they relax to their

tetragonal counterparts (e.g., zinc-blende to β-tin type). A body-centered tetragonal CN phase with 1:1 stoichiometry is predicted to be highly stable; it has a bulk modulus of 243 GPa and an interesting atomic structure, with complicated C-C and N-N dimerization along the c axis. Another wave in the theoretical exploration C:N = 1:1 was initiated by the discovery of "polymeric" nitrogen having a cubic gauche-type structure, cg-N (Fig. 2.9a).[124] Replacing half of the nitrogen atoms in the cg-N by carbon, Wang et al.[125] suggested that a novel carbon nitride phase consisted of $sp^3$ hybridized bonds and possessed a cubic $P2_13$ symmetry with 8 atoms/cell, cg-CN (Fig. 2.9b). The bulk modulus and hardness of the cubic gauche CN were calculated to be 335–348 GPa and 54 GPa, respectively. A further search of hypothetical CN phases by means of ab initio total-energy calculations has indicated the potential existence of 7 other low-energy polymorphic structures of $sp^3$-hybridized CN.[126] Among them, the *Pnnm* structure with 8 atoms per unit cell was found to be energetically more favorable than all previously reported crystalline structures with 1:1 stoichiometry. Furthermore, it has the theoretical hardness of 62 GPa.[126]

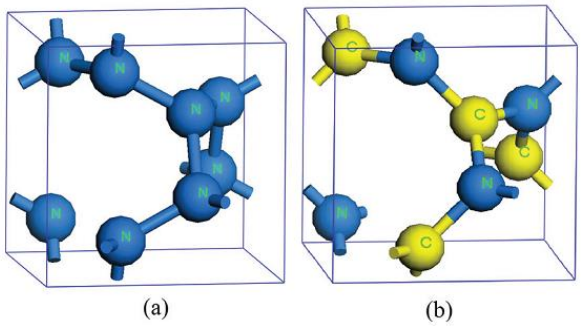


**Fig. 2.9 Unit cells of the simple cubic gauche cg-N (a) and cg-CN (b)[125]**

Aiming to explain nitrogen evolution during the CVD of carbon nitride thin films, Betranhandy et al.[127] have suggested 2 hypothetical models based on a pyrite-type structure with different C:N stoichiometries: $CN_2$ and $C_2N$. In the considered $AX_2$ compounds with the pyrite-type structure, $X_2$ diatomic units are arranged in the octahedral holes of the A-atoms fcc-sublattice. The authors indicated structural instability of both carbon nitrides and a tendency to release $N_2$ and $C_2N_2$ for $CN_2$ and $C_2N$, respectively. As many reports explained the nitrogen substoichiometry of carbon nitrides by an extraordinary stability of $N_2$ molecule, Sandre et al.[128] have proposed many structural models for the composition $C_3N$, making the substitution of one-quarter of carbon atom by nitrogen in the carbon graphite structure. Ab initio calculations have led to 2 graphitic 2-D structures and 2 3-D ones (poly-$C_3N$-a and -b) with orthorhombic symmetry. Authors mainly insist that the dynamic structural transformations from one polymorph to another are favored, which makes very difficult structural characterizations.

In addition to such dense, saturated or $sp^3$-hybridized carbon(IV) nitride structures, many soft unsaturated structural variants have been suggested in the literature. Different graphitic $C_3N_4$ structures[112,113,129,130]; numerous polymeric triazine-, heptazine-, carbodiimide-, and cyanamide-based networks[115,131]; and amorphous $C_3N_4$-phases[132] are considered as suitable precursors for the synthesis of a hard $C_3N_4$ phase and will be referred in the following subsection.

### 2.2.2 $CN_x$ Thin Films via Vapor Deposition

Up-to-date descriptions of the proposed $C_3N_4$ phases and reviews of the experimental results can be found elsewhere[120,133,134]. Numerous attempts to obtain hypothetical phases have been undertaken since the Liu and Cohen publication. Two main preparative approaches can be clearly distinguished: thin films deposition and bulk synthesis. First attempts to obtain $CN_x$ coatings were undertaken already in the 1970s. But after the above-described prediction of metastable β-$C_3N_4$ phase possessing diamond-like properties, an exponential increase of attempts to synthesize the postulated material via gas phase deposition techniques was documented. Currently, scientific databases consist of more than 2,000 papers related to carbon nitride films. The numerous papers have been summarized and critically analyzed in several review articles[120,133–135] allowing to conclude that the existence of crystalline stoichiometric $C_3N_4$ has not been clearly evidenced yet.

Practically all known variants of chemical vapor deposition techniques were applied to produce CNx-coatings. These include thermal low-pressure CVD, microwave- and RF-plasma-enhanced CVD, and laser- or hot filament CVD. The applied physical vapor deposition techniques include ion implantation or ion beam deposition; magnetron, electron cyclotron resonance, and other sputtering methods; laser ablation; vacuum arc deposition; and laser-induced gas phase reaction. The CVD-approaches are dominated by plasma-enhanced techniques, while in the physical vapor deposition (PVD) area, predominantly various kinds of sputtering methods were used. Important deposition parameters like temperature, pressure, precursors, target materials, and substrates were varied in wide range. Some of the obtained films showed an extremely high hardness (e.g., ~65 GPa for coatings with C:N-ratio of 0.6–0.7 obtained by ion beam PVD[136]), which, however, is still significantly below the corresponding values for diamond (~100 GPa). Independent of applied methods and apparatus, several reports on the successful synthesis of partially or fully crystalline coatings were published. Many authors claim unambiguous formation of β-$C_3N_4$, α-$C_3N_4$, cubic, graphitic, unknown crystalline $C_3N_4$ phases, or their mixtures in the obtained coatings.

However, in most cases there are only very small crystallites formed, sometimes with various compositions or mixed with other (amorphous) phases. Their diffraction intensities from XRD and TEM studies and derived lattice constants

match usually relatively poorly with the calculated values for the theoretically proposed modifications. Moreover, a detailed systematic analysis of the published diffraction data have shown that the reported X-ray and/or electron diffraction patterns may also be assigned to different crystalline carbon phases.[134] The elemental composition of the coatings is usually insufficient: such techniques as EDX, XPS, Rutherford backscattering spectrometry, or EELS are, in general, not suitable to provide an exact and reliable quantification of the light elements C, H, N, and O, and even the C:N ratio is usually very difficult to determine for a small single crystal. In many cases, the obvious contamination of the obtained material with hydrogen is ignored. Interpretation of such results on the basis of the C:N ratio is unacceptable, since molecular or polymeric crystalline C/N/H-phases may also be formed. So, it is not unlikely that many of the crystalline phases described in experimental reports contain significant amounts of oxygen, hydrogen, or other elements.

Critical analysis of the existent literature devoted to the preparation of carbon nitride films leads to the conclusion that it is relatively unlikely that the vapor deposition techniques can provide dense crystalline stoichiometric $C_3N_4$—in particular, its existence has not been clearly evidenced yet. To date, the so-obtained deposits are generally mainly amorphous and can eventually contain nanometric CNx crystallites. Nevertheless, amorphous nonstoichiometric CNx-materials are interesting from a fundamental, as well as from a practical, point of view because of their interesting mechanical, tribological, and optical properties. Much of the recent work in the field of carbon nitride coatings is focused on the synthesis and characterization of amorphous, homogeneous materials.[137]

### 2.2.3 Ambient- and Low-Pressure Bulk Synthesis Approaches

Another route to C-N compounds suggested by many authors devotes bulk synthesis approaches, which will provide hard ceramic carbon nitride materials in macroscopic amount. The present section briefly overviews the most significant results on carbon nitrides synthesis under ambient- or "low-" pressure conditions, implying the pressures below 1 GPa. It should be mentioned that the application of such moderate conditions in most cases does not provide dense C-N compounds. Thermal decomposition of organic precursors, moderate temperature synthesis, or solvothermal synthesis in most cases was resulting in amorphous/turbostratic and low-density crystalline (graphitic) carbon nitrides. Nevertheless, the obtained $CN_x$ materials are nitrogen rich and predominantly single phase, so they (in particular, graphitic $C_3N_4$ networks A and B on Fig. 2.10) can be considered as perfect precursors for the production of dense $C_3N_4$.

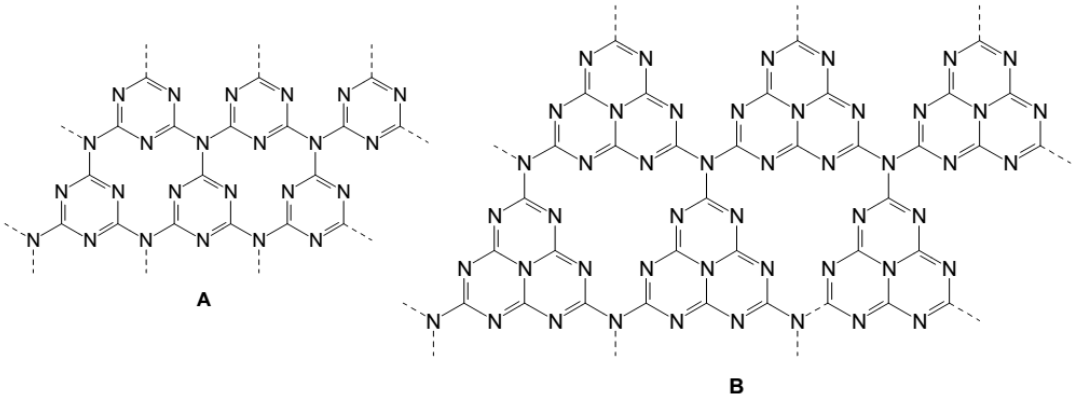


**Fig. 2.10 Examples for graphitic $C_3N_4$ networks with relative high symmetry based on the s-triazin unit (A) and the s-heptazine (tri-s-triazine) unit (B). Structure A was initially predicted to be the thermodynamically most stable $C_3N_4$ modification. However, recent DFT calculations have shown that B is significantly more stable than A.[138]**

### 2.2.3.1 Solid Phase Pyrolysis and Synthesis

Pyrolysis of N,N-diethyl-1,4-phenylen-diammonium-sulfate ($C_{10}H_{18}N_2O_4S$) in a nitrogen atmosphere at 800 °C and in the presence of $SeO_2$ as catalyst results in a heterogeneous product containing crystalline carbon nitride with a zinc blende structure, according to TEM examinations.[139] The authors propose the following reaction:

$$C_{10}H_{18}N_2O_4S + 8N_2 \rightarrow 3\text{“}C_3N_4\text{”} + CO_2 + 6NH_3 + SO_2$$

The composition of the crystalline product could only be estimated with EELS because of the small crystallite size of 5–50 nm. The crystallites are surrounded by an amorphous matrix with varying nitrogen content.

Thermal treatment of melamine ($C_3H_3N_6$), cyanoguanidine ($C_2H_4N_4$), 1,2,4-triazol ($C_2H_3N_3$), diaminomaleonitrile ($C_4H_4N_4$), polymerised HCN, dicyanoimidazol ($C_5H_2N_4$), TCNE ($C_6N_4$), TCNE with ammonia, and hexaazatriphenylene hexacarbonitrile ($C_{18}N_{12}$) at 700 °C / 225 MPa results in the products with composition deviating from the ideal $C_3N_4$. The observed ammonia release during thermal treatment allowed the authors to conclude that an ideal precursor should contain no or at least the lowest possible hydrogen content.[140]

An alternative method to synthesize the graphitic $C_3N_4$ precursor A (Fig. 2.10) is based on reactions of cyanuric chloride (2,4,6-trichloro-1,3,5-triazine, $C_3N_3Cl_3$) with metal nitrides and/or amides. The major challenge of this approach is the separation of the side product, i.e., the metal chloride, from the polymer. Kawaguchi et al.[141] used lithium nitride and removed LiCl by dissolving in water:

$$C_3N_3Cl_3 + Li_3N \rightarrow \text{“}C_3N_4\text{”} + 3LiCl$$

Two different products were obtained, with the composition $C_3N_{4.5}O_{1.2}H_{4.1}$ and $C_3N_{3.6}O_{1.1}H_{4.2}$. The oxygen content indicates a hydrolysis reaction during the treatment with water. Amorphous carbon nitrides as well as graphitic $C_3N_4$ hollow spheres have been reported to be formed upon reacting cyanuric chloride or fluoride with lithium nitride in a steel or Monel reactor at temperatures between 300 and 500 °C.[142,143] Interestingly, the addition of materials such as glass wool to the educts seems to have a catalytic effect resulting in the formation of hollow spheres with diameters from 30 nm to 1 µm (Fig. 2.11).[142,143] SEM, TEM, FTIR, XRD, and solid-state NMR examinations indicated the presence of spherical $CN_x$ particles with graphitic structure. The authors supported their interpretation with force-field calculations, which indicate that triazine-based $C_3N_4$ structures cross-linked with nitrogen atoms (structure A in Fig. 2.10, Fig. 2.11) tend to form curved layers. Guo et al.[144] have mixed cyanuric chloride with either potassium or nitriding agents, such as $NaN_3$ and $NaNH_2$, and submitted to temperatures of 300, 380 and 220 °C, respectively, in a solvent-free autoclave. While at higher temperatures nitrogen-poor materials were obtained, the lower-temperature treatment (when the organic reagent was mixed with $NaNH_2$) resulted in graphitic carbon nitride with a nitrogen-to-carbon (N/C) ratio of 1.20 and interplanar distance of 3.28 A. The authors proposed that a single layer of the graphitic carbon nitride is composed of triazine rings interconnected by nitrogen bridges (structure A in Fig. 2.10).

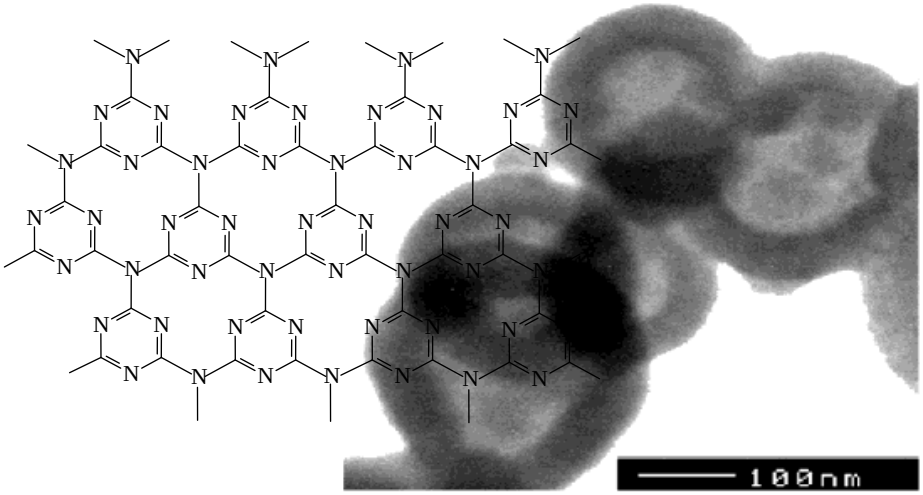


**Fig. 2.11** ***g*-$C_3N_4$: s-triazine-based chemical structure and TEM image of nanosized hollow spheres[142,143]**

Komatsu et al.[145,146] reported preparation of graphitic $C_3N_4$ materials based on the tri-s-triazine nucleus ($C_6N_7$) (e.g., structure B in Fig. 2.10) by ambient pressure chemical synthesis. Pyrolysis of tricyanomelamine or of mixtures of melamine with metal halides like $ZnCl_2$ at temperatures up to 800 °C results in the C/N/H-polymer melon, as supported by IR and mass spectrometry (MS) and

C/H/N elemental analyses.[146] Much more promising appeared to be the reactions of potassium melonate $K_3[(C_6N_7)(NCN)_3]$, with heptazinetrichloride, $C_6N_7Cl_3$.[145] Taking into account the IR and MS examinations, as well as XRD and the C:N-ratio determined by combustion chemical analysis, the author suggested for the synthesized product a network structure like that shown in Fig. 2.10B. Zhao et al.[147] have focused on the de-ammonation polycondensation of melamine at moderate temperatures (300 °C then 600 °C in atmosphere). The resulting carbon nitride nanowires adopted a turbostratic stacking with an interplanar distance of 3.21 A. High nitrogen content ($C_3N_{4.63}H_{1.61}$) and high thermal stability (up to 700 °C) suggested this material as a good precursor for the high-temperature and high-pressure synthesis of dense carbon nitride crystals.

Careful thermal treatment of C–N–H compounds, such as melamine $C_3N_3(NH_2)_3$, dicyandiamide $H_4C_2N_4$, ammonium dicyanamide $NH_4[N(CN)_2]$, or cyanamide $H_2CN_2$ to about 450 °C was found to lead to the formation of a nitrogen-rich condensed molecular structure so-called "melem" (2,5,8-triamino-tri-s-triazine).[148] Melem consists of nearly planar $C_6N_7(NH_2)_3$ molecules that are organized into parallel layers with an interplanar distance of 3.27 A. Being also highly nitrogen rich (the C:N ratio 1:1.67), melem is of significant interest as an intermediate phase on the way to the graphitic $C_3N_4$. Indeed, when heated up to 580 °C, it transforms into a graphitic carbon nitride with an interplanar distance of 3.40 A. Same behavior was observed for guanylurea dicyanamide $[(NH_2)C(=O)NHC(NH_2)_2][N(C{\equiv}N)_2]$, which forms melamine at about 130 °C and leads to a melem by heating at about 380 °C and, upon further heating to 490 °C, transforms into graphitic carbon nitride.[149] An investigation of the thermal behavior of nonmetal tricyanomelaminates in the temperature range of 380–500 °C revealed the formation of a graphitic hydrogenated carbon nitride through the intermediate melem phase.[150] The authors relate the structure of the obtained g-$C_3N_4$ to the "A" structure shown in Fig. 2.10.

Amorphous bulk nitrogen-rich carbon nitrides are produced via slow thermal decomposition of 2,4,6-triazido-1,3,5-triazine $[(C_3N_3)(N_3)_3]$ at 185 °C in a high-pressure reactor.[151] Under autogenous nitrogen pressure (~1 atm), the product with $C_3N_{3.9}H_{1.4}O_{0.2}$ composition (~$C_3N_4$) is obtained, while the application of initial nitrogen pressure of 6 atm yields a solid with one of the highest reported nitrogen-to-carbon ratios corresponding to $C_3N_5$, $C_3N_{4.7}H_{1.3}O_{0.4}$. Both products were found to have significant $sp^2$ carbon bonding in a conjugated doubly bonded network. Electron microscopy reveals that these powders have a glassy microstructure with large irregular pores and voids. Similar amorphous nitrogen-rich carbon nitride material, $C_3N_{4+x}$ where $0.5 < x < 0.8$, is obtained through the rapid decomposition of the trichloromelamine $[(C_3N_3)(NHCl)_3]$

upon heating above 185 °C.[152] The ideal decomposition should occur according to the following equation:

$$[(C_3N_3)(NHCl)_3] \rightarrow C_3N_4 + 3HCl + (2\text{-}x)/2{*}N_2$$

IR, NMR, optical, and X-ray photoelectron spectroscopy revealed in the product primarily $sp^2$ hybridized carbon centers and triazine ($C_3N_3$) rings bridged by nitrogen species. The authors have shown that pressure is not essential for high nitrogen content in resulting layered carbon nitrides.

Spherical carbon nitride nanoparticles with a graphitic structure were also synthesized using a template process.[153] A nanoporous silica matrix was soaked with liquid cyanamide ($CH_2N_2$) and dried. The carbon nitride material was obtained via heating the monolith under $N_2$ flow at 550 °C followed by treatment with hydrofluoric acid to remove the matrix. The authors have reported high nitrogen content (N/C = 1.56) and suggested the s-heptazine-based structure (B-type in Fig. 2.10) for the single layer of g-$C_3N_4$. The oxygen and hydrogen content of the synthesized material was not, however, specified.

Semencha et al.[154] reported simple methods for preparing crystalline carbon nitrides—namely, *g*-$C_3N_4$ and β-$C_3N_4$. The submicrometer-sized graphitic crystallites were obtained via thermal decomposition of a mixture of sodium and potassium thiocyanates at 450 °C. Reaction of carbon tetrachloride $CCl_4$ with ammonia $NH_3$ at an elevated temperature was claimed to lead to β-$C_3N_4$. The $CN_x$ phases were investigated using TEM, XRD, IR spectroscopy, and MS. Because of a poor agreement of experimental XRD patterns with that of the theoretically predicted ones, the presence of nonindexed XRD peaks, and the absence of any data on elemental composition, further characterization of the synthesized materials is indispensable.

Very recently Goglio et al.[155] suggested another simple method to synthesize carbon nitrides, including a low-compressibility $CN_x$-polymorph. The carbon nitride material was obtained through the decomposition of commercial thiosemicarbazide ($H_2NC(S)N_2H_3$) powder at ambient pressure and 600 °C under nitrogen flow. Besides the presence of a graphitic $CN_x$ phase, a nanocrystalline material is obtained and is identified as a cubic carbon nitride with a cell parameter of 3.163 Å. The authors report a high bulk modulus of 355 GPa for the cubic phase, which is still below those from numerous theoretical predictions. Finally, a bulk elemental combustion analysis of C, H, N, O, and S indicated no sulfur and high nitrogen content, but also showed the presence of significant H and O amounts. The composition of the cubic phase was not determined.

Another ambient-pressure approach toward $C_3N_4$ is presented by Schmidt and Jansen.[156] Using $C_2N_2O$, a hydrogen-free inorganic polyisocyanate obtained by the polymerization of molecular cyanogen isocyanate (NC–NCO), they

prepared a phase-pure 3-D structured C–N network by a carefully controlled polycondensation reaction. Only gaseous $CO_2$ was released, providing amorphous and porous $C_3N_4$ at 400 °C. Further densification of this inorganic cross-linked polymer up to 2.3 g/cm$^3$ was achieved by annealing in the presence of elemental mercury as a catalyst. The densified $C_3N_4$ network was analyzed using elemental analysis; IR, Raman, and electron paramagnetic resonance spectroscopy; thermal analysis, and MS studies. The authors have concluded that the obtained material with the composition $C_3N_4$ is best described as an inorganic resin-like thermosetting network (Fig. 2.12), structurally related to the well-known melamine-based resins (polytriazines).

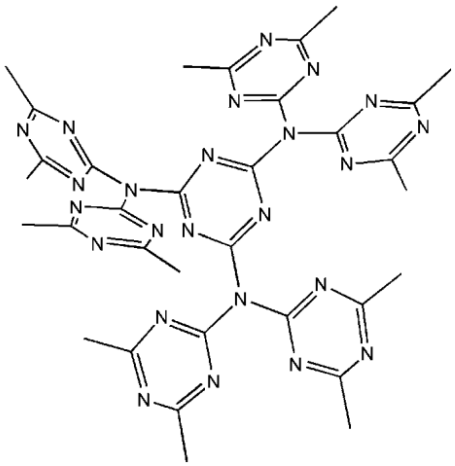

**Fig. 2.12 The 3-D resin-like structural model for $C_3N_4$[156]**

### 2.2.3.2 Solvothermal Route

Of all the synthesis methods for the carbon nitrides, the solvothermal process is considered to be of significant interest because the moderate temperature conditions are able to prevent the loss of nitrogen, and the chemical reactivity of the precursors at the interface between solid and liquid phases or between solvated species can be strongly improved. Montigaud et al.[157] tried to prepare the triazine-based structure A (Fig. 2.10) via solvothermal techniques at 250 °C / 130 MPa starting from cyanuric chloride and melamine in the presence of ethyl-diisopropylamine. The product was characterized by XRD, reflection electron microscopy, EDX, Raman, and XPS. The resulting poorly crystallized graphitic phase had an N/C ratio of 1.28 and contained hydrogen. It is very likely that the C/N/H-polymer melon was formed. Melon, $[C_6N_9H_3]_n$, contains only 1.5 wt% hydrogen; therefore, its composition is very close to the carbon(IV) nitride stoichiometry. Treatment of the same reagents in the presence of nickel with supercritical benzene as a solvent at 400 °C and autogenously pressure (or even without solvent) results in the formation of nitrogen-rich graphitic carbon nitride hollow spheres (10–40 nm in size) with an N/C equal to 1.6.[158] In this case, nickel is claimed to be necessary to induce a polycondensation reaction. FTIR, UV–vis, XPS, and photoluminescence

spectroscopic studies of the carbon nitride materials show that the products reserve the s-triazine-based structure (A, Fig. 2.10). The solvothermal condensation of melamine without a secondary reagent with pure hydrazine ($NH_2NH_2$) as a dehydrogenating agent was also studied at higher pressure and temperature conditions ($P$ = 3 GPa, $T$ = 800–850 °C) in a belt apparatus.[159,160] The product was characterized with XRD, SEM, XPS, EMPA, elemental analysis, and IR spectroscopy. A hydrogen content of 2 wt% was reported, indicating the presence of a C/N/H phase. The resulting material was a carbon nitride with a new unpredicted graphitic structure having an orthorhombic cell and a composition close to $C_3N_{3.36}O_{0.14}H_{1.24}$. Similar solvothermal conditions were applied to test 2 further triazine derivatives for their suitability to prepare a $C_3N_4$-material: 2-amino-4,6-dichloro-1,3,5-triazine and 5-azacytosin.[161] The products also showed relatively high hydrogen contents and/or significant oxygen impurities.

Solvothermal reaction of $CCl_4$ with $NH_4Cl$ at 400 °C in a stainless steel autoclave was reported to provide graphite-like $C_3N_4$ nanocrystals without any catalyst.[162] The obtained material exhibited very good crystallinity and its XRD pattern is consistent with graphite-like $C_3N_4$. IR spectroscopy indicated the presence of C=N, C–N, and N-H bonds. The overall elemental composition was not reported.

Further attempts to synthesize carbon nitride material via a solvothermal route involved cyanuric chloride $C_3N_3Cl_3$ as a source of both carbon and nitrogen. The reactant was usually mixed with different additives able to trap chloride anions or/and to supply additional nitrogen (e.g., alkali metals or their nitrides, $NaNH_2$ or $NaN_3$) in a nonpolar solvent ($C_6H_6$ or $C_6H_{12}$). In these experiments, moderate pressure and temperature conditions have been developed in a solvothermal environment. Lu et al.[163] tried to reproduce the solvothermal carbon nitride synthesis using cyanuric chloride with lithium nitride as reactants in benzene solution at 300–400 °C / 5–7 MPa. They claimed the formation of α- and β-$C_3N_4$. Nevertheless, the reported N/C ratio was very low compared with the theoretical value (0.66–0.76 vs. 1.33), and a number of nonindexed XRD peaks implied the presence of unknown crystalline phase(s). Here further characterization is necessary to unambiguously identify the structure and chemical nature of the phases observed. In order to investigate the nitridation mechanism, Guo et al.[164] have performed nitridation of $C_3N_3Cl_3$ using $NaN_3$ as the nitriding agent according to the following chemical equation:

$$C_3N_3Cl_3 + 3NaN_3 \rightarrow C_3N_4 + 3NaCl + 4N_2$$

The reaction has been carried out in the presence of benzene as the solvent at 220 °C for 15 h. The obtained material is composed of high-quality carbon nitride nanotubes having a graphite-like $sp^2$ bonded structure confirmed by XPS. Elemental analysis has shown the atomic N/C ratio of 1.25, which is very

close to the theoretical value for $C_3N_4$ (1.33). However, the presence of hydrogen bonded to nitrogen was detected. An equivalent benzene-thermal synthesis with $NaNH_2$ instead of $NaN_3$ at moderate temperatures (180–220 °C)[165] has led to the material mainly consisting of graphitic carbon nitride nanosized crystallites with N/C ratio 1.39, in agreement with chemical reaction:

$$C_3N_3Cl_3 + 3NaNH_2 \rightarrow C_3N_4 + 3NaCl + 2NH_3$$

The N–H bonds, however, were still present in the product. The reaction of cyanuric chloride with sodium metal at 250 °C without a catalyst in the presence of cyclohexane as solvent, in contrast to the above 2 experiments, resulted in carbon nitride with an atomic N/C ratio of 1.[166] Analysis of the XRD, FTIR, and XPS data suggested a graphite-like $sp^2$-bonded structure composed of blocks of s-triazine rings bridged by carbon-carbon atoms in the bulk carbon nitride. The TEM revealed spherical particles with an average diameter of 50 nm. Carbon nitrides having CN stoichiometry were prepared from the same reagents by Li et al.[167] between 230 and 290 °C and 1.8 and 4.5 MPa in a stainless steel autoclave. CN nanotube bundles were formed at 230 °C and 1.8 MPa using $NiCl_2$ as a catalyst. Without any catalyst, aligned nanoribbons were formed at 290 °C and 3 MPa, while microspheres consisting of hundreds of nanoribbons were formed at 260 °C and 3.5–4.5 MPa.

Recently, well-crystallized graphitic carbon nitride was prepared from $C_3N_3Cl_3$ and $NaN_3$ in $CCl_4$ at 180 °C without any catalyst.[168] The elemental analysis of the prepared sample indicated that the average composition was $C_3N_{4.88}H_{3.87}O_{1.58}$, with the N/C ratio to be 1.63, which is higher than the expected one (1.33) of the $C_3N_4$ empirical stoichiometry. The presence of hydrogen and oxygen in the sample was explained by hydrolysis during the washing procedure and/or by the presence of $–NH_x$ end groups. XPS and FTIR studies confirmed a graphite-like $sp^2$ bonded structure of the A-type (Fig. 2.10). TEM investigation revealed the presence of nanometer-size spherical particles and crinkly lamellas.

When comparing the results obtained by solvothermal methods, one can notice that the obtained morphologies of carbon nitrides are very different (microspheres of nanoribbons, nanotube bundles, nanospheres, lamellas, etc.) even when the only difference deals with the concentration of reagents and a slight modification in their ratios. Then the mechanisms responsible for all these morphologies are very sensitive to all experimental parameters (concentration, temperature, reducing agent amount, catalyst presence, and pressure), which underlines the great complexity of the phenomena involved in the solvothermal route.

### 2.2.4 HP-HT Synthesis of Dense C-N Phases

Despite many claims of making new $CN_x$ films and $C_3N_4$ crystallites, the scientific community still doubts the existence of dense $C_3N_4$ phases other than the graphite-like ones.[110,169,170,171] After years of unsuccessful attempts to synthesize the new $C_3N_4$ phases, Badzian et al. argued that based on chemical considerations, the "extensive network with C-N single bonding has never been documented and only very local C-N bonds are known as in amino acids".[170] The difficulties faced in the synthesis of carbon nitrides with a $C_3N_4$ stoichiometry are most probably related to their low thermodynamic stability with respect to carbon and nitrogen, as indicated by the positive values of their enthalpies of formation.[172] Taking this issue into account, together with theoretical studies mentioned in the previous section, as well as keeping in view the reported successes in the high-pressure synthesis of other nitrides, it becomes clear that HP-HT techniques similar to the synthesis of diamond and c-BN should be applied to prepare hard $C_3N_4$ materials (Fig. 2.13). Using suitable precursors with high nitrogen content may allow obtaining carbon nitride materials of good crystallinity in macroscopic amounts, which will also facilitate their characterization.

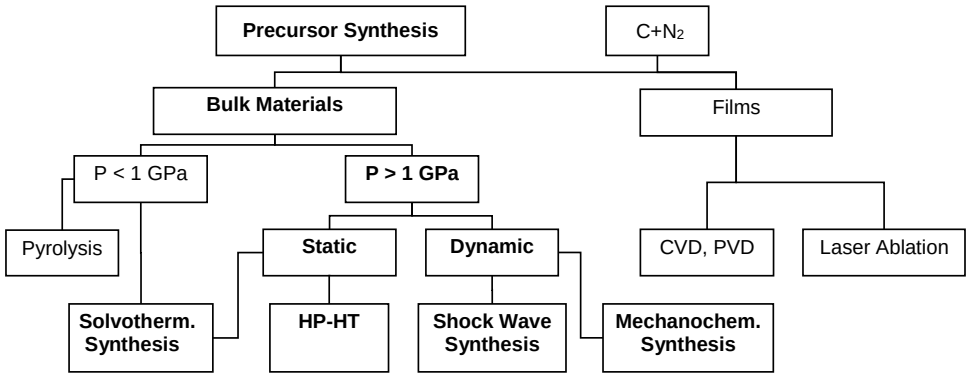


**Fig. 2.13 The diagram presents an overview of the reported experimental routes to produce $C_3N_4$ phases. The bold route indicates the most promising synthesis pathways to dense $C_3N_4$.**

An overview of the reported attempts to synthesize dense carbon nitride polymorphs under pressures exceeding ~1 GPa is listed in Table 2.3 and includes the utilized precursors, synthesis conditions, characterization methods, and main results. Even though most of the products obtained from the high-pressure experiments are amorphous materials with nitrogen contents much lower than the expected value of 57 at% for $C_3N_4$ ($x < 1.33$ for $CN_x$), several groups have reported the synthesis of polycrystalline materials consisting of small α-, β-, and c-$C_3N_4$ crystallites embedded in an amorphous carbon nitride matrix. Moreover, a recently conducted synthesis of several new C-N-based crystalline phases demonstrates how little is known about the behavior of the C-N compounds under high pressure.

**Table 2.3 Experimental details and main results related to the HP-HT synthesis of carbon nitrides**

| Starting Materials | Synthesis Conditions | Analyses Methods | x in $CN_x$ | Claimed Phases, Contaminations, Comments | Ref. |
|---|---|---|---|---|---|
| ***Static High-Pressure Synthesis*** | | | | | |
| $[C_3N_3(NH_2)_3 + NH_2NH_2]$ | 2.5–3 GPa 800-850 °C | FTIR, XPS, XRD, REM, TEM, ESCA | 1.14–1.34 | Cryst. graphitic $C_3N_{3.36}O_{0.14}H_{1.24}$ | [129, 160] |
| $[C_3N_3(NH_2)_3 + C_3N_3Cl_3]$ | 1.0–1.5 GPa 500–550 °C | XRD, TEM, EELS, FTIR, NMR | 1.50 | Crystalline $C_6N_9H_3 \cdot HCl$ with hexagonal graphitic structure | [173] |
| $C_3N_3(NH_2)Cl_2$ $C_3N_3(NH_2)(OH)_2$ | 3.0 GPa 450–1100 °C | XRD, FTIR, EA | 0.80–1.46 | cryst. $C_3N_{2.4}O_{0.7}H_{2.23}$ , $C_3N_{4.4}H_{4.4}$; unknown structure | [161] |
| $C_3N_3(NH_2)_3$ | 5.0 GPa 400–900 °C | EA, FTIR, XPS, XRD | 0.17–1.91 | T = 650 °C: partially cryst. graphitic CNx + melamine + unknown; H<br>T > 900 °C: amorphous carbon, low N content | [174] |
| a-$C_xN_yH_z$ | 6–7 GPa 300–400 °C | FTIR, XRD, Raman | 0.25 | Cryst. β-$C_4N$ + graphite + disordered carbon; O | [175] |
| $[C_6Cl_6 + 3NaN_3]$ | 7.7 GPa 400–500 °C | HR-TEM, EELS, XRD, FTIR, Raman | 0.70–1.94 | Nanosized hexagonal graphitic crystallites in amorphous matrix; O, H | [176] |
| $C_3N_3(NH_2)H_2$ catal.: NiMnCo, Co | 7 GPa 1400 °C | EDX, XRD, REM, | 1.09–1.44 | Partially cryst. α-$C_3N_4$ + β-$C_3N_4$ + catal. + unknown phase | [177] |
| $C_6N_4$ | 18–42 GPa 2000 °C | TEM, EELS, EDX, FTIR, Raman | 0.56-0.88 | Amorphous sp2-bonded $CN_x$ + carbon | [172, 178] |
| $[C_6N_4 + 2C_3N_{12}]$ | 115 GPa 2500 °C | XRD | n.d. | Cryst. $CN_x$, nitrogen content? | [179] |
| $[C_{60} + N_2]$ | 30 GPa, 2000–2500 °C | XRD | n.d. | Cryst. cubic phase; nitrogen presence? | [180] |
| $C_3N_4H_{2.5}$ | 4.8 GPa 950 °C | EELS, SIMS, XRD | 1.1 | Turbostratic-CN | [181] |
| a-$C_3N_4$ | 8.5 GPa 500 °C | XRD, TEM | n.d. | Cryst. cubic $CN_x$, nitrogen content? | [143] |
| g-$C_3N_4$ | 23–38 GPa <2700 °C | XRD, SEM, EDX | 1.29–1.47 | Unsolved cubic $C_3N_4$ + diamond | [182] |
| $C_2N_4H_4$ | 27–41 GPa 1700–2300 °C | TEM, EELS, EDX, SIMS, Raman | 1.61 | Well crystalline (~1 µm) orthorhombic "defect-wurtzite" $C_2N_2(NH)$ | [171] |
| a-$C_3N_4$ + cr-$CN_x$ film | 3–7.7 GPa, 300–1200 °C | XRD, XPS, TEM | n.d. | Cryst. α-$C_3N_4$ + β-$C_3N_4$ + unknown phase<br>nitrogen content? | [183] |
| ***Shock-Wave Compression Synthesis*** | | | | | |
| $C_3N_3Cl_3$, $C_3N_3H_3$, $C_3N_3(OH)_3$ | 15–50 GPa 1000–3000 °C | EA, XRD | 1.0 | Nanocrystalline cubic $CN_x$ (H, O, Cl) | [184] |
| $NaN(CN)_2$+$CI_4$+ $NaN_3$ | 20–25 GPa | TEM, EELS, IR | 0.09–0.15 | Cubic $sp^3$-bonded $CN_x$ nanocrystallites embedded in amorphous matrix (low N content) | [185] |
| $NaN(CN)_2$+$CI_4$/$CBr_4$ | 13–45 GPa | XRD, EA | 0.38–1.3 | Amorphous or poorly crystallized graphitic $CN_x$ | [186] |
| Graphitic $C_3N_2$ | 30 GPa 2700 °C | TEM, EELS, EDX, XRD,EA | 0.55 | Cubic heterodiamond $C_2N$ | [187] |
| a-$C_3N_{3.9}O_{0.9}$ (1) $C_2N_4H_4$ (2) | (1): 42–44 GPa 2200–2400 °C<br>(2): 28 GPa 280 °C | XRD | n.d. | Cryst. β-$C_3N_4$ + monoclinic phase. nitrogen/oxygen content? | [188] |

**Table 2.3 Experimental details and main results related to the HP-HT synthesis of carbon nitrides (continued)**

| Starting Materials | Synthesis Conditions | Analyses Methods | x in $CN_x$ | Claimed Phases, Contaminations, Comments | Ref. |
|---|---|---|---|---|---|
| ***Mechano-Chemical Synthesis*** | | | | | |
| Graphite + $NH_3$ | High energy ball milling | XRD, EELS, FTIR, XPS, TEM, EA | n.d. | Nanocryst. β-$C_3N_4$ embedded in amorphous carbon. Nitrogen content? | [189] |
| Graphite + $N_2$ | High energy ball milling | XPS, IR | <0.12 | Amorphization of graphite, weak nitridation | [190] |
| Nanosized graphite + $NH_3$ | High energy ball milling | XRD, FTIR, EELS, TEM, Raman, EDX, XPS | ~1.33 | Nanosized β-$C_3N_4$ embedded in amorphous carbon | [191] |
| Ball milled graphite + $NH_3$ | High energy ball milling 350 -450 °C + $NH_3$ | XRD, TEM, XPS, EELS, FTIR | ~1.33 | β-$C_3N_4$ nanorods | [192] |
| Ball milled graphite + $NH_3$ flow | 1100 °C + $NH_3$ flow | XRD, TEM, Raman, EELS, FTIR, EDX | ~1.33 | Graphitic $C_3N_4$, excellent crystallinity | [193] |
| Ball milled graphite + $NH_3$ flow | (1): 1050 °C + $NH_3$ flow; (2): 1350 °C + $NH_3$ flow of g-$C_3N_4$ from (1) | XRD, TEM, EELS, EDX | ~1.33 | (1) Graphitic g-$C_3N_4$, excellent crystallinity (2) $sp^3$-bonded pseudocubic $C_3N_4$ | [194] |
| $C_3N_3Cl_3$ + $Li_3N$ | High energy ball milling | XRD, SEM, XPS, TEM, FTIR | 1.23–1.3 | Graphitic carbon nitride | [195] |

One of the first noteworthy HP-HT syntheses of carbon nitrides has been attempted in an LH-DAC, where the molecular precursor TCNE ($C_6N_4$) was subjected to up to 2500 °C and 42 GPa.[172,178] TEM, SAED, EELS, and EDX analysis revealed the formation of amorphous $sp^2$-bonded carbon nitrides. The amount of nitrogen incorporated into the network increases with pressure, ranging from 24% (~$C_3N$) at 18 GPa to 38% at 42 GPa (~$C_3N_2$), which was the most nitrogen-rich carbon nitride prepared under pressure by that time. The authors argued that, in agreement with their thermodynamic analysis, pressures of 40 GPa are insufficient for the synthesis of $sp^3$-bonded carbon nitrides. Interestingly, that heating of a mixture of buckminster-fullerene $C_{60}$ with nitrogen in LH-DAC to 2,500 °C at pressures up to 30 GPa resulted in a 3-D carbon nitride in which the XRD pattern was consistent with a dense crystalline cubic system.[180] The proposed crystal structures were not compatible with any theoretical $C_3N_4$, thus suggesting the formation of an unpredicted carbon nitride. However, further characterization of the high-pressure product in order to prove the presence of nitrogen and to determine the structure was not performed.

Dymont et al.[175] have heat-treated the amorphous C-N-H precursor at 7 GPa by means of a toroid-type apparatus. Among various carbon phases, the authors also detected a crystalline carbon nitride with a hexagonal structure ($a$ = 6.65 Å, $c$ = 4.82 Å). After comprehensive XRD, IR, and Auger electron spectroscopy analysis, the model of the hexagonal β-$C_4N$ structure was

proposed, which is derived from the theoretical $C_3N_4$ structure by replacing some of the nitrogen atoms with carbon and forming C–C bonded pairs. Crystalline carbon nitride has been also synthesized from 3-amino-1,2,4-triazine, $C_3N_4H_4$, having ($C_3N_3$) a molecular skeleton in the presence of a nickel-based alloy or cobalt as a catalyst at similar pressures of 7 GPa and temperature of about 1,400 °C.[177] SEM showed rod-like C-N crystals of several micrometers in size having 47–62 at% of nitrogen. Based on XRD, the authors claimed the presence of α-$C_3N_4$ and β-$C_3N_4$ crystals with lattice constants of a0 = 6.425, c0 = 4.715, and a0 = 6.419, c0 = 2.425, respectively, in reasonable agreement with earlier ab initio calculations. Recently, Kim and Zorov[183] reported preparation of a mixture of crystalline α-, β-$C_3N_4$, and an unknown phase at 7 GPa and 550 °C from amorphous carbon nitride (a-$C_3N_{4.2}$) in a toroid-type apparatus. To promote crystallization of the dense phase, the author used crystalline carbon nitride films, obtained by laser-electric discharge method, as crystallization seeds. The exact composition of the HP products was not determined.

In 2007 the LH-DAC synthesis of a new well-crystallized compound with an N/C ratio of 3/2—namely, carbon nitride imide, $C_2N_2(NH)$—in which all of the carbon atoms are tetrahedrally coordinated was reported.[171] The crystals of $C_2N_2(NH)$ were formed at HP-HT conditions from a single source precursor 1-cyanoguanidine (dicyandiamide, $C_2N_4H_4$):

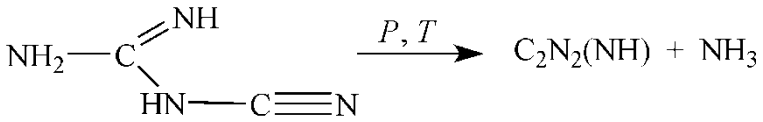


After the laser heating, the products were examined in-situ in a DAC by Raman spectroscopy. The recovered samples were investigated by means of TEM, EELS, and nano-SIMS (secondary ion mass spectrometry). Treatments of dicyandiamide at P < 27 GPa and T < 2,000 K yielded black amorphous $CN_x$ products. At higher P-T conditions the formation of a new optically transparent phase having a characteristic Raman spectrum was observed. The TEM investigation of the recovered products revealed the presence of a well-crystallized material (Fig. 2.14a). The N/C ratio of the crystals was determined by EELS to be 1.61 ± 0.06. The electron-energy loss near-edge fine structure of the EELS spectra proofed the formation of tetrahedrally coordinated C and N atoms with $sp^3$-hybridization in the synthesized material. Additionally, quantitative nano-SIMS measurements revealed the presence of hydrogen in the recovered crystals with an H/C ratio of 0.5 ± 0.15. Thus, the resulting composition of the synthesized material could be expressed as $C_2N_3H$, corresponding to $C_2N_2(NH)$.[171] The crystal structure of the new compound was determined by combining SAED data, experimentally measured composition, and first-principles calculations. Only a defect-wurtzite (dwur) structure type gave good agreement with the electron diffraction and EELS data, especially

regarding the $sp^3$-hybridized N sites. The SAED patterns for different zone orientations suggested an orthorhombic cell with the space group $Cmc2_1$ and lattice parameters $a$ = 7.546(2) Å, $b$ = 4.434(8) Å, and $c$ = 4.029(8) Å for the new dwur-$C_2N_2(NH)$ compound (Fig. 2.14b). The density of the carbon nitride imide (3.21 g/cm$^3$) was found to be close to that of diamond (3.52 g/cm$^3$), while the calculated bulk modulus of $C_2N_2(NH)$ of 277 GPa is significantly lower than those for diamond or predicted dense $C_3N_4$ polymorphs.

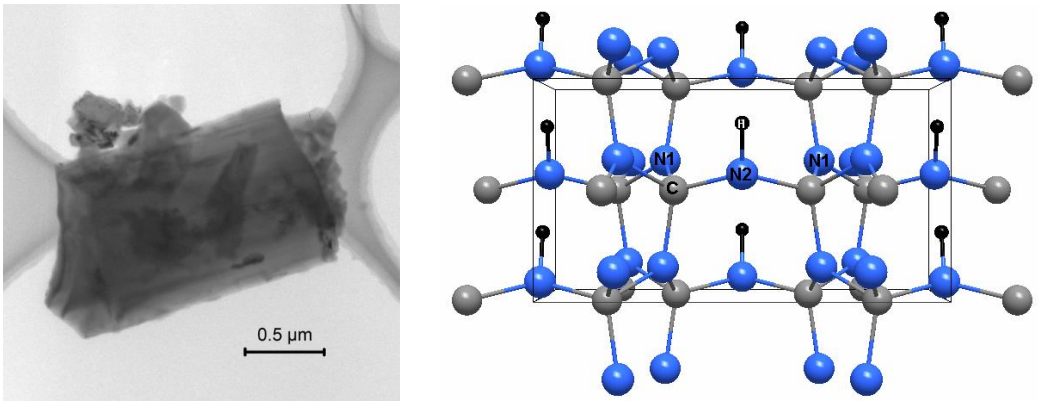


(a) (b)

**Fig. 2.14 a) Bright field TEM image of the $C_2N_2(NH)$ crystal synthesized at P = 41 GPa and T > 1700 °C and b) crystal structure of the defect wurtzite-type carbon nitride imide, dwur-$C_2N_2(NH)$[171]**

The above finding was confirmed by Salamat et al.[196] The authors have obtained XRD patterns in the DAC at high pressure and during decompression, confirming that no phase transitions occur upon release of pressure and recovery to ambient conditions. Analysis of the XRD patterns from different zones resulted in an orthorhombic *C*-centered cell with $a_0$ = 7.618 Å, $b_0$ = 4.483 Å, and $c_0$ = 4.038 Å, which supported the defect-wurtzite structure type (Fig. 1.14b) for the synthesized $C_2N_2(NH)$ (space group $Cmc21$) analogous to those of $Si_2N_2(NH)$ and $Si_2N_2O$ (sinoite). The $C_2N_2(NH)$ is suggested to be a promising precursor for dense $C_3N_4$, which could form above 40 GPa via further polycondensation reaction accompanied by complete elimination of $NH_3$:

$$3\ C_2N_2(NH) \rightarrow 2\ C_3N_4 + NH_3$$

The 2 hardest materials studied (diamond and cubic BN (*c*-BN)) were successfully synthesized under HP-HT conditions by direct conversion of a graphite-like phase with $sp^2$ bonding to a cubic phase with $sp^3$ bonding.[197] Naturally, one can assume that the experiment with direct conversion of the graphite-like $C_3N_4$ to diamond-like phases should provide an answer to the question of the existence of dense $C_3N_4$ phases. Thermodynamic analysis conducted by Badding et al.[172,198] showed that direct phase transition should occur at pressures above 50 GPa at 1300 K. Figure 2.15 shows the computed phase boundary between the cubic phase of $C_3N_4$ and diamond + nitrogen from Odintsov and Pepekin[199] and Horvath-Bordon et al.[200] If temperatures of 2,000–

2,500 K (typical for the direct synthesis of diamond from graphite) are applied, pressure of at least 50 GPa is required for *g*-$C_3N_4$ → dense $C_3N_4$ phase transition. If temperatures of 1,200–1,500 K are required to overcome the activation barrier for the *g*-$C_3N_4$ → dense $C_3N_4$ phase, then the optimal pressure for synthesis of the dense $C_3N_4$ phase should be between 20 and 40 GPa (Fig. 2.15).

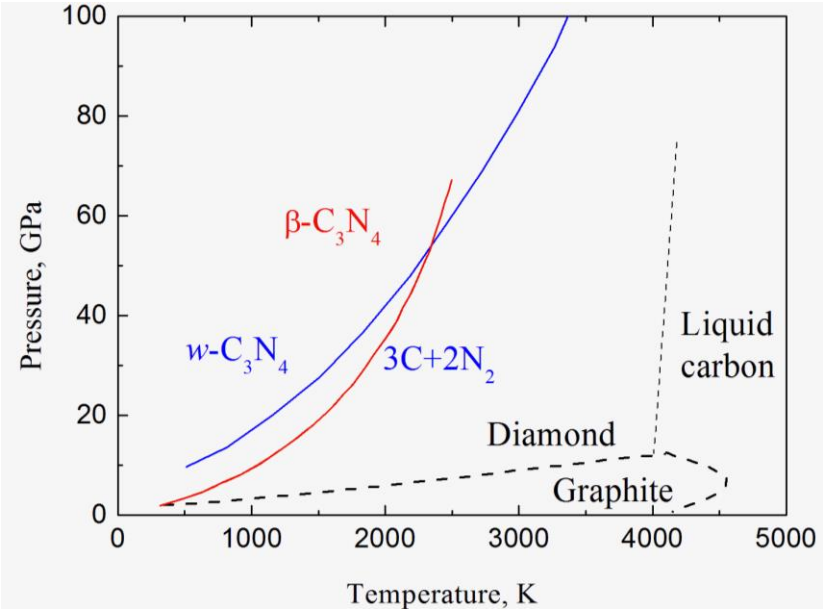


**Fig. 2.15 Computed phase boundary between carbon + nitrogen and the dense phases of $C_3N_4$: willemite-type phase w-$C_3N_4$ (blue line[200]) and β-$C_3N_4$ (red line[199]). For comparison, the phase diagram of carbon is shown by dashed lines.**

Indeed, Khabashesku et al.[143] synthesized nanocrystals of a dense $C_3N_4$ phase treating nanosized spherical powder of $C_3N_4$ at 8.5 GPa and 500 °C. TEM analysis of the product indicated the presence of well-faceted crystallites embedded in a graphic carbon nitride phase. The diffraction patterns obtained from these crystallites were indexed by a cubic cell with the lattice parameter of 5.3–5.4 Å, which is in good agreement with the theoretical value of 5.397 Å.[113] The authors also concluded that the temperature of the "nanosize-spherical-$C_3N_4$ → dense-$C_3N_4$" transition should be lower than that of the crystalline *g*-$C_3N_4$ → dense-$C_3N_4$ transformation. Using a well-characterized graphitic phase[165,201] with the LH-DAC technique has led to the discovery of a new cubic $C_3N_4$ (c-$C_3N_4$) and monoclinic *m*-$C_3N_4$ phases.[182] A cubic phase was recovered at ambient conditions from the graphite-like $C_3N_4$ (*g*-$C_3N_4$) phase subjected to pressures between 16 and 30 GPa and temperatures between 1600 and 3,000 K.[182] The density of the cubic phase (2.62 g/cm$^3$) is less than that predicted for the high-pressure phases but is 12% denser than the low-pressure graphitic phase ($\rho$ = 2.336 g/cm$^3$). The same research group took another approach to synthesize a dense $C_3N_4$ phase at HP-HT conditions: they used the above-mentioned c-$C_3N_4$ phase as a starting material. The c-$C_3N_4$ was converted into a new monoclinic (m-$C_3N_4$) phase at a pressure of 50 GPa and high

temperature. The XRD pattern of the recovered sample contained more than 30 well-defined peaks, which were indexed with a monoclinic unit cell having the following parameters: $a$ = 5.607Å; $b$ = 7.628 Å; $c$ = 4.226 Å, and $\beta$ = 126.915. The authors, however, noted that the observed XRD patterns are strongly dependent on the P-T synthesis conditions when starting with $g$-$C_3N_4$ ($g$-$C_3N_4$ nanospheres[143] or turbostratic $g$-$C_3N_4$ phases) materials.[165] They explain this finding by the possible existence of several structures with similar energies but different equilibrium volumes, for which the formation will strongly depend on the preparation conditions.[202]

With respect to dynamic high-pressure techniques, several shock-wave syntheses of dense (nano)crystalline $C_3N_4$ phases were reported. In particular, the cubic heterodiamond $C_2N$ phase was obtained by shock compression of graphitic $C_3N_2$ around 30 GPa and 3,000 K.[187] The recovered product was analyzed using authentic methods such as TEM, SAED, EELS EDX, powder XRD, IR spectroscopy, and CHN/S/O combustion elemental analysis. The $C_2N$ heterodiamond was found to consist of $sp^3$-bonded carbon and nitrogen atoms settled within a cubic diamond-like cell with a lattice constant of 3.51 Å, 1.6%–1.9% smaller than that of diamond. A series of shock recovery experiments up to 50 GPa on 3 nitrogen-rich C-N-based materials[188] have shown that an amorphous C–N–O material and dicyandiamide $C_2N_4H_4$ transform to a new carbon nitride phase ("phase-X") as well as to β-$C_3N_4$ at peak shock pressures of 28–44 GPa. The powder XRD of recovered samples allowed to index the "phase-X" with a monoclinic cell having parameters of $a$ = 0.981 nm, $b$ = 0.723 nm, $c$ = 0.561 nm, $\beta$ = 95.28°, and $V_{cell}$ = 0.3966 $nm^3$. The composition of the sample—in particular, N/C ratio and O-content—was not determined.

High-energy ball mills may also be used to generate high pressures exceeding 5 GPa as well as high temperatures. The high $P$-$T$ conditions occur at localized spots during impacts between the balls in the reaction mixture. Fahmy et al.[189] were the first to try the reaction of pure graphite with liquid ammonia in a high-energy ball mill. Examination of the products with XRD, EELS, FTIR, XPS, high-resolution TEM, and elemental analyses revealed a nanocrystalline phase that could be attributed to β-$C_3N_4$.

Another research group published several reports on the mechanochemical synthesis of β-$C_3N_4$.[191,192] Graphite nanopowder was reacted with ammonia in a high-energy ball mill to produce nanosized β-$C_3N_4$ particles. Subsequent thermal annealing of the ball-milled powder at 300–450 °C under flow of $NH_3$ gas resulted in the formation of nanorods (Fig. 2.16). Examination of the products by XRD, FTIR, high-resolution TEM, XPS, and EELS supported the formation β-$C_3N_4$ phase. Surprisingly, the ammonolysis of the high-energy ball-milled amorphous nanostructured graphite powders at 1,050 and 1,350 °C was reported to result in crystallization of graphitic- and pseudocubic-$C_3N_4$, respectively.[194] The XRD, TEM, EELS, and EDX were used to analyze the

structure, bonding, and composition (N/C ~1.33) of the synthesized materials. The true elemental composition (namely, the hydrogen and oxygen content) of the products remains unclear.

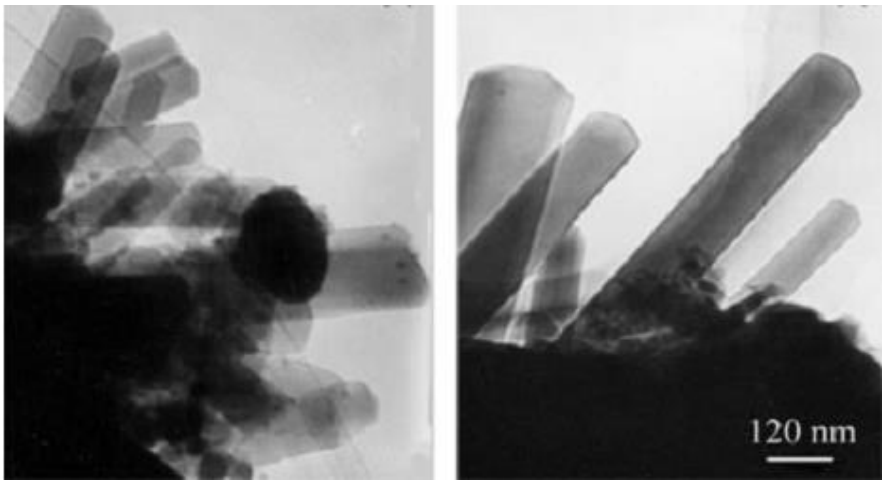


**Fig. 2.16 Low-magnification TEM images of β-$C_3N_4$ single-crystal nanorods obtained via reaction of graphite nanopowder with ammonia in a high-energy ball mill followed by the thermal treatment under $NH_3$ flow[192]**

## 2.3 B-C Compounds

Within B-C-N system binary compounds, which should be certainly mentioned, are boron carbides. The well-known "$B_4C$" itself combines a number of important properties like high hardness, high thermal and ionizing radiation stability, chemical inertness, and neutron absorption. (Strictly speaking, boron carbide, commonly referred to as $B_4C$ ($B_{12}C_3$), may have compositions varying between $B_{13}C_2$ and $B_{12}C_3$.[203,204]) Discovered more than a century ago, this compound was extensively studied and now has a number of useful applications.[203,205] For a long time boron carbide was considered the third hardest material after diamond and c-BN and still the hardest one above 1,300 °C.[203,205] On the other hand, the interest in the high-pressure studies of the boron-carbon system originated from the fact that doping of diamond with other elements has a drastic effect on its properties—in particular, doping with boron turns it from an insulator into a semiconductor or even into a quasi-metallic electrical conductor with high chemical resistance.[206] Moreover, boron-doped diamond was reported to be a type-II superconductor with a transition temperature of $T_c$ = 5 K,[207] while heavily boron-doped diamond (20 at% of B) is predicted to be a superconductor with $T_c$ up to 55 K.[208] However, employment of the common CVD and HP-HT synthesis methods allows one to incorporate a limited amount of boron (~2–3 at%) into the diamond lattice. The diamond-like B-C phases with high boron content (which can be increased by using extreme P-T conditions) are expected to combine the best properties of diamond and boron carbide, which could be further extended to advanced optoelectronic applications.

### 2.3.1 HP-HT Synthesis of Diamond-like B-C Phases

Most of the earlier HP-HT experiments in the B-C system were related to the synthesis of the boron-doped diamond. The main starting material for such experiments was a mixture of boron or boron carbide $B_4C$ with graphite powders. Thus, Ekimov et al.[207,209] investigated interaction in the $B_4C$(B)–C system in the toroid-type apparatus at pressures of 8–9 GPa and temperatures of 2,500–2,800 K. They reported the formation of a superhard polycrystalline diamond material containing less than 5 wt% $B_4C$. The increase in the lattice parameter of the synthesized diamond, observed via Raman spectroscopy and NMR studies, confirmed the formation of heavily boron-doped diamond with boron content estimated to reach ~2 at% (the overall boron content being 2.8 at%). The authors also tried HP-HT synthesis from homogeneous mixtures of naphthalene ($C_{10}H_8$) with o-carborane ($C_2B_{10}H_{12}$) or with amorphous boron, so that the B-content was varied from 0 to 10 at%. They observed that under employed P-T conditions, the level of boron doping of diamond reaches the limit already for 5 at% of boron in the starting material and is still lower than the B-doping level observed for the $B_4C$(B)–C system.[210] Using the mixture of $B_{13}C_2$ and graphite with a C/B ratio of 13 (~7 at% B) as a starting material, Dubrovinskaia et al.[211] performed experiments in a MAP at pressures from 9 to 20 GPa and temperatures 2,500–2,700 K. The chemical composition and texture of the samples were studied using SEM, TEM/parallel EELS, and EPMA. The overall B content was determined to be 2.6 at% for the sample synthesized at 20 GPa and 2700 K and 1.8 at% for the sample synthesized at 9 GPa and 2600 K. XRD data revealed the presence in boron-doped diamond of a very small amount of a boron-rich phase ($B_{50}C_2$) together with traces of the starting $B_{13}C_2$. The Raman spectra and increased lattice constants of the synthesized diamond crystals are in agreement with earlier reported heavily B-doped diamond phases.

For a long time it has been known that boron atoms can substitute carbon atoms in the structure of graphite, thus forming a graphite-like solid solution. Lowell[212] synthesized boron-doped graphite by thermal treatment of a mixture of graphite flakes and $B_4C$ to 2,350 °C and reported the maximum boron solubility of 2.35 at%. Since that time a number of graphite-like B-C phases (boron-substituted graphites) with boron content up to 50 at% were successfully prepared by thermal chemical vapor deposition methods (e.g., Kouvetakis et al.[62,213]). Since the graphitic structures are the usual precursors for HP-HT synthesis of superhard diamond-like phases (graphite → diamond, h-BN → c-BN), the boron-substituted graphites are considered to be perfect precursors for diamond-like B-C phases. However, HP-HT treatment of turbostratic graphite-like g-$BC_3$ at 20 GPa and 2,300 K using a MAP resulted in a bulk composite material consisting of intergrown boron carbide $B_4C$ and B-doped diamond with 1.8 at% B. The material was found to exhibit semiconducting behavior and extreme hardness of approximately 88 GPa comparable with that of single-

crystal diamond.[214] Subjecting the same g-$BC_3$ to shock pressures ranging from 10 to 30 GPa resulted only in local segregation of g-$BC_3$ and its partial transformation into a mixture of amorphous boron carbide and carbon. No expected diamond-like phases were observed in the shock products, probably due to the low shock temperatures (~600 K) reached in the samples.[215]

In contrast to above experiments, a direct transformation of the g-$BC_{1.6}$ phase to a diamond-like c-$BC_{1.6}$ phase in an LH-DAC at 2,230 K and 45 GPa was reported.[216] The recovered samples were examined using both synchrotron-based X-ray diffraction and confocal micro-Raman spectroscopy at ambient conditions. XRD examination revealed the presence of another orthorhombic or hexagonal phase in the less heated areas. The lattice parameter of the c-$BC_{1.6}$ phase was found to be slightly higher than that of diamond, thus supporting the theoretical prediction that incorporation of the B atoms into a diamond structure should lead to a negligible distortion of the cubic diamond cell.[217] The same research group continued LH-DAC experiments using other g-$BC_x$ starting materials (x = 4 and 3) at pressures above 40 GPa and temperatures above 2,000 K and claimed the formation of corresponding diamond-like c-$BC_4$ and c-$BC_3$ phases.[218] Their cubic lattice parameters were found to be 3.587 and 3.589 Å as well as the C/B ratio (determined by EPMA/EELS) to be $3.9 \pm 0.3$ and $2.8 \pm 0.7$, respectively.

Solozhenko et al.[219] have performed a systematic investigation of phase transformations of turbostratic g-$BC_x$ phases at pressures up to 25 GPa and temperatures up to 2,500 K using both an LH-DAC and MAP technique. In situ HP-HT experiments with g-BC and g-$BC_3$ in the 3–7 GPa pressure range using MAP and energy-dispersive XRD revealed no phase transformation up to 2000 K in both compounds. At pressures above 20 GPa in the 2,000–2,500 K range, t-$BC_x$ phases ($1 \leq x \leq 4$) decompose into boron-doped diamond (1–2 at% B) and boron carbides ($B_4C$ and $B_{50}C_2$) that are accompanied by the formation of cubic B-C phases (c-$BC_z$) with lattice parameters up to 2% higher than that of diamond. From these findings the authors concluded that the synthesis of a pure cubic B-C phase may be expected only for g-$BC_x$ with a lower B-content (i.e., $x \geq 5$). Indeed, g-BC5 compressed to 24.0 GPa and heated above 2200 K transformed to a (pseudo)cubic $BC_z$ phase. Since no amorphous phase has been observed in the recovered products by TEM and Raman spectroscopy, the authors suggested the formation of a c-$BC_5$ phase, the composition of which was further confirmed by EELS and EPMA analysis. At higher temperatures the cubic phase was found to decompose to boron-doped diamond and $B_4C$. In contrast to the other reported c-$BC_x$ phases, the lattice parameter of c-$BC_5$ (3.635 Å) was reported to be higher than that of both diamond and c-BN. Significantly, the authors were able to produce the sintered polycrystalline bodies (~1 $mm^3$) at similar P-T conditions using MAP. The Vickers hardness of these samples was found to be ~71 GPa, which is close to the hardness of

nanostructured bulk c-$BC_2N$. The authors also reported for c-$BC_5$ a remarkable indentation fracture toughness of 9.5 $MPa \cdot m^{1/2}$ and thermal stability up to 1,890 K in a nonoxidizing environment. These findings make diamond-like c-$BC_5$ an exceptional superabrasive superior to diamond.

### 2.3.2 Potential Superhard B-C Phases

In contrast to carbon nitrides and boron-carbon nitrides, theoretical exploration of superhard diamond-like B-C phases and the calculation of their properties has begun quite recently. The interest in diamond-like $BC_x$ structures has originated from the knowledge that superhard diamond-like structures are usually derived from their graphitic counterparts. In turn, graphitic structures of boron–carbon phases, g-$BC_x$, are also well known to exist in various stoichiometries with x greater than or equal to 1. Potential diamond-like phases can be formed from a unit cell or a supercell of diamond by replacing C atoms with boron at the various lattice positions according to the nominal lattice stoichiometry. Thus, various stoichiometries like BC, $BC_2$, $BC_3$, $BC_5$, and $BC_7$ were investigated, and structures of different symmetries (cubic, tetragonal, orthorhombic, hexagonal, or trigonal) were derived depending on the composition and positions of B-atoms (Table 2.4).

Among all considered $BC_x$ compositions, diamond-like c-$BC_5$ attracted the interest of experimentalists and theoreticians. The recent synthesis of c-$BC_5$ in macroscopic amounts using MAP[219] provided the community with the initial experimental data on its structure (XRD and Raman spectrum) and properties (extreme hardness and stiffness). This was followed by theoretical work using DFT calculations, where Calandra et al.[220] have shown that superhard c-$BC_5$ is metallic, making it the hardest conductor studied to date, and superconducting with a $T_c$ = 45 K, the largest $T_c$ ever for a phonon-mediated superconductor. Because of the similar atomic numbers of boron and carbon, the position of B in the cell could not be determined using XRD. Consequently, the structure of the synthesized c-$BC_5$ was assigned to a pseudocubic cell with $a_0$ = 3.635 Å. However, Calandra et al. have shown that c-$BC_5$ should adopt a hexagonal structure, which is compatible with a cubic symmetry for $c/a = \sqrt{6} \approx 2.45$ (Fig. 2.17). Performing volume and force optimization of a 6-atom hexagonal diamond-like supercell with 2 C atoms replaced by boron, the authors have found that the obtained c/a ratio was only slightly larger than the ideal one for cubic symmetry. Thus, the $BC_5$ cell can be obtained via a small elongation of the cubic cell along the cubic (111) axis (Fig. 2.17).

**Table 2.4 Structural parameters, bulk moduli, shear moduli, and estimated hardness (if available) of the predicted superhard diamond-like $BC_x$ phases calculated employing GGA (LDA). The experimental values for diamond, c-BN, and recently discovered c-$BC_5$ are given for comparison.**

| Compd/Structure | | V/atom (Å$^3$) | a (Å) | b (Å) | c (Å) | B (GPa) | G GPa) | H (GPa) | Ref. |
|---|---|---|---|---|---|---|---|---|---|
| Diamond[1] | | … | 0.3567 | 0.3567 | 0.3567 | 442-433 | 534-544 | 60–150 | [1,50] |
| c-BN[1] | | … | 0.3616 | 0.3616 | 0.3616 | 369-401 | 409 | 46–80 | [1,50] |
| c-$BC_5$[1] | | … | 3.635 | 3.635 | 3.635 | 335 | … | 71 | [219] |
| BC | cubic | … | 3.790 (3.745) | 3.790 (3.745) | 3.790 (3.745) | … | … | … | [217] |
| $BC_2$ | t-*I*4$_1$/*amd* | … | 2.520 | 2.520 | 11.919 | 349 | 319 | 56 | [221] |
| $BC_3$ | tetragonal | … | 3.553 (3.509) | 3.553 (3.509) | 3.913 (3.876) | 352 (379) | (344) | … | [217,222] |
| | tetr-*P*-42*m* | 5.975 | 3.513 | 3.513 | 3.871 | 361 | 337 | 41 | [223] |
| | tetr-*P*-42*m* | … | 2.510 | 2.510 | 3.915 | 359 | … | 66 | [224 |
| | o-*Pmma*-a | … | 2.513 | 2.520 | 7.788 | 354 | … | 62 | [224] |
| | o-*Pmma*-b | … | 2.484 | 2.531 | 7.891 | 352 | … | 65 | [224] |
| | trigonal | … | 3.685 (3.642) | 3.685 (3.642) | 3.685 (3.611) | 337 (378) | … | … | [217] |
| $BC_5$ | tetragonal | 5.993 | 3.633[2] | … | … | 385 | 405 | … | [225] |
| | hex-*P*3*m*1 | 5.871 | 3.608[2] | … | … | 376 | 394 | … | [226] |
| | hex-*P*3*m*1 | 6.02 | 2.55 | 2.55 | 6.39 | 337 | … | 83 | [227] |
| | hex-*P*3*m*1 | 6.006 (5.805) | 2.552 (2.522) | 2.552 (2.522) | 6.392 (6.324) | 379 (407) | 386 (410) | 62 | [228] |
| | hex-*P*3 | (5.867) | (2.539) | (2.539) | (6.303) | (410) | … | … | [229] |
| | hex-*P*3*m*1 | … | 2.210 (2.161) | … | 6.694 (6.326) | (405) | (372) | … | [223] |
| | o-*Pmma*-2 | 6.007 | … | … | … | 379 | … | 70 | [230] |
| | o-*Pmma*-I | … | 2.488 | 2.498 | 11.214 | 382 | … | … | [231] |
| | o-Pmma-II | … | 2.472 | 2.495 | 11.346 | 388 | … | … | [231] |
| | tetr-*I*-4*m*2 | … | 2.525 | 2.525 | 11.323 | 376 | 379 | 80 | [232] |
| | trig-*P*-1 | … | 4.455 | 4.459 | 4.462 | 370 | 374 | 79 | [232] |
| | h-*P*3*m*1-II | 6.02 | 2.532 | 2.532 | 13.017 | 401 | … | … | [233] |
| $BC_7$ | c-*P*-43*m* | … | 3.621 (3.581) | 3.621 (3.581) | 3.621 (3.581) | 387 (418) | (412) | … | [217,223] |
| | o-*Amm*2 | … | … | … | … | 388 | 430 | 49.5 | [234] |
| | hex | 5.933 (5.733) | … | … | … | 387 (417) | 399 (421) | 63 | [228] |
| | *P*-4*m*2 | … | 2.516 | 2.516 | 7.450 | 377 | 421 | 75 | [235] |
| | *P*-4*m*2 | … | 2.514 | 2.514 | 7.466 | 388 | 419 | 78 | [236] |
| $B_4C_3$ | α-*P*31*c* | 7.86 | 7.085 | 7.085 | 5.061 | 231 | … | 60 | [237] |
| | β-*P*63/*m* | 7.61 | 6.750 | 6.750 | 2.701 | 203 | … | 56 | [237] |
| | c- *I*-43*d* | 7.19 | 5.860 | 5.860 | 5.860 | 260 | … | 65 | [237] |
| | pc-*P*-42*m* | 7.89 | 3.809 | 3.809 | 3.809 | 220 | … | | [237] |
| | cs-*F*d-3*m* | 6.11 | 6.996 | 6.996 | 6.996 | 333 | … | 64 | [237] |

[1]Experimental values
[2]Effective cubic lattice parameter derived from the volume of the unit cell

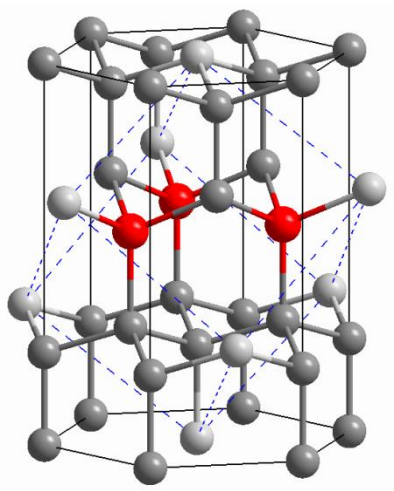

**Fig. 2.17 A representative atomic arrangement in the hexagonal supercell of c-$BC_5$[220] with carbon and boron atoms represented by gray and red spheres, respectively. The hexagonal supercell is compatible with a cubic symmetry (dashed blue line) for c/a = √6 ≈ 2.45.**

Based on Calandra and Mauri's structural model[220], Jiang et al.[225] considered a 12-atom hexagonal supercell and, via replacing 2 of the carbon atoms with boron, constructed 9 nonequivalent structures. The authors found only a small total-energy difference between the considered ordered configurations and the fully disordered state of $BC_5$ (with boron randomly distributed in the diamond lattice). Moreover, the calculated volume per atom, bulk modulus, and XRD pattern of the disordered $BC_5$ structure were in good agreements with experimental data.[219] The authors concluded that the c-$BC_5$ phase synthesized at HP and HT may be disordered in nature.

Yao et al.[232] have shown that recently synthesized diamond-like $BC_5$ is metastable and suggested the existence of a thermodynamically stable tetragonal (*I*-4*m*2) polymorph of $BC_5$. The predicted phase is expected to be harder than c-$BC_5$, metallic, and superconducting with an estimated superconducting critical temperature $T_c$ of 47 K. Another candidate structure with trigonal *P*-1 symmetry was found to fit very well with the experimental XRD pattern of c-$BC_5$, being, however, energetically less favorable. Li et al.[230] suggested another 2 energetically more preferable orthorhombic (*Pmma*) structures for c-$BC_5$. Their simulated XRD patterns, Raman modes, and Vickers hardness revealed remarkable agreement with the experimental data. Both structures were also found to be hole-conducting and superconducting with a critical temperature of 11–23 K. The main result of the theoretical studies of potential c-$BC_5$ structures and other diamond-like B-C phases are summarized in Table 2.4. All of the considered c-$BC_x$ are expected to be ultra-incompressible and superhard. Moreover, they may exhibit conductivity and superconductivity with a remarkably high $T_c$ of 11–48 K.[221–224,226–228,233–235,238] The combination of such properties suggests that they are an extremely superabrasive and promising functional material for electronics extreme

environments. Also, notice the trend in the mechanical properties: the larger the concentration of boron in the considered B-C phase, the lower the elastic moduli of c-$BC_x$ and the less hard the material would be. Last but not least, the incorporation of large amounts of boron also affects the conducting character of c-$BC_x$.

## 2.4 Summary

During last 2 decades, many studies were dedicated to the exploration of the B-C-N phase system. Undoubtedly, the synthesis of diamond-like boron carbon nitrides, c-$BC_2N$ and c-$BC_4N$, and boron carbide, c-$BC_5$, is the most remarkable achievement in the search of novel superhard materials. These dense phases were obtained under high static pressures above 20 GPa and temperatures about 2,000 K, employing various precursors, either single-source graphitic phase or an amorphous mechanical mixture of the constituting compounds. Furthermore, c-$BC_{2.5}N$ heterodiamond was successfully obtained as a nanocrystalline powder via shock compression of its graphitic counterpart above 30 GPa and 2,700 K. As the authors emphasized, one of the most important factors in the successful synthesis of dense diamond-like B-C-N phases lies in the nature and quality of the starting materials employed. A serious achievement was that the preparation of macroscopic single-phase samples made possible a detailed examination of properties of the high-pressure products. Both c-$BC_xN$ and c-$BC_5$ were confirmed to be superhard, with a hardness of ~70–80 GPa, approaching that of diamond, and possess exceptional fracture toughness, high thermal stability, and oxidation resistance. Moreover, while c-$BC_xN$ reveals semiconducting behavior, c-$BC_5$ is a conductor and potential high-$T_c$ superconductor. Thus, these novel compounds not only represent exceptional superabrasives surpassing diamond, but also, thanks to their intriguing functional properties, can expand the boundaries of high-temperature electronics and electrochemistry at extreme conditions.

However, the solid-state structure of the synthesized diamond-like B-C-N phases and their structure-properties relationship still remain a matter of controversy. So far, there is no unambiguous proof of the existence of the experimentally obtained crystalline phases. Thus, there is more detailed research to be done to clarify the composition and structure of the published phases in the B-C-N system. Nevertheless, despite the successful realization of superhard diamond-like B-C-N and B-C phases in macroscopic amounts, commercialization of their production in the form of powders or sintered bodies is quite unlikely at the moment. The reason is that extremely high thermobaric conditions are required for the direct transformation of the suitable precursors—namely, pressures and temperatures above 20 GPa and 2,000 K, respectively. However, it would be of interest to investigate the feasibility of such a transformation using different solvent catalysts (similar to those employed for

the industrial synthesis of diamond and c-BN) to reduce the P-T conditions to commercially utilizable values. A different way to synthesize large amounts of high-pressure B-C-N phases is by the shock-wave technique (e.g., by utilizing explosives). The disadvantage here is that the desired P-T conditions can only be maintained for very short times, which usually result in the formation of ultradispersed powders with reduced crystallinity. Therefore, once the synthesis and purification of the powder product is accomplished, an appropriate sintering technique (including conditions and suitable sintering additives) to obtain dense superhard B-C-N bodies should be developed.

Concerning dense $C_3N_4$, the direct synthesis under extreme static or dynamic pressures and temperatures has unambiguously led to dense C-N phases, although the results are far from numerous. However, in most cases the identification of their structures and compositions (with respect to the amount of nitrogen and contaminations) remains problematic. Moreover, because of the severe pressure and temperature conditions required, such studies are mainly of fundamental character. Another significant point is that the properties predicted for dense $C_3N_4$, such as extreme incompressibility and superhardness, have never been experimentally confirmed. It is worth noting that despite the fact that extreme pressures and temperatures were claimed to be necessary for the $C_3N_4$ synthesis, dense carbon nitrides were also obtained under quite mild conditions—namely, via solvothermal reactions and a high-energy ball-milling process. These 2 routes appear to be very promising in the future, either for crystal growth or large-scale synthesis of dense $C_3N_4$. Significant efforts are being undertaken to investigate and understand the chemistry of dense carbon nitrides and the mechanisms involved during their synthesis. These mechanisms are strongly dependent on the nature of the precursors, catalysts, pressure, temperature, and duration.

# 3. Experimental: Synthesis of Transparent Spinel-Type γ-$Si_3N_4$

Dmytro Dzivenko and Ralf Riedel

## 3.1 High-Pressure, High-Temperature (HP-HT) Synthesis

Commercial silicon nitride powder (Goodfellow, α-$Si_3N_4$ > 85%, particle size < 10 μm, oxygen ~1 wt%, nitrogen > 37.5 wt%) was used as a starting material for high-pressure synthesis. In spite of the declared chemical composition, elemental combustion analysis of the powder employing LECO TC-436 analyser revealed the presence of 2.5 ± 0.1 wt% of oxygen. Nitrogen was found to amount 38.5 ± 0.9 wt%, which is in reasonable agreement with the theoretical value of 39.9 wt%.

The starting $Si_3N_4$ powder was packed into a 3.8-mm-long platinum capsule with an outer diameter of 2 mm, which was preliminary welded, closed at one end, and mechanically sealed after sample loading. The sample loading and capsule-sealing procedures were performed in a glove box under a controlled argon atmosphere to prevent further contamination of the sample powder with oxygen and/or moisture.

For the sample pressurization, a hydraulically driven 6/8 type multianvil (MA) apparatus was employed. The setup consisted of an 18-mm-edge-length Cr-doped MgO octahedron containing the sample in a set of coaxially arranged parts, including a resistance-heated $LaCrO_3$ furnace and a $ZrO_2$ thermal insulation tube that accommodated the cylindrical capsule (Fig. 3.1). The octahedron was placed inside the octahedral volume formed by 8 tungsten carbide cubes with truncated corners. The sample assembly was brought to a pressure of 17 ± 0.5 GPa at room temperature and then heated to 1,825 °C in about 30 min. After holding the maximum temperature (±5 °C) for 1 h, the sample was quenched to room temperature in about 15 s by turning off the heating power. The temperature during experiment was monitored using a W3%Re-W25%Re thermocouple coaxially inserted into the furnace assembly (Fig. 3.1). A detailed description of the MA-press assembly, pressure calibration, and temperature measurement can be found elsewhere.[239]

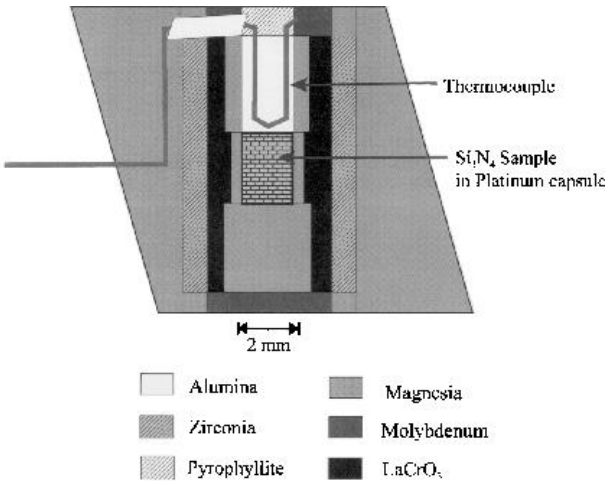


**Fig. 3.1 Cross section of an octahedral pressure assembly used for HP-HT synthesis of γ-$Si_3N_4$**

## 3.2 Sample Characterization

After decompression, the sample capsule (optically intact) was recovered from the pressure medium and embedded in epoxy resin. The capsule cap was removed for further examination by polishing, and 2 slices about 0.3 and 0.25 mm thick were cut from the sample by a diamond wire saw. The sample slices were investigated by optical microscopy, Raman spectroscopy, and powder X-ray diffraction (XRD). Preliminary elemental analysis of the high-pressure product was performed using a scanning electron microscope equipped with an energy dispersive X-ray (EDX) detector. The residual HP product weighing 5.5 mg was completely recovered by cutting and unwrapping the capsule cylinder.

### 3.2.1 Optical Observation

Figures 2.2 and 2.3 show optical micrographs of the 2 slices of the HP product made in reflected and transmitted light. On slice 1, the areas of a light-yellowish "milky" material were observed under reflected light (Fig. 3.2a). These areas appeared to be translucent under transmitted illumination (Fig. 3.2b). Likewise, the translucent phase was observed in slice 2 (Fig. 3.3). The translucent phase is mainly concentrated on the sample surface in contact with the capsule. The rest of the sample (internal volume) is, in contrast, dark gray and opaque.

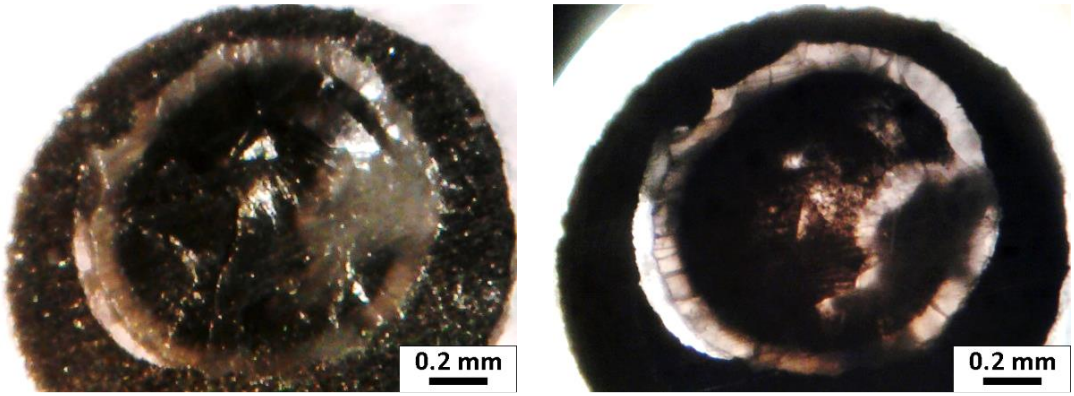


(a) (b)

**Fig. 3.2 The microscopic photographs of "slice 1" of the HP product in a platinum capsule ring taken under combined transmitted and reflected light (a) and in transmitted light only (b)**

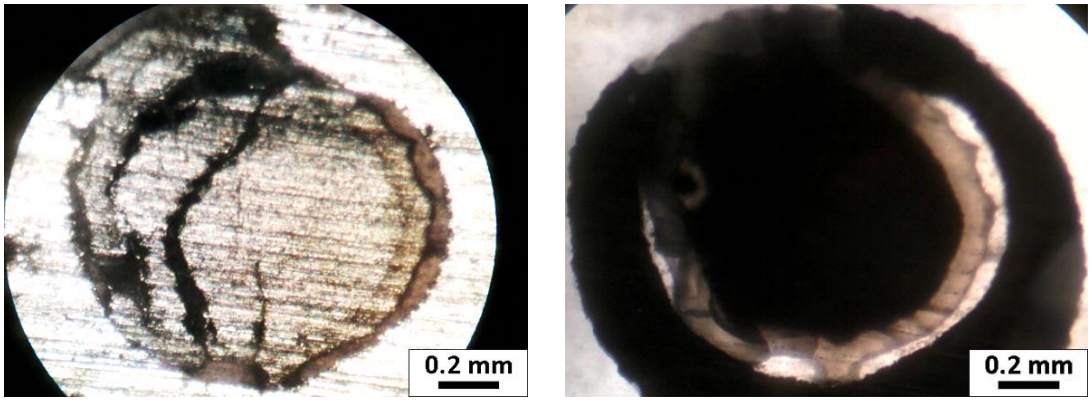


(a) (b)

**Fig. 3.3 The microscopic photographs of "slice 2" of the HP product in a platinum capsule ring taken under combined transmitted and reflected light (a) and in transmitted light only (b)**

### 3.2.2 Raman Spectroscopy

Raman spectra were excited by a HeNe laser with the wavelength $\lambda = 632.8$ nm and measured using a LabRam HR800 spectrometer (Horiba Jobin Yvon). All Raman shifts detected from the translucent areas of slices 1 and 2 (Fig. 3.4a) can be attributed to the cubic spinel $\gamma$-$Si_3N_4$ and are in excellent agreement with the previously reported data.[117,240,241] The dark areas also revealed the main features of $\gamma$-$Si_3N_4$ (bands at 523 and 846 $cm^{-1}$) as well as broad peaks at 123 and 360 $cm^{-1}$ (Fig. 3.4b), which have not been (yet) assigned to any of the known Si-N-O phases and can be probably related to an impurity or defects in $\gamma$-$Si_3N_4$.[240]

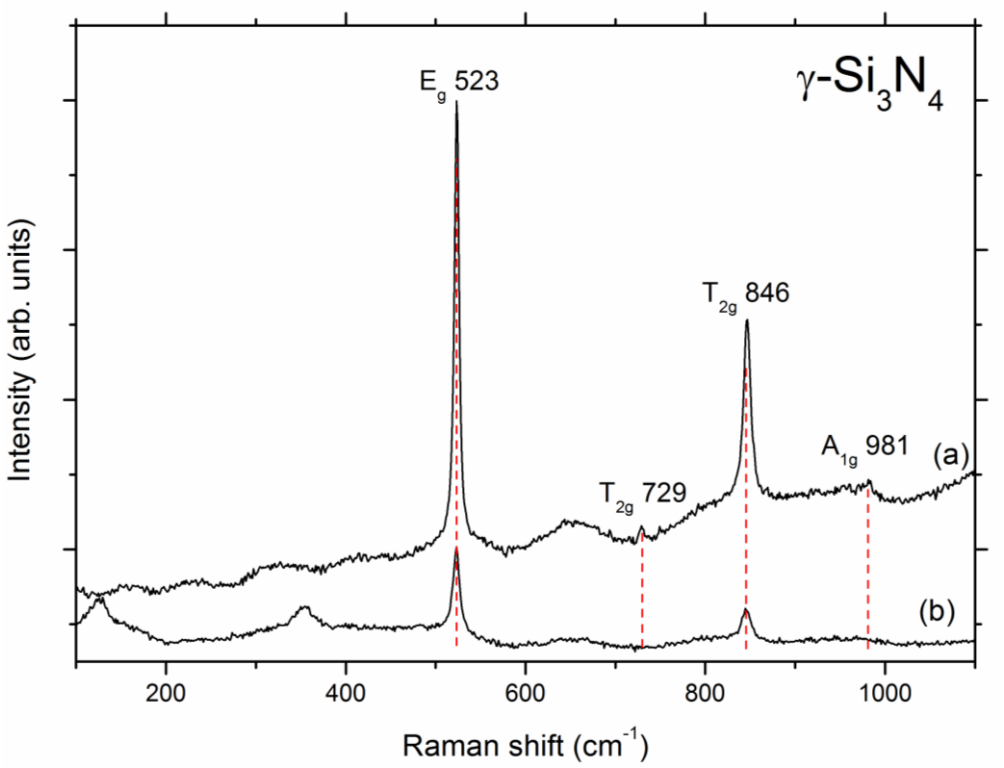


**Fig. 3.4 Typical Raman spectra measured from the translucent (a) and dark (b) areas of the HP product. The characteristic Raman shifts of the γ-$Si_3N_4$ with corresponding Raman-active phonon modes (according to Fang et al.[242]) are indicated.**

### 3.2.3 Powder X-ray Diffraction (XRD)

A powder XRD pattern (Fig. 3.5) was collected from slice 2 in the transmission geometry using a STOE Stadi P diffractometer (Stoe & Cie GmbH) equipped with a Molybdenum X-ray source, a flat Ge (111) monochromator ($\lambda$(Mo-$K_{\alpha 1}$) = 0.70932 Å) and a linear position-sensitive detector covering the 2θ region of 6°. The XRD pattern shows only reflexes of a cubic phase, the structure of which could be attributed to that of spinel type γ-$Si_3N_4$. The refined lattice parameter $a_0$ = 7.7467(6) Å is slightly higher than those reported earlier.[240,241,243] The anion parameter (nitrogen coordinate) is calculated to be 0.2589(2).

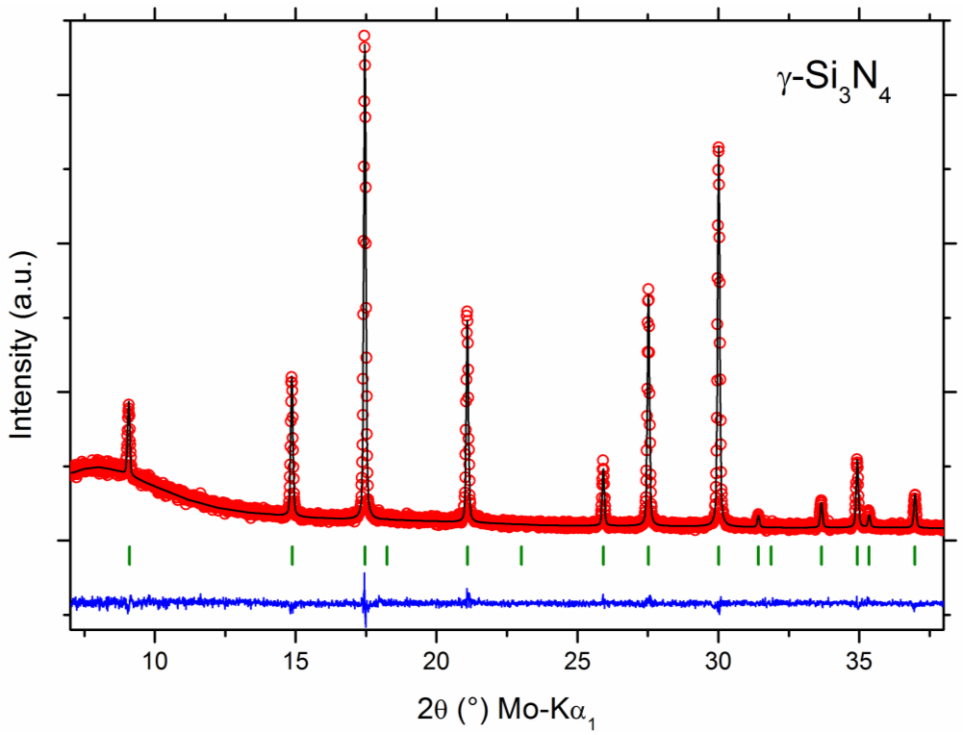


**Fig. 3.5 Powder XRD pattern (red circles) of the HP product (slice 2) measured in transmission "STOE" geometry. The results of the full profile Rietveld refinement for the cubic spinel γ-$Si_3N_4$ and the corresponding difference curve are presented by black and blue lines, respectively. The calculated peak positions of the cubic spinel-type structure (space group *Fd*-3*m*) are denoted by green tick marks. The refinement agreement factors are $R_{Bragg}$ = 7.2%, RF = 6.1%, and $\chi 2$ = 1.2.**

### 3.2.4 Energy-Dispersive X-ray Spectroscopy (EDX)

Preliminary elemental analysis of the HP product (slice 1, unpolished) was performed by means of EDX spectroscopy using a scanning electron microscope (HR-SEM Philips XL30 FEG) equipped with an EDX detector (EDAX Genesis). Semi-quantitative EDX analysis revealed the presence of Si, N, and a small amount of O (as well as C from adhesive carbon tape) throughout the sample (e.g., Fig. 3.6).

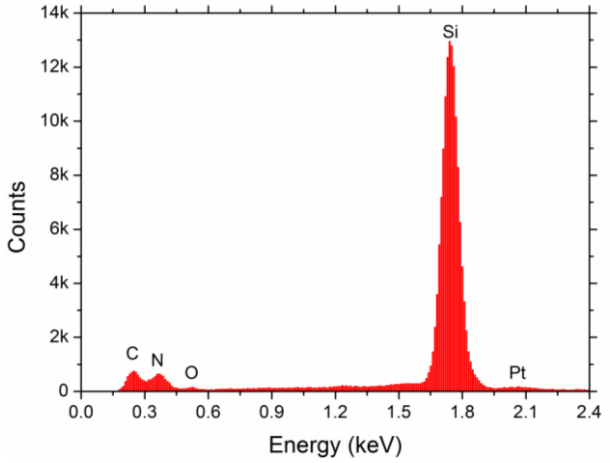


**Fig. 3.6 Typical EDX spectrum measured from translucent part of the HP product. C-K peak is due to the adherent carbon tape.**

However, because of the unprepared sample surface and low resolution of the EDX detector at low energies, the scattering of measured values did not allow an unambiguous conclusion about the compositional difference between translucent and dark sample areas. The element mapping also showed no significant composition variation (Fig. 3.7).

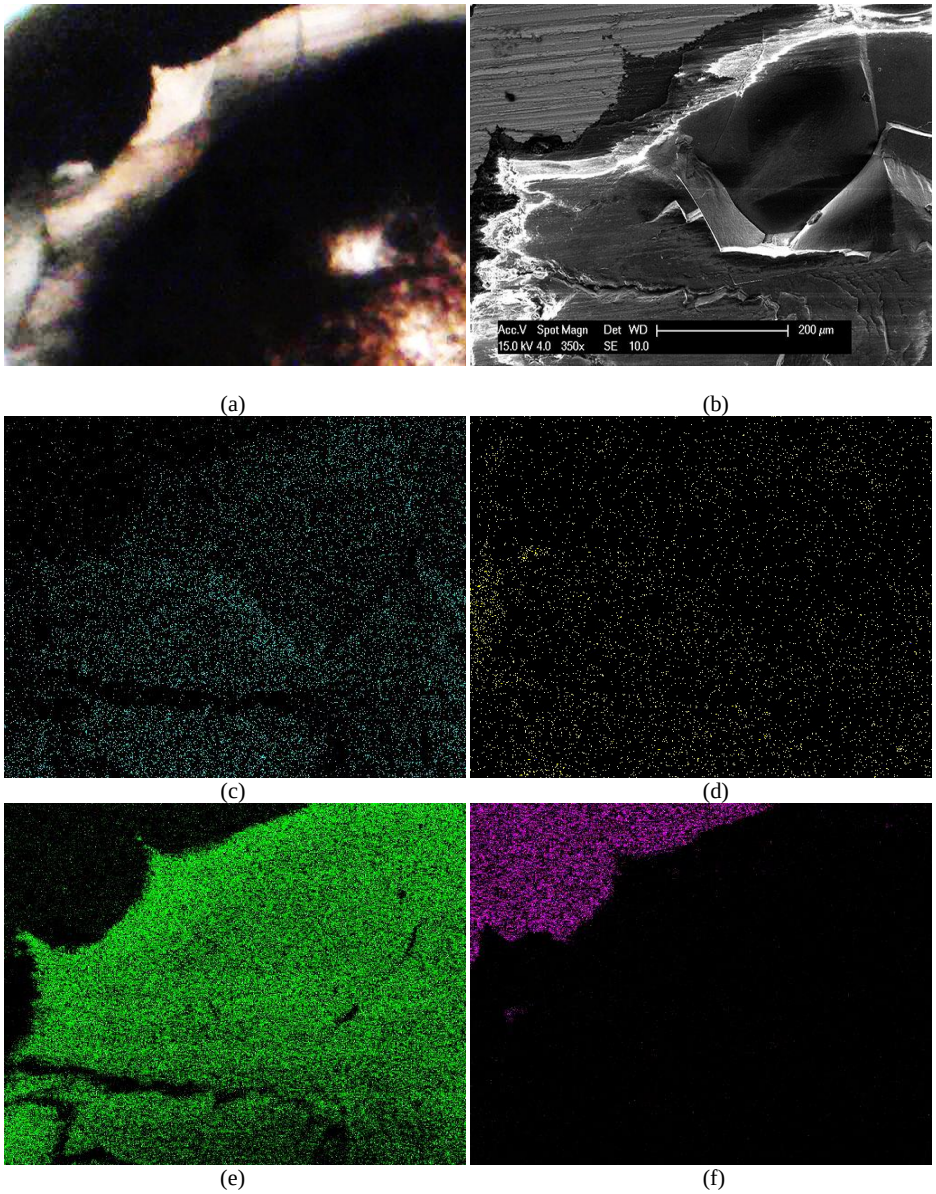


**Fig. 3.7 a) Optical and b) SEM micrographs of the sample surface together with EDX elemental maps for c) nitrogen, d) oxygen, e) silicon, and f) platinum**

## 3.3 Conclusion

The investigation of the HP product allows us to conclude that the major constituent (and the only crystalline) phase of both the translucent and opaque sample parts is γ-$Si_3N_4$. The nature of the sample translucency is not, however, clarified. The resulting translucency and opaque sections of the final product, instead of the transparency that was desired, probably resulted from microstructure or the elemental composition variation (mainly oxygen content) of γ-$Si_3N_4$. The variation of γ-$Si_3N_4$ can result from the temperature/pressure gradients in the sample and oxygen diffusion from the oxidic environment through the platinum capsule into the sample during heating. Moreover, the presence of an insignificant amount of an amorphous oxidic phase[241,243] cannot be excluded. Therefore, further detailed investigation of the HP product with respect to its (micro)structure and elemental and phase composition by means of transmission electron microscopy combined with electron energy loss spectroscopy and electron-probe microanalysis is required. These studies will provide more insight into the relationship between the experimental environment/conditions and the optical properties of the HP product. Thus, optimization of the synthetic approach for obtaining fully translucent γ-$Si_3N_4$ bulks can be possible.

## 4. References for Sections 2 and 3


1. Brazhkin VV, Lyapin AG, Hemley RJ. Philos Mag A. 2002;82(2):231.
2. McMillan PF. Nat Mater. 2002;1(1):19; Solozhenko VL, Gregoryanz E. Mater Today. 2005;8(11):44.
3. Rafaja D, Klemm V, Motylenko M, Schwarz MR, Barsukova T, Kroke E, Frost D, Dubrovinsky L, Dubrovinskaia N. J Mater Res. 2008;23(4):981; Yip S. Nature. 1998;391(6667):532; Veprek S. J Vac Sci Technol A. 1999;17(5):2401; Irifune T, Kurio A, Sakamoto S, Inoue T, Sumiya H, Nature. 2003;421(6923):599; Dubrovinskaia N, Solozhenko VL, Miyajima N, Dmitriev V, Kurakevych OO, Dubrovinsky L. Appl Phys Lett. 2007;90(10):3; Barnett S, Madan A. Phys World. 1998;11(1):45; Tian YJ, Xu B, Yu DL, Ma YM, Wang YB, Jiang YB, Hu WT, Tang CC, Gao YF, Luo K, Zhao ZS, Wang LM, Wen B, He JL, Liu ZY. Nature. 493(7432):385.
4. Badzian AR. Mater Res Bull. 1981;16(11):1385.
5. Knittle E, Kaner RB, Jeanloz R, Cohen ML. Phys Rev B. 1995;51(18):12149.
6. Komatsu T, Nomura M, Kakudate Y, Fujiwara S. J Mater Chem. 1996;6(11):1799.
7. Solozhenko VL, Andrault D, Fiquet G, Mezouar M, Rubie DC. Appl Phys Lett. 2001;78:1385.
8. Zhao Y HD. Preparation of bulk superhard B-C-N nanocomposite compact. United States patent US 7938997 B2 (11/529,657).
9. Zhao Y, Huang J, Zhang J, Shen G, Qian J, Zerda TW. J Mater Res. 2002;17(12):3139.
10. Komatsu T, Samedima M, Awano T, Kakadate Y, Fujiwara S. Journal of Materials Processing Technology. 1999;85(1–3):69.
11. Tian Y, He J, Yu D. BCN crystal with orthogonal structure and its preparing process. Chinese Patent CN 1382622-A; CN 1159213-C (CN 1382622-A CN 104856 15 Feb 2002).
12. Bhattacharya S, Majumder C, Das GP. J Phys Chem C. 2008;112(45):17487; Portehault D, Giordano C, Gervais C, Senkovska I, Kaskel S, Sanchez C, Antonietti M. Adv Func Mater. 2010;20(11):1827.

13. Komatsu T, Tomokuni K. Active boron carbonitride material used for exhaust gas purification has predetermined oxygen content, specific surface area and mean pore diameter. (JP2009119423-A JP298778 19 Nov 2007), 16.

14. Yu J, Wang EG, Ahn J, Yoon SF, Zhang Q, Cui J, Yu MB. J Appl Phys. 2000;87(8):4022; Gago R, Jimenez I, Agullo-Rueda F, Albella JM, Czigany Z, Hultman L. J Appl Phys. 2002;92(9):5177; Kurapov D, Schneider JM, Plasma Chemistry and Plasma Processing. 2005;25(6):613; Tsai PC, Surf Coat Technol. 2007;201(9–11):5108; Ying ZF, Yu D, Ling H, Xu N, Lu YE, Sun J, Wu JD. Diam Relat Mat. 2007;16(8):1579; Krause M, Bedel L, Taupeau A, Kreissig U, Munnik F, Abrasonis G, Kolitsch A, Radnoczi G, Czigany Z, Vanhulsel A. Thin Solid Films. 2009;518(1):77; Mannan MA, Kida T, Noguchi H, Nagano M, Shimoyama I, Hirao N, Baba Y. J Ceram Soc Jpn. 2009;117(1364):503; Castillo HA, Arango PJ, Velez JM, Restrepo-Parra E, Soto G, De la Cruz W. Surf Coat Technol. 2010;204(24):4051; Chen XY, Wang ZH, Ma SL, Ji V, Chu PK. Diam Relat Mat. 2010;19(10):1225; Essafti A, Ech-chamikh E. J Mater Sci. 2011;46(17):5847.

15. Liu AY, Wentzcovitch RM, Cohen ML. Phys Rev B. 1989;39(3):1760.

16. Nozaki H, Itoh S. Phys Rev B. 1996;53(21):14161; Nozaki H. Itoh S. Physica B. 1996;219–20:487; Nozaki H, Itoh S. J Phys Chem Solids. 1996;57(1):41.

17. Bill J, Riedel R, Passing G. Z. Anorg. Allg Chem. 1992;610(4):83.

18. Hubacek M, Sato T. J. Solid State Chem. 1995;114:258.

19. S. Azevedo, Paiva RD. EPL. 2006;75(1):126.

20. Tapas Kar MCU, Scheiner S. J Phys Chem A. 1998;102.

21. Lambrecht WRL, Segall B. Phys Rev B. 1989;40(14):9909.

22. Lambrecht WRL, Segall B. Phys Rev B. 1993;47(15):9289.

23. Tateyama Y, Ogitsu T, Kusakabe K, Tsuneyuki S, Itoh S. Phys Rev B. 1997;55(16):R10161.

24. Mattesini M, Matar SF. Int J Inorg Mater. 2001;3(7):943.

25. Sun J, Zhou X-F, Qian G-R, Chen J, Fan Y-X, Wang H-T, Guo X, He J, Liu Z, Tian Y. Appl Phys Lett. 2006;89(15):151911.

26. Chang J, Chen X-R, Wei D-Q, Yuan X-L. Physica B. 2010;405(17):3751.

27. Sun J, Zhou X-F, Fan Y-X, Chen J, Wang H-T, Guo X, He J, Tian Y. Phys Rev B. 2006;73(4):045108.

28. Yuge K, Seko A, Koyama Y, Oba F, Tanaka I. Phys Rev B. 2008;77(9).

29. Zheng JC, Wang HQ, Wee ATS, Huan CHA. Phys Rev B. 2002;66(9).

30. Yuge K. Phys Rev B. 2011;84(13):134207.

31. Yuge K. J Phys: Condens Matter. 2009;21(5):055403.

32. Zhuang C, Zhao J, Jiang X, Jiang X. J Phys: Condens Matter. 2009;21(40):405401.

33. Sun H, Jhi S-H, Roundy D, Cohen M. Louie S. Phys Rev B. 2001;64(9).

34. Pan Z, Sun H, Chen C. Phys Rev B. 2004;70(17):174115; Pan Z, Sun H, Chen C. J Phys: Condens Matter 2005;17(21):3211.

35. Pan Z, Sun H, Chen C. Phys Rev B. 2006;73(21):214111.

36. Chen S, Gong X, Wei S-H. Phys Rev Lett. 2007;98(1).

37. Kim E, Pang T, Utsumi W, Solozhenko V, Zhao Y. Phys Rev B. 2007;75(18).

38. Zhou X-F, Sun J, Fan Y-X, Chen J, Wang H-T, Guo X, He J, Tian Y. Phys Rev B. 2007;76(10):100101.

39. Zhou X-F, Sun J, Qian Q-R, Guo X, Liu Z, Tian Y, Wang H-T. J. Appl Phys. 2009;105(9):093521.

40. Luo X, Guo X, Liu Z, He J, Yu D, Xu B, Tian Y, Wang H-T. Phys Rev B. 2007;76(9):092107.

41. Luo X, Guo X, Xu B, Wu Q, Hu Q, Liu Z, He J, Yu D, Tian Y, Wang H-T. Phys Rev B. 2007;76(9):094103.

42. Li Q, Wang M, Oganov AR, Cui T, Ma Y, Zou G. J Appl Phys. 2009;105(5):053514.

43. Luo X, Zhou X-F, Liu Z, He J, Xu B, Yu D, Wang HT, Tian Y. J Phys Chem C. 2008112:9516.

44. Luo XG, Li LY, Wang WH, Tian YJ. J Appl Phys. 2011;109(2).

45. Tang MJ, He DW, He L. Physica B. 2011406(17):3154.

46. Luo X, Guo X, Liu Z, He J, Yu D, Tian Y, Wang H-T. J Appl Phys. 2007;101(8):083505.

47. Weihrich R, Matar SF, Betranhandy E. J Phys Chem Solids. 2003;64(9–10):1539.

48. Jiang X, Zhuang C, Li X, Sai L, Zhao J, Jiang X. Diam Relat Mat. 2011;20(7):891.

49. Martinez E, Andújar JL, Polo MC, Esteve J, Robertson J, Milne WI. Diam Relat Mat. 2001;10(2):145.

50. Teter DM. MRS Bull. 1998;23(1):22.

51. VL Solozhenko, SN Dub, NV. Novikov Diam Relat Mat. 2001;10(12):2228.

52. Zhang RQ, Chan KS, Cheung HF, Lee ST. Appl Phys Lett. 1999;75(15):2259.

53. Mattesini M, Matar SF. Comput Mater Sci. 2001;20(1):107.

54. Chen S, Gong XG., Wei S-H. Phys Rev B. 2008;77(1):014113.

55. Zhang Y, Sun H, Chen C. Phys Rev Lett. 2004;93(19):195504.

56. Zhuang C, Li X, Zhao J, Samra HA, Jiang X. J Phys: Condens Matter. 2011;23(46):465401.

57. Zang CP, Sun H. Phys Rev B. 2010;81(1):012106.

58. Miyamoto Y, Rubio A, Cohen ML, Louie SG. Phys Rev B. 1994;50(7):4976.

59. Watanabe MO, Itoh S, Sasaki T, Mizushima K. Phys Rev Lett. 1996;77(1):187.

60. Kosolapova TY, Makarenko GN, Serebryakova TI, Prilutskii EV, Khorphyakov OT, Chernysheva OI. Poroshk Metall. 1971;1:27.

61. F Zhuge, Yamanaka S. J Alloys Compd. 2008;466(1–2):299.

62. Kouvetakis J, Sasaki T, Shen C, Hagiwara R, Lerner M, Krishnan KM, Bartlett N. Synth Met. 1989;34(1–3):1.

63. Krishnan KM, Kouvetakis J, Sasaki T, Bartlett N. MRS Proc., 121, null.1988; Kaner RB, Kouvetakis J, Warble CE, Sattler ML, Bartlett N. Mater Res Bull. 1987;22(3):399.

64. Moore AW, Strong SL, Doll GL, Dresselhaus MS, Spain IL, Bowers CW, Issi JP, Piraux L. J Appl Phys. 1989;65(12):5109.

65. Besmann TM. J Am Ceram Soc. 1990;73(8):2498.

66. Watanabe MO, Itoh S, Mizushima K, Sasaki T. J Appl Phys. 1995;78(4):288; Watanabe MO, Itoh S, Mizushima K, Sasaki T. Appl Phys Lett. 1996;68(21):2962.

67. Kawaguchi M, Kawashima T, Nakajima T. Chem Mater. 1996;8(6):1197.

68. Hegemann D, Riedel R, Dressler W, Oehr C, Schindler B, Brunner H. Chem Vapor Depos. 1997;3(5):257.

69. Kim HS, Choi IH, Baik YJ. Surf Coat Technol. 2000;133–134(0):473; Yuki T, Umeda S, Sugino T. Diam Relat Mat. 2004;13(4–8):1130; Stöckel S, Weise K, Dietrich D, Thamm T, Braun M, Cremer R, Neuschütz D, Marx G. Thin Solid Films. 2002;420–421(0):465.

70. Zhou F, Adachi K, Kato K. Wear. 2006;261(3–4):301; Caretti I, Jiménez I, Gago R, Cáceres D, Abendroth B, Albella JM. Diam Relat Mat. 2004;13(4–8):1532.

71. Wada Y, Yap YK, Yoshimura M, Mori Y, Sasaki T. Diam Relat Mat. 2000;9(3–6):620; H Ling, JD. Wu, J Sun, W Shi, ZF Ying, FM. Li Diam Relat Mat. 2002;11(9):1623; Ying ZF, Yu D, Ling H, Xu N, Lu YF, Sun J, Wu JD. Diam Relat Mat., 2007;16(8):1579.

72. Guan C, Zhao J, Jia F, Zhuang C, Bai Y, Jiang X. Vacuum. 2012;86(10):1499; Ulrich S, Kratzsch A, Leiste H, Stüber M, Schloßmacher P, Holleck H, Binder J, Schild D, Westermeyer S, Becker P, Oechsner H. Surf Coat Technol. 1999;116–119(0):742; Zhou ZF, Bello I, Lei MK, Li KY, Lee CS, Lee ST. Surf Coat Technol. 2000;128–129(0):334; Linss V, Hermann I, Schwarzer N, Kreissig U, Richter F. Surf Coat Technol. 2003;163–164(0):220; Kim DH, Byon E, Lee S, Kim JK, Ruh H. Thin Solid Films. 2004;447–448(0):192; Zhuang C, Zhao J, Jia F, Guan C, Wu Z, Bai Y, Jiang X. Surf Coat Technol. 2009;204(5):713.

73. Lechner M. Darstellung und Untersuchung parakristalliner Borcarbonitride. [PhD thesis]. [München, (Germany)]: Fakultät für Chemie und Pharmazie, Ludwig-Maximilians-Universität München; 1981.

74. D Seyferth, Rees WS. Chem. Mater. 1991;3(6):1106; Rees WS, Seyferth D. Preparation, Characterization, and Pyrolysis of Decaborane (14) -Based Polymers: B4C/BN and BN Procedures. In A Collection of Papers Presented at the 13th Annual Conference on Composites and Advanced Ceramic Materials: Ceramic Engineering and Science Proceedings. John Wiley & Sons, Inc., 2008 p. 837.

75. Maya L. J Am Ceram Soc. 1988;71(12):1104.

76. Maya L. J Am Ceram Soc. 1990;73(9):2714.

77. Riedel R, Bill J, Passing G. Adv Mater. 1991;3(11):551.

78. Bill J, Friess M, Riedel R. Eur. J Solid State Inorg Chem. 1992;29:195; Riedel R. Adv Mater. 1994;6(7–8), 549.

79. Nicolich JP, Hofer F, Brey G, Riedel R. J Am Ceram Soc. 2001;84(2):279.

80. Sauter D, Weinmann M, Berger F, Lamparter P, Müller K, Aldinger F. Chem Mater. 2002;14 (7):2859.

81. Volger KW, Kroke E, Gervais C, Saito T, Babonneau F, Riedel R, Iwamoto Y, Hirayama T. Chem Mater. 2003;15(3):755.

82. Komatsu T. J Mater Chem. 2004;14(2):221.

83. Tian YJ, He JL, Yu DL, Li DC, Zou GT, Jia XP, Chen LX, Yanagisawa O. Radiat Eff Defects Solids. 2002;157(1–2):245.

84. Li XF, Zhang J, Shen LH, Lei WW, Yang DP, Cui QL, Zou GT. J Phys: Condens Matter. 2007;19(42):425235.

85. Bai SZ, Yao B, Xing GZ, Zhang K, Su WH. Physica B. 2007;396(1–2):214; Bai SZ, Bin Y, Su WH. Acta Phys Sinica. 2005;54(10):4627.

86. Raidongia K, Hembram KPSS. Waghmare UV, Eswaramoorthy M, Rao CNR. Z Anorg Allg Chem. 2010;636(1):30.

87. Raidongia K, Jagadeesan D, Upadhyay-Kahaly M, Waghmare UV, Pati SK, Eswaramoorthy M, Rao CNR. J Mater Chem. 2008;18(1):83.

88. Huang FL, Cao CB, Xiang X, Lv RT, Zhu HS. Diam Relat Mat. 2004;13(10):1757.

89. Sun G, Liu ZY, He JL, Yu DL, Tian YJ. Chin Phys Lett. 2007;24(4):1092.

90. Huang J, Zhu YT, Mori H. J Mater Res. 2001;16(04):1178.

91. Filonenko VP, Khabashesku VN, Davydov VA, Zibrov IP, Agafonov VN. Inorg Mater. 2008;44(4):395; Filonenko VP, Davydov VA, Zibrov IP, Agafonov VN, Khabashesku VN. Diam Relat Mat. 2010;19(5–6):541.

92. Yamada K. J Am Ceram Soc. 1998;81(7):1941.

93. Wu Q, Liu Z, Hu Q, Li H, He J, Yu D, Li D, Tian Y. J Phys*:* Condens Matter. 2006;18(41):9519.

94. Yang DP, Li YA, Yang XX, Du YH, Ji XR, Gong XL, Su ZP, Zhang TC. Chin Phys Lett. 2007;24(4):1088.

95. Sasaki T, Akaishi M, Yamaoka S, Fujiki Y, Oikawa T. Chem Mater. 1993;5(5):695.

96. S Nakano, M Akaishi, T Sasaki, S. Yamaoka Chem Mater. 1994;6(12):2246.

97. T Komatsu, S Hosomi, S. Fujiwara J Mater Chem. 2001;11(7):1781; Komatsu T, Kakudate Y, Fujiwara S. J Chem Soc Faraday Trans. 1996;92(24):5067.

98. Hubble HW, Kudryashov I, Solozhenko VL, Zinin PV, Sharma SK, Ming LC. J Raman Spectrosc. 2004;35(10):822.

99. Zinin PV, Solozhenko VL, Malkin AJ, Ming LC. J Mater Sci. 2005;40(11):3009.

100. Tkachev SN, Solozhenko VL, Zinin PV, Manghnani MH, Ming LC. Phys Rev B. 2003;68(5):052104.

101. Guo L-C, Hu W-T, He J-L, Yu D-L, Liu S-M, Li D-C, Tian Y-J. Chin Phys Lett. 2005;22(12):3141.

102. Nicolich FHJP, Gerhard B, Ralf R. J Am Ceram Soc. 2001;84(2):279.

103. Turkevich VLSa.VZ. J Am Ceram Soc. 1997;80(12):3229.

104. Li D, Yu D, Xu B, He J, Liu Z, Wang P, Tian Y. Crystal Growth & Design. 2008;8(7):2096.

105. Li M, Lin P, Gao Y, Gao C. J Appl Phys. 2010;107(7):073508.

106. Tang M, He D, Wang W, Wang H, Xu C, Li F, Guan J. Scr Mater. 2012;66(10):781.

107. Liu X, Jia X, Zhang Z, Zhao M, Guo W, Huang G, Ma H-A. Crystal Growth & Design. 2011;11(4):1006.

108. Liu AY, Cohen ML. Science. 1989;245:841.

109. Cohen ML. Phys Rev *B.* 1985;32(12):7988.

110. Sung CM, Sung M. Mater Chem Phys. 1996;43(1):1.

111. Guo YJ, Goddard WA. Chem Phys Lett. 1995;237(1–2):72.

112. Liu AY, Wentzcovitch RM. Phys Rev B. 1994;50(14):10362.

113. Teter DM, Hemley RJ. Science. 1996;271(5245):53.

114. Mo SD, Ouyang LZ, Ching WY, Tanaka I, Koyama Y, Riedel R. Phys Rev Lett. 1999;83(24):5046.

115. Kroll P, Hoffmann R. J Am Chem Soc. 1999;121(19):4696.

116. Molina B, Sansores LE. Mod Phys Lett B. 1999;13(6–7):193.

117. He J, Guo L, Guo X, Liu R, Tian Y, Wang H, Gao C. Appl Phys Lett. 2006;88(10):101906.

118. Zhao J, Fan C. Physica B. 2008;403(10–11):1956.

119. Kroll P. J Solid State Chem. 2003;176(2):530.

120. Malkow T. Mater Sci Eng A. 2000;292(1):112.

121. Zerr A, Miehe G, Serghiou G, Schwarz M, Kroke E, Riedel R, Fuess H, Kroll P, Boehler R. Nature. 1999;400(6742):340.

122. Côté M, Cohen ML. Phys Rev B. 1997;55(9):5684.

123. Kim E, Chen C, Köhler T, Elstner M, Frauenheim T. Phys Rev Lett. 2001;86(4):652.

124. Eremets MI, Gavriliuk AG, Trojan IA, Dzivenko DA, Boehler R. Nat Mater. 2004;3(8):558.

125. Wang X, Bao K, Tian F, Meng X, Chen C, Dong B, Li D, Liu B, Cui T. J Chem Phys. 2010;133(4):044512.

126. Wang X. J Chem Phys. 2012;137(18):184506.

127. Betranhandy E, Matar SF. Diam Relat Mat. 2006;15(10):1609; Weihrich R, Matar SF, Betranhandy E, Eyert V. Solid State Sci. 2003;5(5):701.

128. Sandré É, Pickard CJ, Colliex C. Chem Phys Lett. 2000;325(1–3):53.

129. Alves I, Demazeau G, Tanguy B, Weill F. Solid State Commun. 1999;109(11):697.

130. Ortega J., Sankey OF. Phys Rev B. 1995;51(4):2624.

131. Vodak DT, Kim K, Iordanidis L, Rasmussen PG, Matzger AJ, Yaghi OM. Chem -Eur J. 2003;9(17):4197; Riedel R, Kroke E, Greiner A, Gabriel AO, Ruwisch L, Nicolich J, Kroll P. Chem Mater. 1998;10(10):2964; Kroke E, Schwarz M, Horath-Bordon E, Kroll P, Noll B, Norman AD. New J Chem. 2002;26(5):508.

132. Lowther JE. Phys. Rev. B. 1998;57(10):5724; Lowther JE. Phys Rev B. 1999;59(18):11683; Weich F, Widany J, Frauenheim T. Phys Rev Lett. 1997;78(17):3326; Weich F, Widany J, Frauenheim T. Carbon. 1999;37(4):545.

133. Kroke E, Schwarz M. Coord Chem Rev. 2004;248(5–6):493.

134. Matsumoto S, Xie EQ, Izumi F. Diam Relat Mat. 1999;8(7):1175.

135. Bewilogua K. Vide. 1996;52(280):213; Muhl S, Mendez JM. Diam Relat Mat. 1999;8(10):1809.

136. Ogata K, Chubaci JFD, Fujimoto F. J Appl Phys. 1994;76(6):3791.

137. Bell J, Chen Z, Olofinjana A. Diam Relat Mat. 2001;10(12):2184; Jelínek M, Kulisch W, Delplancke-Ogletree MP, Vorlíček V, Studnička V, Chvostová D, Trchová M, Sobota J. Diam Relat Mat. 1999;8(10):1857; Tajima N, Saze H, Sugimura H, Takai O. Jpn. J Appl Phys. 1999;38:L1131; Liu XW, Tsai SH, Lee LH, Yang MX, Yang ACM, Lin IN, Shih HC. J Vac Sci Technol B. 2000;18(4):1840; Ju J, Xia Y, Zhang W, Wang L, Tang D. J Non-Cryst Solids. 2000;278(1–3):213; Liu XW, Tseng CH, Lin JH, Chao LT, Shih HC. Surf Coat Technol. 2001;135(2–3):184; Liu XW, Lin JH, Tseng CH, Shih HC. Mater Chem Phys. 2001;72(2):258; Wilson EK. Chem Eng News Arch. 2004;82(22):34; Long W, Shun Y, Bing Y. Rare Met Mater Eng. 2002;31:96; Cui FZ, Li DJ. Surf Coat Technol. 2000;131(1–3):481.

138. Gracia J, Kroll P. J Mater Chem. 2009;19(19):3013.

139. Martin-Gil J, Martin-Gil FJ, Sarikaya M, Qian MX, JoseYacaman M, Rubio A. J Appl Phys. 1997;81(6):2555.

140. Maya L, Cole DR, Hagaman EW, J Am Ceram Soc. 1991;74(7):1686.

141. Kawaguchi M, Tokimatsu Y, Nozaki K, Kaburagi Y, Hishiyama Y. Chem Lett. 1997;10:1003.

142. Zimmerman JL, Williams R, Khabashesku VN, Margrave JL. Nano Lett. 2001;1(12):731; Khabashesku VN, Zimmerman JL, Margrave JL. Chem Mater. 2000;12 (11):3264.

143. Khabashesku VN, Margrave JL. Adv Eng Mater. 2002;4(9):671.

144. Guo Q, Yang Q, Yi C, Zhu L, Xie Y. Carbon. 2005;43(7):1386.

145. Komatsu T. J Mater Chem. 2001;11(3):802.

146. Komatsu T. J Mater Chem. 2001;11(3):799; Komatsu T, Nakamura T. J Mater Chem. 2001;11(2):474.

147. Zhao YC, Yu DL, Zhou HW, Tian YJ, Yanagisawa O. J Mater Sci. 2005;40(9–10):2645.

148. Jürgens B, Irran E, Senker J, Kroll P, Müller H, Schnick W. J Am Chem Soc. 2003;125(34):10288.

149. Lotsch BV, Schnick W. Chem Mater. 2005;17(15):3976.

150. Lotsch BV, Schnick W. Chem Mater. 2006;18(7):1891.

151. Gillan EG. Chem Mater. 2000;12(12):3906.

152. Miller DR, Wang J, Gillan EG. J Mater Chem. 2002;12(8):2463.

153. Groenewolt M, Antonietti M. Adv Mater. 2005;17(14):1789.

154. Semencha AV, Pozdnyakov OF, Pozdnyakov AO, Blinov LN. Glass Phys Chem. 2008;34(1):103.

155. Goglio G, Foy D, Pechev S, Majimel J, Demazeau G, Guignot N, Andrault D. Diam Relat Mat. 2009;18(4):627.

156. Schmidt CL, Jansen M. J Mater Chem. 2010;20(20):4183.

157. Montigaud H, Tanguy B, Demazeau G, Courjault S, Birot M, Dunogues J. C R Acad Sci Ser II b. 1997; 325:229.

158. Li C, Yang X, Yang B, Yan Y, Qian Y. Mater Chem Phys. 2007;103(2–3):427.

159. Montigaud H, Tanguy B, Demazeau G, Alves I, Birot M, Dunogues J. Diam Relat Mat. 1999;8(8–9):1707.

160. Montigaud H, Tanguy B, Demazeau G, Alves I, Courjault S. J Mater Sci. 2000;35(10):2547.

161. Courjault S, Tanguy B, Demazeau G. C R Acad Sci Ser II c. 1999;2(9–10):487.

162. Bai Y-J, Lü B, Liu Z-G, Li L, Cui D-L, Xu X-G, Wang Q-L. J Cryst Growth. 2003;247 (3–4):505.

163. Lu Q, Cao C, Li C, Zhang J, Zhu H, Kong X, Duan X. J Mater Chem. 2003;13 (6):1241; Lu Q, Cao C, Zhu H. Chin Sci Bull. 2003;48(6):519; Lu Q, Cao C-B, Zhang JT, Li C, Zhu H-S. Chem Phys Lett. 2003;372(3–4):469; Cao C-B, Lu Q, Zhu H-S. Diam Relat Mat. 2003;12(3–7):1070.

164. Guo Q, Xie Y, Wang X, Zhang S, Hou T, Lv S. Chem Commun. 2004;0(1):26.

165. Guo Q, Xie Y, Wang X, Lv S, Hou T, Liu X. Chem Phys Lett. 2003;380(1–2):84.

166. Mu T, Huang J, Liu Z, Han B, Z Li, Y Wang, T Jiang, H. Gao J Mater Res. 2004;19(06):1736.

167. Li J, Cao C, Hao J, Qiu H, Xu Y, Zhu H. Diam Relat Mat. 2006;15(10):1593.

168. Zhang J, Liu W, Li X, Zhan B, Cui Q, Zou G. Mater Res Bull. 2009;44(2):294.

169. Goglio G, Foy D, Demazeau G. Mater Sci Eng R-Rep. 2008;58(6):195; Badzian A, Badzian T. Int J Refract Met Hard Mater. 1997;15(1–3):3.

170. Badzian A, Badzian T, Roy R, Drawl W. Thin Solid Films. 1999;354(1–2):148.

171. Horvath-Bordon E, Riedel R, McMillan PF, Kroll P, Miehe G, van Aken PA, Zerr A, Hoppe P, Shebanova O, McLaren I, Lauterbach S, Kroke E, Boehler R. Angew Chem. 2007;46(9):1476.

172. Badding JV, Nesting DC. Chem Mater. 1996;8(2):535.

173. Zhang ZH, Leinenweber K, Bauer M, Garvie LAJ, McMillan PF, Wolf GH. J Am Chem Soc. 2001;123(32):7788.

174. Ma HA, Jia XP, Chen LX, Zhu PW, Guo WL, Guo XB, Wang YD, Li SQ, Zou GT, Zhang G, Bex P. J Phys: Condens Matter. 2002;14 (44):11269.

175. Dymont VP, Nekrashevich EM, Starchenko IM. JETP Lett. 1998;68(6):498; Dymont VP, Nekrashevich EM, Starchenko IM. Solid State Commun. 1999;111(8):443; Dymont VP, Smurov I. Mater Sci Eng. B. 2001;82(1–3):39.

176. Andreyev A, Akaishi M, Golberg D. Diam Relat Mat. 2002;11(12):1885; Andreyev A, Akaishi M, Golberg D. Chem Phys Lett. 2003;372(5–6):635.

177. He DW, Zhang FX, Zhang XY, Qin ZC, Zhang M, Liu RP, Xu YF, Wang WK. J Mater Res. 1998;13(12):3458.

178. Nesting DC, Badding JV. Chem Mater. 1996;8(7):1535.

179. Nesting DC, Kouvetakis J, Badding JV. In Proceedings of the 5th NIRIM International Symposium on Advanced Materials (ISAM'98), 1998 March 1–5; Tsukuba, Japan.

180. Nguyen JH, Caldwell WA, Benedetti LR, Kruger MB, Jeanloz R. Mater Res Symp. 1998;499:303; Nguyen JH, Jeanloz R. Mater Sci Eng. A. 1996;209(1–2):23.

181. Solozhenko VL, Solozhenko EG, Lathe C. J Superhard Mater. 2002;24:95; Solozhenko VL, Solozhenko EG, Zinin PV, Ming LC, Chen J, Parise JB. J Phys Chem Solids. 2003;64(8):1265.

182. Ming LC, Zinin P, Meng Y, Liu XX, Hong SM, Xie Y. J Appl Phys. 2006;99(3):033520.

183. Kim JI, Zorov NB. J Korean Phys Soc. 2004;44(5):1071; Kim JI, Zorov NB. J Korean Phys Soc. 2008;53(6):3675.

184. Komatsu T. Production method of cubic carbon nitride material. Japan Patent P2000-51678A. 2000.

185. Collins C, Thadhani N, Iqbal Z. Carbon. 2001;39(8):1175.

186. Shibata K, Sekine T. Solid State Commun. 2006;139(10):501.

187. Komatsu T. Phys Chem Chem Phys. 2004;6(5):878.

188. Liu JJ, Sekine T, Kobayashi T. Solid State Commun. 2006;137(1–2):21.

189. Fahmy Y, Shen TD, Tucker DA, Spontak RL, Koch CC. J Mater Res. 1999;14(6):2488.

190. Alcala MD, Sanchez-Lopez JC, Real C, Fernandez A, Matteazzi P. Diam Relat Mat. 2001;10(11):1995.

191. Yin L-W, Li M-S, Luo G, Sui J-L, Wang J-M. Chem Phys Lett. 2003;369(3–4):483; Yin L-W, Li M-S, Liu Y-X, Sui J-L, Wang J-M. J Phys: Condens Matter. 2003;15(2):309.

192. Yin LW, Bando Y, Li MS, Liu YX, Qi YX. Adv Mater. 2003;15(21):1840.

193. Fei Z-Y, Liu Y-X. Chin Phys Lett. 2003;20(9):1554.

194. Gong Z-G, Li M-S. Chin Phys Lett. 2003;20(9):1540.

195. Zhao H, Chen X, Jia C, Zhou T, Qu X, Jian J, Xu Y, Zhou T. Mater Sci Eng B. 2005;122(2):90.

196. Salamat A, Woodhead K, McMillan PF, Cabrera RQ, Rahman A, Adriaens D, Cora F, Perrillat JP. Phys Rev B. 2009;80 (10):104106.

197. Wentorf RHJ. J. Chem. Phys., 26 (4), 956 (1957); F. P. Bundy, J Chem Phys. 1962;38(3):631.

198. Badding JV. Annu Rev Mater Sci. 1998;28:631.

199. Odintsov VV, Pepekin VI. Propellants Explos Pyrotech. 1997;22(1):34.

200. Horvath-Bordon E, Riedel R, Zerr A, McMillan PF, Auffermann G, Prots Y, Bronger W, Kniep R, Kroll P. Chem Soc Rev. 2006;35(10):987.

201. Ming LC, Zinin PV, Manghnani MH, Carvalho T, Hong SM, Xie Y. Microsc Microanal 2005;11:2028.

202. Hart JN, Claeyssens F, Allan NL, May PW. Phys Rev B. 2009;80(17):174111.

203. Thevenot F. J Eur Ceram Soc. 1990;6(4):205.

204. Greenwood NN, Earnshaw A. Chemistry of the elements. Oxford: Butterworth-Heinemann;1998.

205. Telle R, Sigl LS, Takagi K. Boride-based hard materials. In: Riedel R, editor. Handbook of Ceramic Hard Materials. Weinheim:WILEY-VCH; 2000. p. 802.

206. Granger MC, Xu J, Strojek JW, Swain GM. Anal Chim Acta. 1999;397(1–3):145; Yano T, Popa E, Tryk DA, Hashimoto K, Fujishima A. J Electrochem Soc. 1999;146(3):1081; Isberg J, Hammersberg J, Johansson E, Wikström T, Twitchen DJ, Whitehead AJ, Coe SE, Scarsbrook GA. Science. 2002;297 (5587):1670.

207. Ekimov EA, Sidorov VA, Bauer ED, Mel'nik NN, Curro NJ, Thompson JD, Stishov SM. Nature. 2004;428(6982):542.

208. Moussa JE, Cohen ML. Phys Rev B. 2008;77(6):064518.

209. Ekimov EA, Sadykov RA, Mel'nik NN, Presz A, Tat'yanin EV, Slesarev VN, Kuzin NN. Inorg Mater. 2004;40(9):932; Ekimov EA, Sidorov VA, Mel'nik NN, Gierlotka S, Presz A. J Mater Sci. 2004;39(15):4957.

210. Ekimov EA, Sidorov VA, Rakhmanina AV, Mel’nik NN, Timofeev MA, Sadykov RA. Inorg Mater. 2006;42(11):1198.

211. Dubrovinskaia N, Dubrovinsky L, Miyajima N, Langenhorst F, Crichton WA, Braun HF. Z Naturforsch B: Chem Sci. 2006;61:1561.

212. Lowell CE. J Am Ceram Soc. 1967;50(3):142.

213. Kouvetakis J, Kaner RB, Sattler ML, Bartlett N. J Chem Soc Chem Commun. 1986;0(24):1758; Way BM, Dahn JR, Tiedje T, Myrtle K, Kasrai M. Phys Rev B. 1992;46(3):1697; Fecko DL, Jones LE, Thrower PA. Carbon. 1993;31(4):637; Shirasaki T, Derré A, Ménétrier M, Tressaud A, Flandrois S. Carbon. 2000;38(10):1461.

214. Solozhenko VL, Dubrovinskaia NA, Dubrovinsky LS. Appl Phys Lett. 2004;85(9):1508.

215. Resseguier T de, Kurakevych OO, Chabot A, Petitet JP, Solozhenko VL. J Appl Phys. 2010;108(8):083522.

216. Zinin PV, Ming LC, Kudryashov I, Konishi N, Manghnani MH, Sharma SK. J Appl Phys. 2006;100(1):013516.

217. Lowther JE. J Phys: Condens Matter. 2005;17(21):3221.

218. Ming LC, Zinin PV, Liu XR, Nakamoto Y, Jia R. J Phys: Conf Ser. 2010;215(1):012135; Zinin PV, Ming LC, Ishii HA, R Jia, Acosta T, Hellebrand E. J Appl Phys. 2012;111(11):114905.

219. Solozhenko VL, Kurakevych OO, Andrault D, Le Godec Y, Mezouar M. Phys Rev Lett. 2009;102(1):015506.

220. Calandra M, Mauri F. Phys Rev Lett. 2008;101(1):016401.

221. Xu L, Zhao Z, Wang L-M, Xu B, He J, Liu Z, Tian Y. J Phys Chem C. 2010;114(51):22688.

222. Nkambule SM, Lowther JE. Solid State Commun. 2010;150 (1–2):133.

223. Liu Z, He J, Yang J, Guo X, Sun H, Wang H-T, Wu E, Tian Y. Phys Rev B. 2006;73(17):172101.

224. Liu H, Li Q, Zhu L, Ma Y. Phys Lett A. 2011;375(3):771.

225. Jiang C, Lin Z, Zhao Y. Phys Rev B. 2009;80(18):184101.

226. Wang Y-J, Wang C-Y. J Appl Phys. 2009;106(4):043513.

227. Lazar P, Podloucky R. Appl Phys Lett. 2009;94(25):251904.

228. Liang Y, Zhang W, Zhao J, Chen L. Phys Rev B. 2009;80(11):113401; Zhang Q, Wang S-m, Liang Y-c. J Zhejiang Univ Sci A. 2011;12(3):177.

229. Nakae N, Ishisada J, Dekura H, Shirai K. J Phys: Conf Ser. 2010;215(1):012116.

230. Li Q, Wang H, Tian Y, Xia Y, Cui T, He J, Ma Y, Zou G. J Appl Phys. 2010;108(2):023507.

231. Xi S. Chin Phys Lett. 2010;27(1):16101.

232. Yao Y, Tse JS, Klug DD. Phys Rev B. 2009;80(9):094106.

233. Zhang J-D, Cheng XL. Comput Mater Sci. 2011;50(7):2249.

234. Dong B, Tian F, Duan D, Jin X, Cui T, Zou G. Diam Relat Mat. 2011;20(3):454.

235. Liu H, Li Q, Zhu L, Ma Y. Solid State Commun. 2011;151(9):716.

236. Xu L, Zhao Z, Wang Q, Wang L-M, Xu B, He J, Tian Y. J Appl Phys. 2011;110(1):013501.

237. Guo X, He J, Xu B, Liu Z, Yu D, Tian Y. J Phys Chem C. 2007;111(37):13679.

238. Yang J, Sun H, He J, Tian Y, Chen C. J Phys Condens Matter. 2007;19(34):346223.

239. Rubie DC. Phase Transitions. 1999;68(3):431; Frost DJ, Poe BT, Tronnes RG, Liebske C, Duba A, Rubie DC. Physi Earth Planet Inter. 2004;507:143–144.

240. Jiang JZ, Kragh F, Frost DJ., Stahl K, Lindelov H. J Phys: Condens Matter. 2001;13(22):L515; Jiang JZ, Stahl K, Berg RW, Frost DJ, Zhou TJ, Shi PX. EPL. 2000;51(1):62.

241. Schwarz M. High pressure synthesis of novel hard materials: spinel-$Si_3N_4$ and derivatives [PhD thesis]. [Darmstadt (Germany): FB Material- und Geowissenschaften, TU Darmstadt; 2005.

242. Fang CM, de Wijs GA, Hintzen HT, de With GJ. Appl Phys. 2003;93(9):5175.

243. Schwarz M, Miehe G, Zerr A, Kroke E, Poe BT, Fuess H, Riedel R. Adv Mater. 2000;12(12):883.

## List of Symbols, Abbreviations, and Acronyms

| | |
|---|---|
| 2-D | 2-dimensional |
| 3-D | 3-dimensional |
| Ar | argon |
| $B_4C$ | boron carbide |
| $BBr_3$ | boron tribromide |
| BCN | boron-carbon-nitrogen |
| c-BCN | cubic boron-carbon-nitride |
| c-BN | cubic boron nitride |
| $CCl_4$ | carbon tetrachloride |
| CHN/S/O | carbon, hydrogen, nitrogen, sulfur, oxygen |
| CVD | chemical vapor deposition |
| DAC | diamond anvil cell |
| DEPT | distortionless enhancement by polarization transfer |
| DFT | density functional theory |
| dwur | defect-wurtzite |
| EDX | energy-dispersive X-ray |
| EELS | electron energy loss spectroscopy |
| EPMA | electron probe microanalysis |
| EPR | electron paramagnetic resonance |
| FTIR | Fourier-transform infrared |
| g-$BC_2N$ | graphitic $BC_2N$ |
| GGA | generalized gradient approximation |
| h-BCN | hexagonal boron–carbonitride |
| He | helium |
| HP | high pressure |

| | |
|---|---|
| HT | high temperature |
| LDA | local density approximation |
| LH-DAC | laser-heated diamond anvil cell |
| $Li_3N$ | lithium nitride |
| MA | multianvil |
| MAP | multianvil press |
| MS | mass spectrometry |
| $N_2$ | nitrogen gas |
| N/C | nitrogen carbon ratios |
| NMR | nuclear magnetic resonance |
| Pt | platinum |
| PVD | physical vapor deposition |
| REM | reflection electron microscopy |
| SAED | select area electron diffraction |
| SEM | scanning electron microscope |
| SIMS | secondary ion mass spectrometry |
| TCNE | tetracyanoethylene |
| TEM | transmission electron microscopy |
| THF | tetrahydrofuran |
| w-BCN | wurtzite boron-carbonitride |
| XPS | X-ray photoelectron spectroscopy |
| XRD | X-ray diffraction |

1 (PDF) DEFENSE TECHNICAL INFORMATION CTR DTIC OCA

2 (PDF) DIRECTOR US ARMY RESEARCH LAB RDRL CIO LL IMAL HRA MAIL & RECORDS MGMT

1 (PDF) GOVT PRINTG OFC A MALHOTRA

49 (7 HC, 42 PDF) DIR USARL
RDRL CIH C
P CHUNG
D GROVE
J KNAP
RDRL WM
P BAKER
B FORCH
J MCCAULEY (6 HC)
P PLOSTINS
RDRL WML B
I BATYREV
B RICE
D TAYLOR
N WEINGARTEN
RDRL WML H
B SCHUSTER
RDRL WMM
J BEATTY
R DOWDING
J ZABINSKI
RDRL WMM B
G GAZONAS
RDRL WMM E
C HILTON
S KILCZEWSKI
J LASALVIA
P PATEL
J SINGH
J SWAB
RDRL WMP
S SCHOENFELD
RDRL WMP B
C HOPPEL
D POWELL
S SATAPATHY
M SCHEIDLER
T WEERASOORIYA
RDRL WMP C
R BECKER
S BILYK
T BJERKE
D CASEM
J CLAYTON (1 HC)
D DANDEKAR
M GREENFIELD
R LEAVY
M RAFTENBERG
S SEGLETES
C WILLIAMS
RDRL WMP D
R DONEY
RDRL WMP E
S BARTUS
RDRL WMP F
N GNIAZDOWSKI
RDRL WMS
M VANLANDINGHAM

INTENTIONALLY LEFT BLANK.